Staphylococcus aureus Dysbiosis and the Role of Glycative Stress

A Dissertation Submitted in Partial Fulfillment of the Requirements for the Degree of

Doctor of Philosophy

Graduate School of Life and Medical Science

Doshisha University

Author: Haasbroek Kyle

Year:2019

Student ID: 1414 19 2001

Supervisor: Prof. Yoshikazu Yonei

Kyoto, Japan

November, 2021

Abstract

Glycation is a non-enzymatic reaction that occurs between reducing sugars and proteins that occurs under physiological conditions. The final products of the glycation reaction are called advanced glycation endproducts (AGEs). AGEs impair protein function, promote inflammation, and disrupt a variety of processes in various tissues. Glycative stress contributes to the pathology of diseases associated with aging, as well as the general aging process itself. AGEs accumulate in the body over time, and under conditions of hyperglycemia glycative stress is heightened.

It has been thought that because bacteria are short lived with high protein turnover that glycative stress via non-enzymatic glycation is not a significant factor for their physiology. However, in recent years glycative stress has been observed to occur in bacteria. Glycation and AGEs are not only relevant for the survival and growth of bacteria, but also alter the human body in ways that promote infection.

Two major skin microbes that inhabit the skin microbiome are *Staphylococcus epidermidis* and *S. aureus.*

S. epidermidis is a beneficial species. *S. epidermidis* produces antimicrobial peptides that inhibit the colonization and growth of pathogens. The presence of *S. epidermidis* also stimulates improved immune response by host skin cells, and inhabits ecological space that may otherwise be inhabited by pathogens.

S. aureus is a potential pathogen. It is present among a plurality of the population, and the leading cause of skin infection. Colonization with *S. aureus* causes inflammation in the skin and nasal epithelia. *S. aureus* frequently forms biofilms on surgical implants, catheters, and skin lesions.

Several conditions are strongly linked with skin lesions and *S. aureus*. Atopic dermatitis, psoriasis, and diabetes mellitus all show elevated abundance of *S. aureus*, associated with increased severity of symptoms and risk of infection. While the etiology of these disorders varies, all are associated with increased glycative stress throughout the body and accumulation of AGEs in the skin. I have also observed and increased abundance of *S. aureus* on the skin of healthy seniors, who have significantly increased fluorescent AGE accumulation in the skin compared to young adults.

I hypothesized that AGEs may increase pathogenicity of *S. aureus*, and conducted testing to examine the *in vitro* effects of glycated keratin.

Results

Previously, a loss of cell viability from elevated glucose and AGEs from was observed in *S. epidermidis*. Expanding testing to *S. aureus*, a similar reduction in cell viability was observed in both species. Exposure to glycated keratin triggered membrane damage and cellular aggregation in *S. aureus*. It was observed that *S. aureus* metabolizes fluorescent AGEs from high molecular weight forms to low.

Glycated keratin induced biofilm formation in a dose dependent manner, and high molecular weight AGEs had a significantly stronger biofilm promoting effect at the same dosage. Exploring potential topical treatments against elevates skin AGEs and *S. aureus* biofilm formation, we examined the biofilm inhibitory effects of several known AGE crosslink breakers in the AGE-biofilm model. Astaxanthin, clove extract, and rosemary extract demonstrated a strong ability to inhibit AGE-induced *S. aureus* biofilms.

A review of the literature was conducted regarding the potential interactions between glycative stress, *S. aureus* colonization, and viral infection that may play a role in the increased vulnerability to COVID19 reported in those with diabetes. Finally, a stable form of sodium hypochlorite was tested for its skin safety and bactericidal efficacy against *S. aureus* for use as a hand sanitizer. It was determined to be a safe product, and demonstrated effectiveness at sterilizing *S. aureus.*

Conclusion

The aging microbiome of the skin is characterized by increasing abundance, in absolute and relative terms, of *S. aureus*. AGEs produced from glucose and keratin triggered cellular aggregation and biofilm production in *S. aureus*. The presence of elevated concentrations of AGEs in the skin likely exacerbates *S. aureus* dysbiosis. Treatments to reduce the buildup of AGEs in the skin may help to reduce the severity of skin lesions, recurring staph infections, and other risks of *S. aureus* carriage in those experiencing elevated glycative stress. Such preventative measures may also help to avoid the overuse of antibiotics and the development of further antibiotic strains of *S. aureus* and other bacteria.

Acknowledgements

I would like to extend my deepest gratitude to my supervising professor Dr. Yonei, for affording me the opportunity to come and study in Japan in the Anti-Aging Medicine laboratory, for providing essential guidance and assistance as I completed my graduate studies. I was able to gain wonderful experiences and develop my knowledge and abilities while learning in a supportive environment.

I would also like to extend my thanks to Dr. Yagi, Dr. Takabe, and Dr. Sakiyama, without whose support and advice my research would not have been possible.

To all my lab mates who were working besides me for the past few years, thank you for your help and assistance while I was learning, for your comradery, and our shared collaboration.

And finally, I would like to thank my family and Catherine for their continued support and encouragement.

Haasbroek Kyle

November 24th, 2021

Kyoto, Japan

Table of Contents

1. INTRODUCTION

1.1. Glycative Stress

Glycation, also known as the Maillard reaction, is a non-enzymatic process that occurs between reducing sugars and protein or lipids. In addition to the well-known browning reaction that occurs during the cooking process, glycation also occurs under physiological conditions in living organisms. The resulting products of these reactions are called Advanced Glycation Endproducts (AGEs). AGEs contribute to the aging process and the pathogenesis of various age-associated illnesses such as diabetes mellitus [1,2] and neurodegenerative disease [3]. When AGEs form in association with proteins, they disrupt protein function and can cause the formation of protein aggregates [4] that are difficult for the body to breakdown and remove. AGEs also activate the Receptor for AGEs (RAGE), triggering an inflammatory response [5]. AGEs accumulate in the body over time and may interfere with a variety of processes from bone homeostasis [6] to the functioning of the immune system [7].

Aging of the skin also involves glycative stress [8,9]. AGEs form crosslinks between collagen fibers, reducing the skin's elasticity and forming wrinkles. Glycation of keratin too has been detected in the skin [10], hair [11], and nails [12]; the relative degree of glycation increases with chronological age [13], and is similarly elevated in those with diabetes. The accumulation of AGEs can also trigger melanogenesis and discolouration [14], further contributing to the physical signs of aging. In recent years, beauty products and dietary supplements are sold which aim to inhibit glycation and breakdown AGE cross-links and aggregates in the skin and throughout the body in order to maintain a healthy and youthful appearance. The healthy state of the skin is also of vital importance to overall health: the thinning and stiffening of the epidermidis that comes with age weakens the skin's barrier function, increasing the risk of injury and infection.

1.2. Glycative Stress and Bacteria

Bacteria are overlooked when it comes to glycation as it is thought of as a slowly occurring reaction that takes months to years to accumulate glycative stress in mammalian/eukaryotic cells; this it at odds with the very short lifespan and generation time of bacterial cells. However,

glycation does occur in bacteria: non-enzymatic glycation and endogenous bacterial AGEs were first reported to be observed in *E. coli* [15].

Glycative Stress is also a significant enough phenomenon in bacteria to appear to have applied enough evolutionary pressure for anti-glycation mechanisms to develop. Demonstrate that *E. coli* breakdown accumulated AGEs intracellularly and secrete them as < 3kDa units, using an unknown metallo-protease [16]. Bacterial secreted AGEs may also have clinical/physiological significance in humans, as secreted AGEs are found to trigger an increase in pro-inflammatory cytokines in mammalian cells via RAGE [17].

Research also suggests that glycopeptidase Gcp (OSGEP in humans) is responsible for preventing the accumulation of glycated proteins in *E. coli* [18]. This protein is preserved in all three domains of life, emphasizing its physiological importance to all life, although its homologs play different roles in different species, usually as a chaperone molecule. However, the sequence is highly conserved across species despite the different functions, suggesting that a shared function may also be maintained, one that is relevant to all life: the defense against non-enzymatic glycation and its consequences, which can occur in any biological system.

1.3. The Human Microbiome

As a part of many systems within the body that change and/or deteriorate with age, it is also of vital importance to consider the communities of symbiotic bacteria that inhabit a diverse range of environments throughout the body, making up the human microbiomes. Shifts in the makeup and abundance of the species inhabiting the human microbiomes have been reported to occur over time with age, leading to distinct patterns of bacterial populations between the gut flora of from infanthood to young adults and the elderly [19,20]. The changes in the makeup of the microbiomes can progress through a process of ecological succession, with early colonizing species preparing the environment for later arrivals before arriving at a relatively stable climax community. Disturbances such as antibiotic treatment, injury, disease, and aging itself can alter the human environment, leading a healthy microbiome to fall out of balance. This is called dysbiosis, where shifts in species of the microbiome disrupt stable homeostasis. Dysbiosis can present as an overabundance of potentially pathogenic species, such as *C. difficile* in the gut [21], or the chronic colonization of the lungs that co-occurs with cystic fibrosis [22,23]. While the gut microbiome has

been a focus for study due to its important role in digestive health [24] and role in the gut-brain axis [25], other ecological niches on the body have seen less attention, such as the skin.

The skin plays a crucial role in maintaining separation between the nutrient rich and vulnerable body and the environment, with its barrier function maintaining distinction from the environment, preventing the loss of water and nutrients, and preventing invasion by hostile pathogens. While relatively dry and low in nutrients, the surface of the skin is nevertheless home to a diverse ecology of microorganisms that first colonize the surface of the body during birth. Humans inherit their skin microbiome from those closest to them in their early lives through physical contact, and a general pattern of succession of species can be recognized during infancy [26].

What role, if any, the species of the skin microbiome play in general health is still only beginning to be understood; the skin microbiome includes many uncharacterized and unculturable species. For the purposes of this research, I chose to focus on the genus *Staphylococcus*, due to their ubiquity, ease of culturing, and important role in human health.

1.4. *Staphylococcus epidermidis*

S. epidermidis is a gram-positive Firmicute, and a ubiquitous inhabitant of the human skin microbiome. It exists in a commensal symbiotic relationship with its human host, providing numerous beneficial effects. *S. epidermidis* can help prime the immune response of native keratinocytes, bolstering skin immunity and promoting the production of host antimicrobial peptides (**Liu 2020**). *S. epidermidis* also produces its own antimicrobial peptides in order to compete against rival species, which includes pathogens such as *S. aureus* (**Newstead 2020**), *P. acnes* [27], and Group A *Streptococcus* [28]. Some strains have even shown the ability to disrupt *S. aureus* biofilms [29].

1.5. *Staphylococcus aureus*

S. aureus is a gram-positive Firmicute that frequently inhabits the skin and nasal epithelia of humans. *S. aureus* is a major pathogen that is a frequent cause of skin infections in hospital and community settings, including antibiotic resistant varieties (i.e., MRSA). It is one of the most common cause of skin and soft tissue infections, which are often recurring: among patients treated for *S. aureus* skin infections, recurrent infection rates after 6 months are as high as 51%

[30]. *S. aureus* proteases harm the skin's barrier function and can induce apoptosis in keratinocytes [31]**.** *S. aureus* frequently colonizes skin lesions [32], its abundance is positively correlated with symptom severity [33], and its presence slows wound healing [34]. *S. aureus* can enter the bloodstream and cause potentially fatal systemic infection, and carriage of the bacterium is a risk factor for post-surgery infection [35,36]. *S. aureus* can also cause bacterial pneumonia, particularly in co-infection with viruses such as Influenza A [37,38] and SARS-CoV-2 [39]. *S. aureus* forms biofilms on the body and on medical implants and catheters, increasing its pathogenicity and protecting constituent cells from the body's immune response, antibiotics, and competing bacteria.

1.6. Glycative Stress and *S.* aureus Dysbiosis

S. aureus dysbiosis is strongly associated with skin disorders linked to high glycative stress. The formation of skin lesions is a major complication of diabetes mellitus, and responsible for a plurality of hospitalizations of diabetic patients [40]. Non-lesions skin is also affected, with a significant increase in *S. aureus* abundance and a loss of non-*S. aureus* staphylococcal species reported on the diabetic foot [41]. Nasal carriage of *S. aureus* is also significantly elevated in those with diabetes [42], and carriage rates are further elevated in those with high fasting blood glucose levels [43] and increased levels of glycated hemoglobin [44]. The incidence rate of *S. aureus* bacteremia is also significantly greater in diabetes [45].

The same phenomenon can be observed in lesions skin disorders unrelated to diabetes as well. Atopic Dermatitis (AD) is a skin disorder characterized by dry and cracked skin that is linked to a loss of function mutation in the protein filaggrin [46]. Severity of AD is correlated with *S. aureus* abundance [47], which is elevated on those with AD on both lesional and non-lesional skin [48]. This colonization is characterized by biofilm formation, which allows *S. aureus* to persist on the skin in high concentrations [49,50]. Surprisingly, it has been discovered that AGE content in the skin of those with AD is significantly elevated compared to healthy controls [51].

Psoriasis is an inflammatory skin disorder that leads to excessive keratinocyte proliferation and the formation of lesional plaques on the skin [52]. Psoriasis is also associated with elevated *S. aureus* colonization and abundance [53,54]. Blood and skin glycative stress markers are also elevated [55,56].

Despite their disparate etiologies, diabetes, atopic dermatitis, and psoriasis are all associated with skin lesions, *S. aureus* dysbiosis and biofilm formation, elevated glycative stress markers, and AGE accumulation in the skin. Glycation of keratin in the stratum corneum is significantly elevated in those with diabetic skin ulcers [57]. and among hospital patients suffering from microbial eczema [58]. Observing this association, it was hypothesized that AGEs may play a causative role in *S. aureus* dysbiosis, leading to increased risk of infection in those under a high glycative stress burden.

During my master's research, I examined the composition of the Staphylococcal skin population of the volar forearm of healthy young adults and elderly participants (see **Table 1**). A significant increase in *S. aureus* abundance and loss of *S. epidermidis* carriage was observed on the elderly skin, which was coincident with an increase in skin fluorescent AGE content. *S. aureus* dysbiosis may be a risk for those with elevated glycative stress, regardless of the lack of co-morbid illnesses like diabetes or atopic dermatitis.

1.7. Role of Glycative Stress in Other Bacterial Diseases

While the effects of glycative stress on aging and the pathogenesis of various diseases has come to be better understood in the recent years, knowledge about its interactions with bacteria is still quite scarce. While it has been known for some time that AGEs in culture media may influence the growth of some microorganisms under laboratory conditions [59], the implications for human health in more complex systems are still prime targets for study. Among that little research has already been published, there are indications that glycative stress is a factor in some infectious disease. Glycation of the bladder epithelium increases the binding affinity of *E. coli* [60], facilitating bacterial adhesion and infection, partially explaining the increased frequency of UTIs in diabetes. Dietary AGEs may impact the gut microbiome [61], and coffee melanoidins have been reported to modulate adhesion by *H. pylori* in the stomach [62].

1.8. Research Aim

In order to better understand age-related changes in the skin microbiome, with consideration of glycative stress, I examined the effects of glycative stress induced by exogenous AGE exposure on *Staphylococcus epidermidis* (Master's research [63]), and here primarily *Staphylococcus aureus*. Based on the reported roles of *S. aureus* dysbiosis in diseases associates with high levels of

glycative stress, it was hypothesized that exogenous host AGEs may affect *S. aureus* in ways that promote increased pathogenicity.

2. MATERIALS AND METHODS

2.1. Glycation Model

Glycated keratin solutions used in testing were produced by incubating proteins with glycating agents in accordance with the recipes outlined by [64]. The final concentration of the solution consisted of 50 mM phosphate buffer (pH 7.4), 0.60 mg/mL keratin (Nacalai Tesque, Kyoto, Japan), and 40 mM glucose. Solutions were incubated at 60°C for 10 days to accelerate the glycation process. After incubation, ultrafiltration was performed using Amicon Ultra Centrifugal Filters according to the manufacturer's instructions (Merck Millipore Ltd, Cork, Ireland) to remove unreacted glucose and concentrate solutions. Protein concentration of glycated keratin solutions was measured by BCA Protein Assay (Thermo Fisher Scientific, MA, USA) according to the manufacturer's instructions.

2.2. High-Performance Liquid Chromatography

HPLC analysis and pentosidine measurement of glycated keratin solution was performed using the following column type:

Column:	Cadenza CD-003, 5 µm (Imtakt, Kyoto, Japan)
Column	Size: 150 x 4.6 mm I.D.

Device settings were as follows:

Eluent Fluid:	A: 100 mM citric acid / acetonitrile = 995 / 5
	B: acetonitrile
Time Program:	0-15 min (0% B)
	15.5-20.5 min (50% B)
	20.5-60 min (0% B)
Flow Speed:	1.0 mL/min
Column Temp.:	20°C
Detection:	Ex: 325nm, Em: 385 nm
Injection Volume:	20 µL
Sample Cooler:	4°C

2.3. Bacterial Strains and Growth Conditions

S. epidermidis NBRC100911 (ATCC 14990) and *S. aureus* NBRC100910 (ATCC 12600) were purchased from the National Institute of Technology and Evaluation Biological Resource Center (Tokyo, Japan).

S. aureus ATCC 12600 is a moderate biofilm producer that contains all the components of the *ica* gene complex that regulates the production and secretion of poly-beta-1,6 N-acetyl-D-glucosamine, the polysaccharide component biofilms [also known as polysaccharide intercellular adhesin (PIA)]. ATCC 12600 also possesses SigB, which plays a role in autolysis and the release of DNA in the formation of eDNA biofilms. It lacks biofilm associated protein (Bap), which is necessary for some types of PIA-independent biofilm formation. However, Bap is generally not found in humans trains of *S. aureus*, but is more common in bovine varieties.

2.4. Bacterial Growth Conditions

Planktonic bacterial cultures were grown in Tryptic Soy Broth (TSB) at 37°C, with 250 rpm shaking. Solid media cultures were grown on either Tryptic Soy Agar or Mannitol Salt Agar at 37°C. Colony counting of agar plates was performed after 24 to 72 hours of incubation. All growth media used was purchased from Becton, Dickinson, and Company (MD, USA). 0.1 M phosphate buffer (pH 7.4) with 0.14M NaCl was used as carbon-free non-growth media.

2.5. Cellular Viability

Bacterial viability of planktonic cultures was determined by plate-counting after serial dilution; Tryptic Soy Agar plates were inoculated in triplicate and incubated at 37°C for 72 hours with daily colony counting. Turbidity assay (OD_{600}) was found to poorly correlate with viable cell concentration in post-logarithmic growth phase cultures containing glycated keratin, and was omitted from the results.

2.6. Cellular Aggregation: Sedimentation Assay

S. aureus is a non-motile bacterium, and cannot move under its own power. Consequently, cells in planktonic solution will slowly settle to the bottom of sample tubes over time without agitation. The rate of this sedimentation depends upon the size of aggregates: larger aggregates settle out of solution more quickly than smaller ones.

5 mL solutions of TSB (supplemented with either 0.5 mg/mL glycated keratin or milliQ as a control) in sterile 12 mL sample tubes were inoculated with *S. aureus* and incubated under planktonic conditions for 24 hours. After incubation, both samples were vortexed and left to sit undisturbed at 4°C. Periodically, 150 µL aliquots were collected from near the air-liquid interface at the top of each solution and their turbidity was measured by absorbance at 600 nm (OD_{600}) in triplicate.

2.7. Cellular Aggregation: Image Analysis

Planktonic cultures were supplemented with either milliQ (control) or 0.5 mg/mL glycated keratin (AGE+) and incubated for 24 hours. After incubation, samples were vortexed and 2 µL aliquots were collected, transferred to microscope slides, and flame fixed. Slides were observed via brightfield microscopy, and images were captured at a maximum magnification of 400X. Image analysis was performed using ImageJ (National Institutes of Health) analysis software. Briefly, images were converted to black and white and size of cells and cellular aggregates was measured (size represented by area in µm2).

2.8. Biofilm Crystal Violet Assay

Biofilm assay was performed as previously reported [65]. 1 mL solutions of TSB were prepared, with the desired amount of glycated keratin added per sample type. Each solution was inoculated with 1:100 volume (10 µL) of *Staphylococcus* overnight stock and thoroughly vortexed before pipetting 100 µL aliquots of each sample into the wells of a sterile un-treated 96-well plate (8 replications per sample). The outer wells of each plate were filled with purified water to prevent evaporation of test wells. Plates were then sealed and incubated at 37°C for 48 hours before staining with 1.0 mg/mL crystal violet solution for 10 minutes. After staining, plates were gently washed with water twice and left to dry overnight. Each dried and stained biofilm well was solubilized using 200 µL of 30% glacial acetic acid solution. Finally, the absorbance of 125µL aliquots were measured at 587 nm using a Varioskan Flash Multimode Microplate Reader (Thermo Fisher Scientific, MA, USA).

2.9. Membrane Integrity Test: DNA Release Assay

The membrane integrity assay was performed as previously described [66]. Cells that have sustained membrane damage leak their cytoplasmic contents, and nucleic acids can be detected

photometrically at a wavelength of 260 nm. Aliquots of *S. aureus* overnight culture were collected and the cells resuspended in carbon free media (0.1 M phosphate buffer, 0.14 M NaCl), before the addition of 1.0 mg/mL of glycated keratin solution. After incubation at 37°C, samples were centrifuged for 5 minutes at 4500 g and the supernatant collected for absorbance assay at 260 nm using a Varioskan Flash Multimode Microplate Reader (Thermo Fisher Scientific, MA, USA).

2.10. Membrane Integrity Test: Propidium Iodide Assay

Membrane integrity was further examined by propidium iodide staining. 1 mL sample cultures were prepared and inoculated with 10 µL of *S. aureus* overnight stock, before incubation under planktonic conditions. After 24 hours, sample aliquots were centrifuged at 4500 g for 5 minutes. Bacterial pellets were stained with 100 µL of 30 µM propidium iodide (Sigma-Aldrich, MI, USA) in 0.1 M phosphate buffer for 10 minutes in the dark at room temperature. After staining, samples were centrifuged again and washed with phosphate buffer, before final resuspension in 1 mL phosphate buffer. 200 µL aliquots of each sample were transferred in triplicate to a black 96-well plate, and fluorescence emission measured at 617 nm after excitation at 535 nm.

2.11. *In vitro* Fluorescent AGE Measurement

Fluorescent AGE content was measured photometrically as previously described [67]. 200 µL aliquots of solution were transferred in triplicate to black 96-well microplates. Emission at 440 nm after excitation at 370 nm was measured using a Varioskan Flash Multimode Microplate Reader (Thermo Fisher Scientific, MA, USA). Absorption values were normalized to the reference value of 5 µg/mL if quinine sulphate using the following equation:

$$Normalized\ Emission\ Value = \frac{Fluorescence\ Intensity\ of\ Sample}{Fluoresence\ Intensity\ of\ Quinine\ Sulphate} \times 1000$$

2.12. Biofilm Inhibition Materials Preparation

Aminoguanidine, ascorbic acid, and N-Phenacylthiazolium Bromide (PTB) were dissolved directly in milliQ at room temperature.

For rosemary extract, a commercial anti-aging supplement, AGE Breaker (manufacturer), was tested. Capsules of the supplement were ground into a powder and dissolved in 0.1 M phosphate buffer (pH 7.4) at room temperature.

For clove extract, a heated water extraction was performed. 2 g of clove powder was added to 40 mL of milliQ and heated at 80°C for 75 minutes. After heating, the resulting solution was centrifuged at 2500 rpm for 10 minutes and the supernatant was collected as the clove extract solution. Concentration of the solution was determined by measurement of the dry mass of aliquots after evaporation.

Melatonin and Astaxanthin were both solubilized in dimethyl sulfoxide (DMSO) at room temperature.

2.13. Dose-Response Curve Fitting

Logistic curve-fitting was performed in R [68] using the Dose Response Curve package [69].

2.14. Statistical Analysis

Simple descriptive statistical analysis was performed using Excel (Microsoft). Between group statistical difference was calculated using Student's T-test. For multiple comparisons, One-way ANOVA was performed with an α of 0.05, followed by Tukey's test using SPSS Statistics (IBM).

3. IN VITRO EFFECTS OF AGES ON STAPHYLOCOCCUS

3.1. Antimicrobial Effect of AGEs: Background

The earliest reports of the effects of glycative stress on microbial organisms can be found in the literature going back to the early 20th century, although AGEs were not yet known at the time. A 1930 paper [70] describes the effects of heat-sterilized culture media containing sugars on the growth of several species of bacteria. Some, like *S. aureus* and *B. anthracis*, were inhibited, while others including *E. coli*, *B. subtilis*, and *K. aerogenes* were unaffected. The reported inhibition occurred alongside caramelization of the media. However, when glucose was caramelized separately from growth media and added after sterilization, the inhibitory effect disappeared. This strongly implies that the Maillard Reaction and the production of AGEs from glucose and nitrogen sources in the media. Other papers from the time describe a similar phenomenon in other microorganisms, although growth could be inhibited or stimulated depending on the species being cultured. Growth of yeasts such as *S. cerevisiae* [71] or bacteria like *Streptococcus salivarius* [72] was reportedly enhanced. Decades later, when Maillard Reaction Products (aka AGEs) were beginning to be more well-known, a handful of studies examined their mutagenic effects on *S. typhimurium* [73,74], or interactions with gut microbes [75].

The implications of glycation of media under laboratory conditions remains relevant to this day; growth media glycation has been noted to hinder study of difficult to culture extremophile archaea [59]. In the food sciences, it has been reported that melanoidins, AGE polymers formed in foods cooked at high temperatures, have antibacterial properties [76], and may interfere with the adhesion of *H. pylori* to host tissues [62]. AGEs formed in foods prepared at high temperatures may help to prevent spoilage or impact human health through dietary AGE intake. However, the effects on microorganisms of AGEs produced from human or mammalian proteins under physiological conditions is largely unknown.

Previously, I examined the effects of AGEs formed from glucose or fructose and HSA, type I collagen, or keratin on planktonic cultures of *Staphylococcus epidermidis* and observed a consistent growth inhibition/loss of viability that was correlated with fluorescent AGE content.

These tests were performed on wild-type SE of unknown strain isolated from healthy human skin. As I observed a decreased abundance of SE and increased SA on the skin of the elderly, I hypothesized that the two species may differ in susceptibility to the anti-microbial effect of AGEs. As the skin increased in AGE content with age, the aged skin environment may be less hospitable to SE while allowing SA to survive. In order to test this, known strains of SE and SA were chosen for comparative testing. Keratin was chosen as the protein of choice due to its predominance in the stratus corneum of the skin where *Staphylococcus* species reside.

3.2. Detection of Keratin Glycation and the Limitations Thereof

In the past, researchers have utilized colorimetric techniques to measure glycation by reacting glucose adducts with thiobarbituric acid after hydrolysis of glycated proteins [77]. More recently, fluorometric [67] and immunostaining [78] methods have been used to identify glycated proteins. However, these techniques are indirect or relative measures of the amount of glycation or concentration of AGEs, and do not represent in absolute terms the degree of polymerization, or the number of modified amino acid residues present on particular proteins.

More specific measurements of the local chemical changes involved in the glycation of keratin remain unknown. Literature on the topic is not available, and it is considerably difficult to determine. Though interesting, this problem is difficult to solve in the limited time available.

In the current glycation model, glycosylation of keratin (in comparison to keratin solution processed without glucose) was detected by the increase in fluorescence intensity associated with AGEs (Excitation 370 nm, Emission 440 nm), the formation of a specific AGE (pentosidine) measured by High-Performance Liquid Chromatography, and the presence of the characteristic browning that is observed in the Maillard Reaction.

3.3. *S. epidermidis* Loss of Viability due to Glycated Keratin

Addition of glycated keratin to *S. epidermidis* NBRC 100911 growth media was examined for its effects on growth and cell viability as determined by colony counting after serial dilution. Samples with glycated keratin showed typical signs of active growth, developing obvious turbidity, with a peak cell count observed after 24 hours of incubation (24-hour viability shown in **Figure 1**). However, the CFUs/mL at this time were significantly reduced compared to controls. By 72 hours of incubation, viable cell count fell below the concentration of the initial

inoculum (see **Figure 2** for 72-hour viability). The IC_{50} at 72 hours was estimated to be 0.38 mg/mL, and a maximum 2.08 log reduction was observed in CFUs/mL at a glycated keratin concentration of 1.5 mg/mL.

3.4. Free Pentosidine/CML Tests

The glucose-keratin glycation model, as was previously known, demonstrated production of fluorescent AGEs. One such fluorescent AGE that is a common target for study is pentosidine; the pentosidine content of the final glycated keratin solution was measured using HPLC. The solution was determined to contain roughly 11 ng pentosidine / mg keratin (**Figure 3**). In order to test the efficacy of pentosidine in isolation, free pentosidine was introduced into TSB media and inoculated with *S. epidermidis* at concentrations of 10, 50, and 100 ng/mL. At all tested concentrations, free pentosidine failed to produce a significant change in cell viability or growth compared to controls (see **Figure 4**).

In addition to pentosidine, carboxymethyl lysine, a non-fluorescent AGE that is also commonly observed in the epidermis, was also tested in its free form. At dosages of 50, 100, and 1000 ng/mL, no significant loss of cell viability was observed (see **Figure 5**).

3.5. *S. aureus* Loss of Viability due to Glycated Keratin

S. aureus NBRC 100910 was also tested with glycated keratin to observe its effects on cell viability. At a dosage of 1.0 mg/mL, glycated keratin was added to growth media of both S. aureus and *S. epidermidis* for comparison at a concentration of 1.0 mg/mL over 72 hours (see **Figure 6**). Observing the increasing dominance of *S. aureus* on skin high in fluorescent AGEs, it was initially hypothesized that *S. aureus* may be more resistant to glycative stress from exogenous AGEs, and a reduced loss of viability would be observed. Both species experienced a similar loss of cell viability, following the same pattern of growth inhibition. After 72 hours, *S. epidermidis* CFUs in glycated keratin cultures were reduced by 3.6 log compared to control cultures, and S. aureus samples were reduced by 3.1 log. In both species, growth peaked at 24 hours at significantly reduced concentrations than control, followed by a further reduction of viable cells after further incubation (24-hour comparison shown in greater detail in **Figure 7**).

After incubation with glycated keratin, large aggregates that were visible macroscopically were observed to form at the bottom of sample tubes inoculated with *S. aureus*.

3.6. Membrane Damage

It has been reported that the antimicrobial effect of coffee melanoidins on *E. coli* is exerted by membrane damage [79]. I speculated that a similar phenomenon may be involved in the antimicrobial effect observed in *Staphylococcus* from glucose-keratin AGEs.

An assay of extracellular DNA release after addition of 0.5 mg/mL glycated keratin to 0.M phosphate buffer containing resuspended *S. aureus* cells indicated no increase in the release of intracellular contents in glycated keratin conditions over a period of 40 minutes (See **Figure 8**). Additional samples incubated for up to 24 hours also showed no increase in the release of eDNA (not shown), suggesting there was no significant direct membrane damage cause by the mere presence of glycated keratin, as is reported for coffee melanoidins.

A propidium iodide assay was also performed to assess membrane damage in TSB growth media (**Figure 9**), as the media itself interfered with the direct photometric measurement of DNA under these circumstances. *S. aureus* grown in culture media with added glycated keratin (0.5 mg/mL) demonstrated 4.7-fold higher fluorescence intensity than control after 24 hours of incubation, indicating significantly increased membrane permeability and/or release of DNA ($p < 0.001$). To better understand the requisite conditions for this membrane damage to occur, an assay was also performed comparing active growth media and non-growth media with added 0.5 mg/mL of glycated keratin (**Figure 10**). In the non-growth media with added glycated keratin, there was no significant change in the measured results. Only samples in which *S. aureus* passed through its logarithmic growth phase in active growth media in the presence of glycated keratin produced significant fluorescence, indicating significant membrane damage and/or release of eDNA.

3.7. Cellular Aggregation: Sedimentation Assay

S. aureus cellular aggregation in response to glycated keratin was initially quantified by sedimentation assay. As *Staphylococcus* is non-motile, cells will settle at the bottom of culture solutions over time without agitation. The rate of this settlement is dependent upon the size of the cells or cell aggregates, with larger particles accumulating at the bottom of sample tubes at a faster rate. After 24 hours of growth, the turbidity of *S. aureus* cultures with and without added 0.5 mg/mL glycated keratin was measured over time (**Figure 11**). Turbidity of AGE+ culture rapidly fell over the initial 4 hours of observation, while control the culture remained relatively

stable. The sedimentation rate during the first 4 hours of testing was 14 times faster in the glycated keratin culture (0.0014 absorbance units/min) compared to control (0.0001 absorbance units/min). After 24 hours, the AGE+ samples' turbidity had fallen by 88% of initial turbidity, while that of control samples had only decreased by 45%. Following this test, aggregation was quantified more precisely by image analysis.

3.8. Cellular Aggregation: Image Analysis

When observed microscopically, the initial formation of small clumps of up to a dozen cells differentiated glycated keratin cultures from controls in the logarithmic growth phase, roughly 5 hours after inoculation. Microscope captured images of *S. epidermis* and *S. aureus* cellular aggregates were collected after 24 hours of incubation under planktonic conditions, with and without 0.5 mg/mL of added glycated keratin (see **Figure 12**). After conducting an analysis of captured microscope images, AGE+ samples demonstrated significantly greater cellular aggregation compared to controls in terms of aggregate size for both *S. epidermidis* and *S. aureus* (see **Figure 13**). Aggregate size was considerably larger in *S. aureus* than *S. epidermidis*, agreeing with the visual observations of macroscopic aggregates noted in test cultures. Glycated keratin at a concentration of 0.5 mg/mL provoked an 8.0-fold increase in mean aggregate size in *S. aureus*, and a 3.3-fold increase in *S. epidermidis* compared to control samples ($p < 0.001$).

3.9. Cellular Aggregation: Mechanisms and Significance

The most well-known regulatory pathway for aggregation in *S. aureus* is that regulated by the ArlRS two-component system. ArlS is a membrane bound sensor protein that detects a yet unknown signal from the environment, which phosphorylates its cytoplasmic counterpart ArlR. ArlR then activates MgrA [80], which is a global regulator that modulates many processes in *S. aureus* physiology [81], including autolysis and cell surface protein expression. In the case of aggregation, MgrA represses expression of the giant Staphylococcal surface protein, Ebh [82] (**Figure 14**). This protein's large size prevents agglutination by blocking neighboring cells from binding to one another in fibrinogen-based aggregates [83]. Fibrinogen aggregation occurs during infection in the blood and synovial fluid; binding substrates such as fibrin/fibrinogen are ligands for cell surface binding receptors, acting as nucleating agents for the formation of bacterial aggregates. Cells in the interior of aggregates are physically shielded from the environment, and the surface area to volume ratio of the total aggregate is increased, reducing exposure to harmful

substances such as antibiotics [84,85]. Large aggregates are also more difficult for phagocytes to engulf [86]. Bacteria that have lost the ability to aggregate show a significant loss of virulence in animal models of *S. aureus* infection [87–90].

Fibrin-based cellular aggregation during infection occurs rapidly upon addition of human plasma [83] or synovial fluid [91] into buffers containing resuspended *S. aureus* cells, without the need for plentiful energy or nutrient sources (e.g., free glucose, amino acids, etc.). However, in testing glycated keratin did not provoke the formation of aggregates in non-growth media such as phosphate buffer, regardless of growth phase. When aggregates were observed in growth media containing glycated keratin, the process was relatively slow, with initial small aggregates of up to a dozen cells only appearing after roughly 5 hours of incubation.

Aggregation may also occur in response to antibiotic compounds as a response to the induced stress or damage to the cell. I have observed *S. aureus* aggregation in response to certain antimicrobial compounds, and aggregation in response to sub-lethal concentrations of antibiotics is reported in the literature for *S. aureus* [92] and other species [93]. With regards to *S. aureus*, the mechanism for this type of aggregation appears to be less understood, but may rely on the release of eDNA. As observed in the experiments, glycated keratin mediated cellular aggregation co-occurred with significant membrane damage, and neither were observed in samples of *S. aureus* resuspended in buffers containing glycated keratin. This suggests that the mere presence of glycated keratin did not directly damage *S. aureus* membranes or act as a binding substrate for already present cell surface anchors, but relies on an energetic response from the bacteria or occurs only during active replication. I speculate that high demand for amino acids during replication may lead to increased metabolism and uptake of glycated keratin, resulting in the observed growth inhibitory and antimicrobial effects of glycated keratin. The glycative stress exerted by consumed AGEs may promote autolysis and the release of eDNA and/or the production of extracellular polysaccharides (PNAG), which would then act as substrates for both aggregation and biofilm formation.

Aggregation may or may not be accompanied by biofilm formation, but is a step in the formation process as individual cells amass to create the biofilm. Observing the occurrence of aggregation in planktonic cultures, I hypothesized that this may indicate the potential for biofilm formation as

well. Skin disorders associated with *S. aureus* dysbiosis often involve biofilm formation on the skin and in lesions; I formed the hypothesis that glycated keratin may trigger biofilm formation.

4. AGE-MEDIATED BIOFILM FORMATION

4.1. Bacterial Biofilms: Background

Biofilms are a viscous extracellular matrix containing polysaccharides, peptide chains, and eDNA that are secreted by certain bacteria. The viscosity of the biofilm, the density of cells, presence of protective enzymes, and changes in metabolic state of resident bacteria all contribute to increased resistance to antibiotics and host immune response [94]. *S. aureus* readily forms biofilms on catheters and medical implants which can lead to serious infection [95].

In addition to medical plastics, *S. aureus* is also known to form biofilms on the skin itself. Skin lesions resulting from poorly treated diabetes mellitus often form on extremities where they are readily colonized, leading to staph infection. *S. aureus* abundance increases while the diversity of commensal and/or mutualistic *Staphylococcus* species is lost on the feet of diabetic patients [41]. Other skin conditions associated with elevated glycative stress, such as atopic dermatitis [51,96] and psoriasis [56,97], are also characterized by colonization with *S. aureus* [48,98], which forms biofilms in skin lesions and exacerbates the severity of accompanying symptoms. Biofilms contain bacterial proteases that contribute to breaking down skin proteins, and induce apoptosis in keratinocytes [31]. Once the skin's barrier function is impaired, potentially fatal systemic infection is a significant risk factor.

4.2. Glycated Keratin Induces Biofilm Formation

Speculating that the cellular aggregation observed in planktonic cultures may indicate the potential for biofilm formation, biofilm assays were performed in order to quantitatively measure the response of *S. aureus* to glycated keratin AGEs. The initial measurement was performed with *S. aureus* at a glycated keratin concentration of 0.5 mg/mL. Biofilm absorbance was measured at 587nm after 48 hours of stationary incubation.

Figure 15 demonstrates the biofilm response of *S. aureus* alongside several controls. Sterile TSB was used as a background to ensure there was no interference during the crystal violet staining, producing negligible absorbance values (not shown). For the glucose condition, an additional 2.5 mg/mL of glucose was added to TSB, resulting in a final glucose concentration of 5.0 mg/mL. Heated keratin, produced following the same procedure as glycated keratin, but without glucose,

did not differ significantly from control. All sample varieties resulted in significantly less biofilm formation than glycated keratin, which produced the strongest response at 1.9 units. Exposure to glycated keratin resulted in a roughly 10-fold increase in biofilm production compared to heated, un-glycated keratin ($p < 0.001$).

The biofilm response of *S. epidermidis* and *S. aureus* are compared in **Figure 16**. While glycated keratin produced a significant increase in biofilm formation in both species, *S. aureus* produced significantly more biofilm than *S. epidermidis* at the same dosage ($p < 0.001$).

4.3. Biofilm Dose-Response

The dose-response curve of *S. aureus* biofilm production in response to glucose-keratin exposure was also examined. The resulting curve, shown in **Figure 17**, reveals a classic sigmoidal relationship with a midpoint of 0.64 mg/mL of glucose-keratin ($R^2 = 0.99$). Biofilm abundance rises rapidly at increasing dosage below 1 mg/mL, before beginning to plateau at an absorbance value of roughly 3.0 above baseline between a dosage of 2 – 5 mg/mL.

4.4. Heated Keratin Dose-Response

The dose-response relationship of glucose concentration on biofilm formation was examined in more detail. Starting with standard TSB media as a control, with 2.5 mg/mL of glucose, the concentration was raised in 2.5 mg/mL intervals up to a maximum of 10 mg/mL. Biofilm formation was quantified after 48 hours under static conditions (see **Figure 18**).

The addition of glucose to growth media induced mild biofilm formation, peaking with 5.0 mg/mL of glucose at a biofilm abundance 4.4-fold that of standard media. As glucose concentration increased beyond this peak, there was a negative trend in biofilm abundance, as it began to decrease with increasing glucose content.

4.5. Glucose Dose-Response

Heated keratin did not significantly increase biofilm formation compared to controls at a dosage of 1.0 mg/mL in preliminary tests, nor did it at 0.5 mg/mL in the previous biofilm response data (**Figure 15)**. Nevertheless, a wider range of heated keratin concentrations were tested to determine if sufficiently high concentrations may have a stronger effect on biofilm formation. The results of the assay can be seen in (**Figure 19**).

Increasing heated keratin concentration was positively correlated with biofilm abundance, although the magnitude of the increase was small, reaching a maximum absorbance value of only 0.26, roughly 3.2 times that of control, at a keratin concentration of 1.6 mg/mL. In contrast to the sigmoidal curve of glycated keratin, the dose-response of biofilm formation to un-glycated keratin was linear and variance between replicates was large. At the maximum tested dosage of 1.6 mg/mL of heated keratin, glycated keratin produced a 11.1-fold greater biofilm response in *S. aureus*.

4.6. Molecular Weight Fractions

In order to determine whether the molecular weight of glycated keratin had an impact on the biofilm response, intermediate (between 3 – 10 kDa), high (> 10 kDa), and mixed (> 3 kDa) molecular weight fractions were prepared by ultrafiltration. Biofilm assays were performed examining a range of concentrations of each molecular weight fraction of glycated keratin, the results of which are shown in **Figure 20**. Intermediate weight AGEs exhibited a significantly weaker biofilm response than the equivalent concentration of high molecular weight AGEs at the same dosage, plateauing at a dosage of roughly 0.25 mg/mL. The results at 0.25 are shown in greater detail in **Figure 21**. While heavier weight AGEs above 10 kDa promoted a significantly stronger biofilm response, the maximum amount of biofilm at the same dosage was produced by the combined fraction containing all AGEs above 3 kDa in weight.

4.7. Effect of *S. aureus* growth phase on Biofilm Formation

To better understand the context of AGE-induced biofilm formation, the effect of the timing of glycated keratin addition to *S. aureus* cultures during different growth phases was examined. The standard protocol used in previous experiments was to prepare growth media with added glycated keratin (typically 0.5 mg/mL), inoculate samples with *S. aureus*, and begin incubation. In these cases, bacteria passed through their logarithmic growth phase in the presence of glycated keratin, before reaching stationary phase after 12-24 hours of incubation.

For stationary phase addition of glycated keratin, initially 0.5 mg/mL of glycated keratin was directly added to 24-hour overnight cultures of *S. aureus* and transferred to static conditions for a further 48 hours. As a result, there was no significant increase in biofilm formation compared to control samples without glycated keratin (not shown). However, the glucose and other nutrient

content of the growth media was likely exhausted by the initial incubation, potentially leaving no suitable resources for *S. aureus* cells to produce biofilm under these conditions.

In order to remedy this problem, 24-hour culture *S. aureus* cells were resuspended in fresh TSB broth with added 0.5mg/mL glycated keratin and incubated for 48 hours under static conditions (see **Figure 22**). The resulting quantification of biofilm formation indicates that stationary phase cultures reached only 41% the amount of biofilm of those that passed through the logarithmic growth phase in AGE+ media, a significant reduction in biofilm abundance ($p < 0.001$).

4.8. Biofilm Response: Discussion

In response to cellular stress, many bacteria from biofilms to protect themselves from adverse environmental conditions or host immune response. *S. aureus* is known to modulate its biofilm production in response to conditions such as hyperoxia [99], anoxia and hypoxia [100,101], pH [102], high salt and suboptimal temperature [103], and sub-lethal concentrations of alcohol [104]. Based on the experimental observations, it is likely that glycative stress is also a factor in *S. aureus* biofilm formation and regulation.

In *S. aureus* there are several physiological processes that govern biofilm formation. As a natural process of their life-cycle, *S. aureus* may form biofilms from the presence of suitable binding substrates (e.g., fibronectin [105], collagen [106], and keratin [107] depending on strain) for cell-surface adhesins or high concentrations of neighboring cells. As can be seen by the comparative biofilm assays (**Figure 15**) there is a small baseline amount of biofilm formation under normal culture conditions, and non-glycated heated keratin did not significantly alter biofilm formation compared to controls. While it is possible that glycated keratin contains new binding substrates that are compatible for cell-surface binding, loss of viability observed in planktonic cells exposed to glycated keratin and the lack of aggregation in non-growth buffer as previously described suggests that cell-surface binding is unlikely to be the direct cause.

The failure of exogenous pentosidine and CML to trigger any of the effects observed with glycated keratin provide further evidence against a receptor hypothesis; if a cell-surface receptor relating to biofilm formation pathways is sensitive to binding by these AGEs (analogous to human RAGE), it should be expected that the free forms of AGEs unbound to keratin to trigger a similar effect. A database search for receptors with similar binding site structure to RAGE in

Staphylococcus and other bacteria failed to return any similar examples; a highly specific homologous or analogous receptor may not exist. In a study of glycative stress in *E. coli* [108], CML was observed to form within *E. coli* in high glucose cultures over time, and CML formation and mortality were both alleviated by treatment with aminoguanidine (a chemical which inhibits glycation [109]). CML does seem to be related to mortality in *E. coli*. In this case, CML and other AGEs may be forming intracellularly among bacterial proteins, and causing damage or stress internally.

I speculate that the causative mechanism relies on the metabolism of glycated keratin. As part of *S. aureus*'s peptide metabolism, glycated peptides may be taken up by oligopeptide transporters and metabolized intracellularly. Once inside the cell, AGEs would able to exert stress directly by disrupting protein function or interfering with other physiological processes. Those cells experiencing sub-lethal stress respond by upregulating biofilm formation. In the case of glycated keratin being added to stationary phase *S. aureus* cultures, the necessary materials for replication are readily available, but the culture has reached carrying capacity and growth has generally stabilized. Thus, there is significantly reduced protein demand, reduced AGE uptake, and reduced biofilm formation (as seen in **Figure 22**).

4.9. Fluorescent AGE Metabolism: Background

The metabolism of AGEs has been observed in *E. coli* [16,110]. Bacterial AGEs formed during normal metabolism are broken down from high molecular weight forms into low molecular weight forms and secreted from the cell. Exogenous AGEs can also be metabolized, such as carboxymethyl-lysine (CML) by *E. coli* [110] and dietary AGEs by gut bacteria [111]. As AGE metabolism was suspected, I attempted to observe a reduction in fluorescent AGEs in media cultured with *S. aureus*. While such a decrease could be observed (see **Figure 23**), the TSB media itself also fluoresced strongly over the same range as fluorescent AGEs, potentially confounding the results and obscuring a more detailed examination. In order to counter this, 24 overnight stock of *S. aureus* was prepared and resuspended it in non-growth media (0.1 M phosphate buffer) which would not interfere with photometric examination. Understanding that metabolic demand would be greatly reduced in this culture, the results were expected to be small in magnitude, but nevertheless conduced the photometric assay of media supernatant before and

after incubation, and filtered between low (< 3 kDa) and intermediate + heavy (> 3 kDa) molecular weight AGEs.

4.10. Fluorescent AGE Metabolism: Results

The results of the fluorescent AGE measurement following 24 hours of incubation with *S. aureus* are shown in **Figure 24**. High molecular weight fluorescent AGEs (> 3 kDa) were observed to significantly decrease after incubation with *S. aureus*, while low molecular weight AGEs significantly increased ($p < 0.001$). These results seem to agree with speculation regarding breakdown/metabolism of AGEs. The rate of metabolism, and the magnitude of the effects of the resulting glycative stress, are likely to be substantially enhanced in active growth cultures.

4.11. Fluorescent AGE Metabolism: Discussion

While these experiments were initially attempted under the optimal conditions for biofilm formation (inoculation into TSB containing glycated keratin), the media itself interfered with the fluorescence assay and it was not possible to distinguish between changes in AGEs and changes to other media contents. By using non-growth media, it was possible to clearly observe fluorescent AGEs. However, as previously shown in **Figure 8** and **Figure 10**, membrane damage and other glycative stress effects were greatly reduced under these conditions, as were the metabolic demands of *S. aureus*. While significant results were still observed, the absolute magnitude of the changes in fluorescent AGEs was relatively small. I suspect that under optimal conditions the metabolism of AGEs would be substantially higher, leading to a higher glycative stress load, thus provoking a stronger stress reaction in the form of greater biofilm formation.

A recent study on CML metabolism in *E. coli* [110] showed that CML dipeptides were preferentially metabolized by the bacterium before free CML. During the earlier studies with *S. epidermidis*, attempts were made to replicate the observed effects of glycated proteins using free CML and free pentosidine (see **Figure 4** and **Figure 5**) , two AGEs that form in the skin and are used as markers of skin glycation [112]. Despite testing dosages reaching orders of magnitude higher than the amount of pentosidine measured in the glucose-keratin glycation model (roughly 11 ng/mg of keratin), free pentosidine and free CML failed to exert any observed effect on *S. aureus* viability, in contrast to that observed with glycated keratin. The primary nutritional peptide transporter of *S. aureus*, Opp-3, has broad specificity and is capable of transporting

peptide chains 3 to 8 residues in length [113]. Using this transporter, *S. aureus* would be incapable of taking up free AGEs composed of a single amino acid residue, explaining the lack of effect of free AGEs if cellular uptake is necessary.

4.12. Biofilm Formation Mechanisms

There are several known pathways that contribute to biofilm formation in *S. aureus* based on the production and secretion of various components that make up the extracellular matrix of the biofilm itself. *S. aureus* biofilms may be primarily composed of a single component, or a combination of several or all of them. Biofilm phenotypes may differ due to the strain of *S. aureus* or the circumstances and environmental context under which it develops.

Polysaccharide Intercellular Adhesin (PIA or PNAG) is the primary polysaccharide produced by *Staphylococcus*, consisting of a polymer of ~20% deacetylated N-acetylglucosamine [114]. PIA production is regulated by the *icaADCB* gene cluster, which is found in both *S. aureus* [100] and *S. epidermidis* [115]. In addition to its role as a structural component of biofilms, PIA also provides protection against immune response [116]. While *ica* is regulated by the ArlRS two-component system in *S. epidermidis*, *ica*-related biofilm formation is independent of ArlRS in *S. aureus* [117]. In *S. aureus*, *ica* is controlled by *Staphylococcus* Accessory Regulator SarA, which is itself activated by Alternative Sigma Factor σ^B [118], which modulates the response to a variety of cellular stressors in various Gram-positive bacteria [119], including *S. aureus* [120,121]. However, the precise mechanism through which σ^B is activated by stress or a noxious environment is still poorly understood.

Biofilm extracellular matrix may also be composed of proteins, whether they are sourced from the host such as fibrin/fibrinogen, or secreted bacterial proteins. Biofilm associated protein (Bap) is a major component of protein-based biofilms in *S. aureus* and other bacteria [122], which can form independently of PIA biofilms in strains lacking *ica* [123]. However, it is primarily found in livestock strains of *S. aureus*, such as those that cause Staph infections in cows [124], and has not been observed in human clinical strains [125]. Bap is not present in the genome of the tested strain, *S. aureus* NBRC100910. Furthermore, as the *in vitro* models do not contain fibrin or fibrinogen, the AGE-mediated biofilms observed do not involve these proteins. Thus, it is likely that other biofilm components play a more prominent role in AGE-induced biofilm formation.

Extracellular DNA can also act as a trigger of *S. aureus* biofilms [126,127]. The eDNA released from damaged or auto-lysed cells becomes a major part of the biofilm itself, and upregulates biofilm formation in surviving cells. Membrane damage by AGEs could lead to an increase in mortality and biofilm formation due to the leakage of intracellular contents, such as eDNA. As mentioned previously in the discussion regarding cellular aggregation, ArlRS regulates some autolysis pathways in *S. aureus*, although this can differ by strain [128]. Two known proteins, CidA and LrgA, play a significant role in *S. aureus* cell death and autolysis. Both proteins share similarity with holins [129], bacteriophage proteins that produce pores in bacterial membranes [130]. CidA is a holin-like protein that promotes cell lysis and the release of DNA, contributing to biofilm development [131]. LrgA, on the other hand, is an anti-holin that inhibits cell lysis [132]. Expression of LrgA is regulated by the LytSR two-component system, and contributes to DNA-related biofilm formation [133].

The precise mechanism of AGE-mediated biofilm formation is still unclear, and there are many potential targets for further study. Examination of the expression of these various proteins and their genes will provide insight into the role AGEs in *S. aureus* biofilm formation and pathogenicity. Considering the current experimental data, it is clear that the release of DNA is involved in the response to glycated keratin exposure. Nevertheless, the involvement of other biofilm regulatory mechanisms, such as polysaccharide production, cannot be ruled out at this stage.

5. BIOFILM INHIBITION BY AGE BREAKING COMPOUNDS

5.1. Anti-Glycating and AGE Breaking Compounds

Due to the role of glycative stress in aging process and various related diseases, preventing and treating glycative stress are important factors for sustaining overall health and delaying the decline associated with old age. Preventative measures such as controlling blood sugar levels to dampen glucose spikes, avoiding ultraviolet damage to the skin, and reducing intake of things like cigarettes and alcohol that promote glycative stress is crucial to reduce the formation of AGEs in the first place. Anti-glycating compounds inhibit the glycation reaction from occurring, reducing the buildup of AGEs within body tissues. In the case of already formed AGEs, AGE breaking compounds react directly with AGE crosslinks or glycated protein aggregates to break them down and allow them to be excreted from the body.

Anti-glycating and AGE breaking compounds can be found in dietary supplements and cosmetic treatments that seek to prevent aging. Considering the role of AGEs in skin disorders associated with *S. aureus* skin dysbiosis and the experimental results of the link between glycated proteins and biofilm formation, it can be predicted that reducing glycative stress will likely be an important preventative measure to prevent infection in high-risk populations, such as those with diabetes or the elderly living in care facilities. In the case of active lesion formation and infection with *S. aureus*, topical treatment with AGE breakers may help to reduce glycative stress and ameliorate dysbiosis and the associated symptoms. However, the potential interactions of various AGE breakers with the *S. aureus* biofilm system are unknown. In these experiments, the ability of known AGE breaking compounds to inhibit the formation of AGE-mediated biofilms in *S. aureus* under static conditions was tested *in vitro* in order to evaluate their potential for use in topical applications on the skin. A summary of the effective dosages of the tested materials can be found in **Table 2**.

5.2. Aminoguanidine: Background

Aminoguanidine is known for its ability to inhibited the non-enzymatic reaction that leads to the formation of AGEs, and is commonly used as a reference for testing novel glycation inhibitors. It

does not have any AGE breaking ability against already formed AGEs. Nevertheless, it was tested for its activity in the AGE biofilm model.

5.3. Aminoguanidine: Results

As a preliminary test, aminoguanidine (AG) was tested at a typical dosage (0.1 mg/mL) against the equivalent concentration of glycated keratin (0.1 mg/mL). As predicted, aminoguanidine had no significant impact on biofilm formation after 48 hours (see **Figure 25**).

High glucose levels are well known to stimulate biofilm formation, so AG was also tested in high glucose (5.0 mg/mL) culture conditions. Again, there was no significant change in biofilm formation due to AG.

5.4. Aminoguanidine: Discussion

Aminoguanidine was tested early in the experimental process, before biofilm inhibition testing protocol was fully optimized and standardized, as it was for the other compounds tested. Due to the lack of preliminary results, and the fact that AG is not an AGE breaker, more detailed experiments, such as dosage effect, were not carried out.

While AG failed to inhibit biofilm formation, it has been reported in the literature that AG products against glycative stress exerted by high glucose levels in *E. coli* [108] and other microorganisms such as yeasts. Yeast grown with aminoguanidine at standard glucose concentrations have increased longevity compared to glucose alone, experienced a benefit of a similar magnitude as observed in calorie restricted cultures [134]. In order to replicate the same phenomenon in *S. aureus*, a range of aminoguanidine concentrations were tested in elevated glucose cultures. Surprisingly, viable cell counts were significantly decreased in a dose-dependent manner in high glucose samples (with some recovery at the highest AG dosage of 12.8 mg/mL), as shown in **Figure 26**. The effects of aminoguanidine require more examination and replication, however they are not strictly relevant to biofilm inhibition so further testing was postponed in favor of more relevant materials.

5.5. Ascorbic Acid: Background

Ascorbic acid, also known as Vitamin C, is an essential dietary nutrient that is necessary for a variety of physiological processes in the human body, including wound repair and collagen

production [135]. Ascorbic acid is also an antioxidant [136] with antibacterial activity [137], and the ability to disrupt exopolysaccharide biofilm formation in *E. coli* [138], *S. mutans* [139], *B. subtilis* [140], and *S. aureus* [141]. Ascorbic acid is a glycation inhibitor [142,143] via its antioxidant activity and ability to ionically bind to proteins, competitively inhibiting the binding of glucose.

5.6. Ascorbic Acid: Results

Ascorbic acid was tested for its antimicrobial and antibiofilm effects. Under planktonic conditions, total growth inhibition was observed at dosages of 1.5 mg/mL and higher (**Figure 27**). Under static conditions with AGE-mediated biofilm formation, *S. aureus* was able to survive and grow at all ascorbic acid concentrations, likely due to the biofilm's protection. Positive controls with only ascorbic acid and no AGEs show a moderate dose-dependent increase in biofilm formation (one to three times baseline), shown in **Figure 28**.

In AGE positive cultures, ascorbic acid significantly reduced biofilm formation at dosages above 2 mg/mL (**Figure 27**). A peak reduction in biofilm abundance of 40% was observed at 3 mg/mL, with the inhibitory effect weakening and stabilizing with further increases in ascorbic acid concentration.

5.7. Ascorbic Acid: Discussion

Ascorbic acid, or vitamin C, appeared to be a strong candidate for treating biofilms: it has been reported [141] that AA prevents biofilm formation in MRSA by impairing EPS production and downregulating *ica*, and consequently inhibiting PNAG production. In current testing, AA moderately inhibited biofilm formation at a dosage of 3 mg/mL, but failed to completely inhibit biofilm formation as was previously reported. However, at the tested dosages, ascorbic acid fully inhibited planktonic growth of *S. aureus*. Static cultures with AGE-mediated biofilm formation survived to produce significant biomass, suggesting that the antimicrobial effects of AA were protected against by the biofilm.

A similar result was reported by [144], who observed that the minimal inhibitory concentration of ascorbic acid prevented biofilm formation entirely, and sub growth-inhibitory concentrations significantly inhibited *ica*-dependent biofilm formation in a dose dependent manner in *S. aureus*. Again, the results showed that ascorbic acid concentrations above the planktonically inhibitory

concentration failed to prevent the formation of biofilms, and only moderately inhibited biofilm production.

This discrepancy suggests that AGE-induced biofilm formation may be *ica*-independent, which would explain the lack of efficacy. Strategies that are typically effective in the inhibition of primarily PIA biofilms may be less effective in the treatment of AGE-related skin infections involving SA.

5.8. Astaxanthin: Background

Astaxanthin is a carotenoid produced by the algae *Haematococcus pluvialis*, and found in high concentrations in animals that consume the algae, such as salmon, shrimp, and crabs. Astaxanthin is a strong anti-oxidant [145] and anti-inflammatory compound, and is commercialized as a dietary supplement for these properties. Astaxanthin has also been found to exert anti-glycation effects [146,147]. Previous work in the lab has examined the effects of dietary astaxanthin intake in both animal and human models; astaxanthin was found to ameliorate high fat diet induced gut dysbiosis in mice, and improved reported gastro-intestinal symptoms (e.g., constipation) in human participants [148].

5.9. Astaxanthin: Results

Astaxanthin exhibited weak antimicrobial/growth inhibitory effect on *S. aureus* planktonic cultures (see **Figure 29**). At a dosage of 0.06 mg/mL astaxanthin, growth was significantly enhanced by a small amount. At 0.6 mg/mL, astaxanthin was saturated in the growth media solution, and CFUs/mL did significantly decrease, but not substantially.

Under static conditions, astaxanthin alone reduced baseline biofilm formation at all tested dosages by roughly half (**Figure 30**). In the AGE positive samples, astaxanthin significantly reduced biofilm formation in a dose-dependent manner, achieving total inhibition beyond a concentration of roughly 0.4 mg/mL (**Figure 29**). Logarithmic curve-fitting was preformed, and indicated an Age-related IC50 of 0.06 mg/mL (**Figure 31**). The standard deviation of absorbance values was quite large for astaxanthin samples at low dosages due to large variance in biofilm loss and detachment between replicate samples.

5.10. Astaxanthin: Discussion

While biofilm formations itself was inhibited, astaxanthin also appeared to have been incorporated into the biofilm itself, changing the white colour of the unstained biofilm into a pale red. In addition to direct inhibition, the ability of the existing biofilm to adhere to the surface of the microwell plats appeared to be impaired. Remaining biofilms were easily detached by gentle washing with milliQ, while biofilms in the lowest dosage wells were strongly adhered and could not be removed even by vigorous shaking, as is typical of standard *S. aureus* biofilms. When high concentration astaxanthin planktonic samples were examined microscopically, aggregation of *S. aureus* around particles of astaxanthin was observed (**Figure 32**). This suggests that astaxanthin may be a competitive ligand for cell surface anchors, weakening surface attachment.

5.11. Clove Extract: Background

Cloves are produced from the dried flowers of the plant *Syzygium aromaticum*. Cloves are typically used as a culinary spice, but also have a centuries long history of use in traditional medicine for their anti-inflammatory properties. Modern research has demonstrated the powerful antioxidant [149] and anti-inflammation [150] activity of clove extracts. A significant active component of clove is eugenol [151], which has additionally demonstrated anti-carcinogenic/anti-tumor [152,153], and antimicrobial effects [154]. Recently, research in my lab has found that extract from clove powder has powerful age cross link breaking activity, which is mediated by the compound biflorin. Considering these properties, the combined effects of eugenol and biflorin make clove extract a strong candidate for use in the age-biofilm system for potential treatment of SA dysbiosis and associated skin lesions, although clove extract may also exert a cytotoxic on human skin cells effect at sufficient dosages [155].

5.12. Clove Extract: Results

Clove extract exerted a strong antimicrobial/bacteriostatic effect, with a significant loss of cell viability in a dose-dependent manner after 24 hours in planktonic conditions. A maximum 3.4 log reduction in CFUs was observed at the highest tested dosage of 1.5 mg/mL, with a roughly 1 log reduction at 0.05 mg/mL (Figure **33**).

For the biofilm assay, clove was incredibly effective. Biofilm formation was completely inhibited at all tested dosages, ranging from 0.05 mg/mL to 2 mg/mL. Macroscopic cellular

aggregates were visible in sample wells, and it appeared that *S. aureus* cells did not adhere to the surface of the plate wells when clove extract was present in solution at dosages above 1.25 mg/mL. Positive control test of clove extract did not significantly alter baseline biofilm production (**Figure 34**).

5.13. Melatonin: Background

Melatonin is an indoleamine hormone primarily known for regulating the circadian rhythm and sleep-wake cycles. In addition to this important physiological role, melatonin has also been discovered to have antioxidant and anti-inflammatory behavior [156]. Melatonin has been shown to protect against AGEs and promote wound healing in diabetic mice [157], as well as exhibiting glycation inhibiting [158] and AGE crosslink breaking activity [159]. Due to these properties, melatonin is a strong candidate for testing in the AGE biofilm model, and may additionally be useful in the treatment of diabetic and other skin lesions.

Some bacteria, such as gut microbe *E. aerogenes*, demonstrate circadian rhythms in behavior and gene expression that are regulated by host secretion of melatonin [160]. Stress induced reduction in host melatonin secretion can also lead to gut dysbiosis promoting intestinal dysfunction, which can me ameliorated by exogenous melatonin treatment [161,162]. In fact, some bacteria produce melatonin themselves [163].

Melatonin has shown efficacy in treating bacterial infections of *S. aureus* and *E. coli*, although via its anti-inflammatory effects [164] There are mixed reports regarding the antibacterial activity of melatonin. It was reported that it appears to inhibit the growth of some species, including *S. aureus* [165]. Conversely, melatonin has also been found to protect bacteria against antibiotics [166] and mycotoxins [167] whose mechanisms rely on exerting oxidative stress.

5.14. Melatonin: Results

In the viability assay under planktonic conditions, melatonin did not appear to exert any substantial growth inhibitory or antimicrobial effects. At a dosage of 1 mg/mL, melatonin samples demonstrated slightly increased CFUs compared to controls (**Figure 35**).

In the biofilm control tests, melatonin concentration was positively correlated with a slight increase in biofilm abundance (**Figure 36**). With the addition of AGEs, melatonin failed to significantly reduce biofilm formation at most concentrations (**Figure 35**). While 14% inhibition

of biofilm was observed at a dosage of 0.5 mg/ml, further increase in melatonin concentration led to an increase in biofilm abundance at 1.0 mg/mL and 1.5 mg/mL compared to baseline.

5.15. Melatonin: Discussion

While reports indicate that the MIC of melatonin was 250 µg/mL for *S. aureus* ATCC 29123 [165], no such effect was observed at substantially greater dosages in the *S. aureus* strain used in this experiment. Conversely, melatonin at a concentration of 1 mg/mL slightly enhanced *S. aureus* growth after 24 hours under planktonic conditions in current testing. The authors of the study speculate that the antibacterial effect of melatonin is a result of its metal chelating properties, absorbing free iron that is necessary for bacteria to survive and function. If their results are correct, then perhaps differences in the levels of iron in the growth media used may account for the difference; this experiment used a different growth medium, however both varieties of media used are complex media with unknown iron content. If their proposed mechanism for the antibacterial effect of melatonin is correct, then strain differences are unlikely to account for the difference in susceptibility to such a vital mineral.

Testing occurred at significantly greater concentrations than those found under physiological conditions. Secretion of melatonin by the pineal gland fluctuates throughout the day, rising in the evening and peaking during the middle of the night, before falling to daytime levels by morning. Daytime serum concentrations of melatonin are reported at roughly 2-4 pg/mL [168,169]. Aging is correlated with a decrease in melatonin production: peak serum melatonin can reach as high as 100 pg/mL in the young, while falling to around 40 pg/mL in the elderly [170].

Melatonin is also produced endogenously in the skin, where it preserves the integrity of the skin, has antioxidant activity, and protects against UV damage [171]. Melatonin concentrations in the skin can be several times higher than serum levels, ranging from 0.1-4 ng/mg depending on various population factors [172].

Melatonin is reported to enhance diabetic wound healing and protect against glycative stress at concentrations significantly higher than typical physiological levels (1 mM [173] and 10-200 uM [157]). While melatonin may be an effective treatment for skin lesions in diabetes which are often colonized by *S. aureus*, this benefit is primarily from the protective effects of melatonin on keratinocyte and skin physiology. Considering the results of the tests, melatonin is unlikely to

have a significant effect directly on *S. aureus* dysbiosis via anti-microbial or anti-biofilm activity, but will likely enhance healing by the previously mentioned mechanisms.

5.16. N-Phenacylthiazolium Bromide: Background

PTB is a compound known for cleaving the AGE crosslinks that form between proteins such as collagen: these crosslinks are responsible for the increased stiffness and loss of elasticity observed in aged skin. The crosslink breaking abilities of PTB have been demonstrated in both *in vitro* and *in vivo* studies [174]. PTB has shown effectiveness in breaking down AGEs and preventing their accumulation in vascular tissues [175], lens proteins [176], periodontic tissue [177] and bone [178]. Any antibacterial or antibiofilm properties of PTB have not been reported at this time.

5.17. N-Phenacylthiazolium Bromide: Results

In testing the effects of PTB without glycated keratin, PTB provoked significant biofilm formation by itself (see **Figure 37**). With the addition of even a small amount of glycated keratin (e.g., 0.1—0.35 mg/mL), biofilm formation was greatly increased compared to controls.

Only at a high dosage of 20 mmol/L and above did PTB begin to inhibit biofilm formation. (**Figure 38**). This coincided with a substantial loss of cell viability, suggesting that antimicrobial effects of PTB are responsible for the lack of observed biofilm at high dosages. As the biofilm response was strongly enhanced at sub-lethal dosages, PTB may not be suitable for topical use on the skin under all circumstances.

5.18. Rosemary Extract: Background

Salvia Rosmarinus, known commonly as rosemary is a plant that grows in the Mediterranean. The leaves of the plant have long been used as a culinary spice and in traditional medicines. Rosemary extract exhibits strong antioxidant and antibacterial effects [179], and is also known for its glycation inhibiting [180] and AGE cross-link breaking abilities [181] via its active ingredient rosmarinic acid. For this experiment, rosemary extract was utilized in the form of a dietary supplement named AGE Breaker (A2P Sciences, France), marketed as an anti-aging supplement.

5.19. Rosemary Extract: Results

Rosemary exhibited a dose-dependent antimicrobial effect against *S. aureus* under planktonic conditions (**Figure 39**). Control samples of rosemary extract under biofilm conditions indicated a

mild increase in biofilm formation at elevated dosages (**Figure 40**). Under AGE-mediated biofilm conditions, rosemary extract significantly inhibited biofilm formation in a dose dependent manner, achieving total inhibition at a concentration of 2 mg/mL and greater (**Figure 39**). The dose-response relationship of extract concentration and biofilm abundance formed a sigmoidal relationship, and logarithmic curve fitting was performed (**Figure 41**). The IC50 was determined to be roughly 0.5 mg/mL, following. The biofilm inhibitory effect was present even at sub-lethal concentrations of the extract.

6. THE POTENTIAL ROLES OF GLYCATIVE STRESS AND *S. AUREUS* IN COVID19

6.1. COVID19 and Diabetes Mellitus

Starting in early 2020, the SARS-CoV-2 pandemic began to spread across the world, which has impacted countless people. As data about COVID19 (the respiratory infection caused by the SARS-CoV-2 virus) began to be reported, increased susceptibility to infection and severity of symptoms appeared to be elevated among those with diabetes mellitus [182–185]. Pneumonia is a relatively common cause of death among diabetics, who are 1.8 times more likely to develop pneumonia than the general population [186].

In a whole population study conducted in England [187], it was found that death rate of those with COVID19 was significantly elevated in all age groups, with a 3.51 odds ratio for death by SARS-CoV-2 association pneumonia in Type 1 diabetes, and 2.03 in Type 2 diabetes. Additionally, the death rate was highly correlated with blood glucose levels, indicating that those with poor glucose control were ae higher risk of death [188].

An additional reported risk during COVID19 is co-infection: secondary infections, often by bacteria or fungi, leading to the development of pneumonia alongside SARS-CoV-2 viral infection. Co-infection has a significant impact on the outcome of COVID19: patients with co-infection are twice as common in intensive care units than they are under standard care [189]. Case reports indicate that in some hospitals, the incidence of co-infection is as high as 50% among fatal cases [190]. The most common bacterial pathogen reported was *Mycoplasma pneumoniae*, however *S. aureus* has also been reported in fatal cases of bacterial pneumonia coincident with COVID19 [39].

Considering these reports, a literature review was conducted to elucidate the relationship between glycative stress and COVID19 infection, as well as what role *S. aureus* may play in susceptibility to SARS-CoV-2.

6.2. Glycative Stress and Immune Functioning

Glycative stress directly impairs immune response in various ways, including by directly disrupting the functioning of immune cells (summary in **Figure 42**). Diabetes and the resulting glycative stress cause mitochondrial dysfunction [191], which leads to impaired energy production and an increase in fumaric acid, which reacts with proteins to create succinylated proteins [192], disrupting their proper functioning. Endoplasmic reticulum stress also occurs in response to glycative stress, as AGEs are up-taken by immune cells through cell surface scavenger receptors [193,194]. The burden of processing all the scavenged matter leads to a decline in cell functioning and apoptosis [195]. Downstream of these effects, a variety of vital immune cell functions are diminished in those experiencing high levels of glycative stress, increasing vulnerability to infection.

Phagocytosis is a process through which pathogens are engulfed and degraded by neutrophils and macrophages. AGEs suppress macrophage phagocytosis, significantly decreasing phagocytic activity in individuals with Diabetes [196]. Phagocytosis of AGEs can also cause apoptosis, further reducing the number of viable macrophages in addition to reducing their effectiveness (**Gao 2017**).

The ability of cells to move in a specific direction in response to signals from chemical gradients is known as chemotaxis. In the early phase of infection or inflammatory response, neutrophils move towards the appropriate location vie chemotaxis. Neutrophils that are exposed to diabetic donor serum are less able to migrate in response to chemical signals [197]. Additionally, activation of the receptor for AGEs (RAGE) increases the binding of neutrophils to collagen [198], impairing their ability to move through the extracellular matrix. This impairment of chemotaxis slows the response of immune cells.

Additionally, the production of antibodies in response to infection is reduced by glycative stress [199], weakening the ability to target pathogens. At the same time, cytokine production is stimulated by activation of RAGE [200], increasing inflammation, and potentially contributing to the potentially lethal cytokine storm that has been observed during SARS-CoV-2 infection [201].

6.3. Mechanisms of SARS-CoV-2 Infection

The primary transmission routes of SARS-CoV-2 are droplet infection and contact infection. In droplet infection, small droplets of fluid containing viral particles are expelled from an infected person by coughing or sneezing. Drops suspended in the air may be directly inhaled into the bronchial mucosa of the lungs, or encounter the mucosal membranes of the mouth, nose, or eyes. In contact infection, surfaces exposed to viral particles are physically touched, transferring the virus to the skin or hands of a person. If that person then touches a vulnerable are of the body, such as the mucous membranes of the mouth, nose, or eyes, the virus can enter the body and potentially cause infection.

Once SARS-CoV-2 has entered a new host, the virion targets the receptor Angiotensin-Converting Enzyme 2 (ACE2) found on the surface of cells susceptible to infection. ACE2 is expressed by a wide variety of human tissues, including the small intestine, heart, and lungs [202]. The viral spike protein found on the surface of the viral capsule is composed of two subunits, S1 and S2, that are connected by an exposed protein chain designated site S1/S2. The S1 subunit bind to the ACE2 receptor, before site S1/S2 is cleaved by a host protease such as serine proteases TMPRSS2 or furin [203]. Once the spike protein is cleaved the virus fuses with the target cell's cellular membrane [204], releasing its RNA and initiating replication.

In contrast previous coronaviruses such as SARS-CoV-1, SARS-CoV-2 possess a novel 4 amino acid insert at the S1/S2 site that allows it to be cleaved by a broader range of proteases such as proprotein convertase 1, tryptase, TTSP matriptase, and cathepsins B and L [205]. This trait may in part explain the increased infectiousness and pathogenicity of SARS-CoV-2.

6.4. *S. aureus* and Increased Vulnerability to Infection

As previously noted, *S. aureus* carriage is increase on the skin of people with diabetes or skin disorders associated with high glycative stress. *S. aureus* is also present in high abundance in the nasal cavity. Considering the capabilities of *S. aureus* and SARS-CoV-2, the literature was reviewed for potential mechanisms that could contribute to increased susceptibility to COVID19 (summarized in **Figure 43**).

The presence of *S. aureus* and its metabolites triggers increased protease activity in human keratinocytes. *In vitro* human keratinocyte and *in vivo* murine models have demonstrated

increased expression of trypsin and KLK family proteases in the skin after exposure to *S. aureus* [206]. When colonizing the skin, *S. aureus* strongly upregulates protease expression [207]. Additionally strains of *S. aureus* collected from atopic dermatitis skin lesions demonstrate increased proteolytic activity compared to reference strains [208]. The increased proteolytic activity of tissues colonized by *S. aureus* may increase viral fusion and infection rate.

S. aureus employs a wide variety of proteases for the purposes of nutrient metabolism and protection against host immune defenses during infection [209]. Major proteases include: six serine protease-like proteins (SplA – SplF), two cysteine proteases (staphopain A and B), a serine protease (V8), and a metalloprotease (auerolysin). While the ability of bacterial proteases to cleave SARS-CoV-2 spike protein site S1/S2 has not yet been tested, the wide variety and general specificity of many *S. aureus* proteases makes the possibility highly likely. *S. aureus* also secreted protease inhibitors that inhibit proteases from host neutrophils while allowing other serine proteases to remain functional [210], further impeding the immune system from clearing invading pathogens.

The carriage of *S. aureus* may also contribute to the risk of complications during viral infection. In the case of the Influenza A virus, *S. aureus* protein lipase 1 has been reported to increase replication of the virus [38]. In the other direction, Influenza can trigger virulence in otherwise commensal *S. aureus* in the nasal cavity [37], which can lead to pulmonary infection and bacterial pneumonia. Elevated body temperature, such as from a fever, promotes the dissolution of *S. aureus* biofilms; the dispersal of nasal biofilms could lead to high concentrations of *S. aureus* cells being aspirated into the lungs and causing a secondary infection.

6.5. Possibility of SARS-CoV-2 Skin Infection

While SARS-CoV-2 is primarily transmitted through mucous membranes, infection through the skin is also theoretically possible. ACE2, while highly expressed in nasal [211] and oral mucosa [202], it also expressed in keratinocytes at a similar level to that observed in lung tissues [212]. Skin rashes during early SARS-CoV-2 infection have been reported. In a survey of patients with COVD19, 17% reported experiencing a rash as their first symptom [213]. Case studies have also noted skin lesions in some patients [214–216] including the formation of vesicular rashes, which are typically a sign of viral replication in the skin in other diseases such as poxviruses.

While healthy skin is unlikely to be infected by exposure to SARS-CoV-2, damaged skin may provide a pathway for infection. DNA/RNases are produced by the skin to defend against pathogens [217]. The presence of biofilm prevents these enzymes and other antimicrobial peptides from clearing pathogenic *S. aureus*; SARS-CoV-2 coming in to contact with biofilm-colonized skin may prolong its survival, increasing the risk of contact transmission or infection through broken or lesional skin. Further, the release of bacterial protease by *S. aureus* present on the skin not only could assist activation of the SARS-CoV-2 spike protein, but also break down skin proteins, weakening barrier function and promoting the formation of skin lesions.

Viral particles that encounter lesions may be able to enter the body and cause infection. Hospitals have also reported concerns regarding increased of infection in dermatological patients [218,219], and note the increased incidence of dermatitis of the hands due to increases in hand-washing during the pandemic. Despite this, sanitation of the hands is of vital importance, as according to recent research SARS-CoV-2 can survive on human skin for up to 9 hours [220], significantly longer than other viruses like influenza.

6.6. Stable Sodium Hypochlorite

Despite the necessity of hand sanitation during the ongoing pandemic, frequent hand washing with soaps and other detergents damages proteins of the stratum corneum, removes beneficial lipids, and may trigger contact dermatitis [221]. While alcohol-based hand sanitizers are significantly less irritating than washing with soap [222,223], they can still cause dryness. Alcohols such as isopropanol and n-propanol may also perturb keratinocyte functioning and cause significantly more irritation than ethanol [224]. During the initial months of the pandemic, the supply of alcohol-based sanitizers was insufficient and they were frequently out of stock.

Due to these issues, alternative forms of hand sanitation are necessary. Here, a sanitizing solution (AirRish) containing a stable form of sodium hypochlorite (NaClO) was tested for potential use as a hand sanitizer. This included skin safety testing, and an evaluation for its bactericidal efficacy against *S. aureus*.

6.7. Stable Sodium Hypochlorite: Skin Safety Testing

Skin safety testing of 200 ppm stable NaClO solution was conducted with 20 participants between the ages of 20 and 60 (4 makes, 16 females, mean age 39.5 ± 10.7 years). A patch test

was performed over 24 hours using Finn chambers on Scanpor tape (SmartPractice Japan Corporation, Yamato City, Kanagawa Prefecture, Japan). Sample materials, consisting of stable sodium hypochlorite and negative control materials (saline, water, and Vaseline), were applied to filter papers in at a volume of 15 µL. Test units were applied to the backs of participants and left for 24 hours before removal. Skin condition was evaluated at 2 and 24 hours, according to the patch test standardized criteria [225] shown in **Table 3**: evaluations were scored according to the cosmetic skin irritation index, seen in **Table 4**. Skin irritation index was calculated according to the method of Sugai et al. [226]**,** using the following formula:

Skin irritation index = (Overall score of the one with the strongest reaction after 24 or 48 hours / the Number of subjects) ×100

The final skin irritation index score was 0.0 (results summarized in **Table 5**). There were no adverse events or irritation recorded in any of the subjects. As a result, 200 ppm stable sodium hypochlorite was classified as a safe product, and the results published [227].

6.8. Stable Sodium Hypochlorite: *S. aureus* Bactericidal Efficacy

The antibacterial and antiviral efficacy of stable NaClO has been demonstrated at concentrations of 1,000 to 2,000 ppm, where it sees use in surface sterilization. However, the efficacy of the 100 and 200 ppm formulations that are being tested for use as hand sanitizers requires confirmation. As my current lab does not possess the biosafety facilities to enable safe handling of and experimentation on viruses, the antibacterial efficacy of the sanitizing solution was tested against the bacterium *S. aureus*.

Overnight stock of *S. aureus* was prepared in TSB growth media and incubated for 24 hours before testing. 100µL aliquots of *S. aureus* culture was inoculated into 9.9 mL test solutions of 100 ppm and 200 ppm stable NaClO, 70% ethanol, and 0.1M phosphate buffer (pH 7.4) as a control. Solutions were vortexed and incubated for 5 minutes at room temperature, then neutralized by 0.1M phosphate buffer before serial dilution. Viability of *S. aureus* was determined by CFU counting after inoculation and incubation of TSA solid media plates.

All tested sanitizers showed excellent bactericidal efficacy against *S. aureus* (**Figure 44**). No colonies were detected in either 100 ppm or 200 ppm NaClO solutions, with a minimum detection limit of 10 CFU/mL. Stable NaClO was just as effective as 70% ethanol, which also

showed no signs of colony growth. Sanitizing solution samples showed at least a 6.6 log reduction in viable colony counts compared to the 0.1M phosphate buffer control.

7. CONCLUSION

The aging microbiome of the skin is characterized by increased abundance of *S. aureus*, and a loss of *S. epidermidis*. *In vitro* under planktonic conditions, the addition of exogenous AGEs produced from glucose and keratin exert an antibacterial effect against both *S. epidermidis* and *S. aureus*, causing membrane damage and provoking cellular aggregation. At the same time, S. aureus appears to be able to metabolize high molecular weight AGEs, which may play a part in the mechanism of glycated keratin's effects. This requires further study.

Under static conditions, glycated keratin induces biofilm formation, which protects the resident bacteria from noxious stimuli and enhances defenses against host immune response, increasing *S. aureus*'s pathogenicity. The presence of elevated concentrations of AGEs in the skin may promote the formation of *S. aureus* biofilms on the skin, exacerbating existing skin conditions and damaging the skin's barrier function, increasing the risk of serious infection in those with elevated glycative stress. Avenues of research regarding the gene and protein expression of the pathways that regulate *S. aureus* biofilms will provide insight into the causative mechanisms of AGE-mediated biofilm formation.

Treatments to reduce the buildup of AGEs in the skin may help to reduce the severity of skin lesions, recurring staph infections, and other risks of *S. aureus* carriage in those experiencing elevated glycative stress. Astaxanthin, clove extract, and rosemary extract distinguished themselves as candidates for topical use in treatment of *S. aureus* dysbiosis, demonstrating strong biofilm inhibitory effects in addition to their known activity as AGE breakers. Such preventative measures may also help to reduce AGE accumulation and prevent recurring infections, avoiding the overuse of antibiotics and the development of further antibiotic strains of *S. aureus* and other bacteria. Preventing *S. aureus* dysbiosis is vital to avoiding the most common cause of skin infections in humans. Maintaining a healthy and balanced microbiome may also reduce the risk of complications during viral infections such as Influenza and COVID19 in vulnerable populations.

FIGURES AND TABLES

Table 1. Skin Sampling Data

	Young Cohort (20-30 years)	Elderly Cohort (65+ years)	p value
Age (years)	23.5 ± 2.1	79.0 ± 5.7	2.02E-26 ***
Skin Autofluorescence (units)	1.6 ± 0.2	2.8 ± 0.5	3.24E-09 ***
Abundance (CFU/Sample)			
Coagulase-Negative *Staphylococcus*	50.8 ± 73.0	61.4 ± 94.6	7.35E-01
S. aureus	5.5 ± 6.6	55.9 ± 71.6	1.70E-02 *
Total Colony Forming Units	56.3 ± 77.3	117.3 ± 132.2	1.40E-01
***S. aureus* Proportion (%)**	12.0 ± 14.9	50.0 ± 36.8	1.30E-03 **
Detection Rate (%)			
Coagulase-Negative *Staphylococcus*	100	81	4.97E-02 *
S. aureus	69	81	4.49E-01

Coagulase-negative *Staphylococcus* was differentiated from *S. aureus* by colour after growth on Mannitol Salt Agar selective media. The young cohort consisted of 13 volunteers, and the elderly 21Mean ± standard deviation. Statistical difference calculated by Student's t-test. *$p < 0.05$, **$p < 0.01$, *** $p < 0.001$.

Table 2. Biofilm Inhibition Summary

Material	*ED50 (mg/mL)*
Aminoguanidine	n/a
Ascorbic Acid	n/a
Astaxanthin	0.06 mg/mL
Clove Extract	< 0.05 mg/mL
Melatonin	n/a
N-Phenacylthiazolium Bromide	18.7 mmol/L
Rosemary Extract (AGE Breaker)	0.5 mg/mL

Sample concentrations indicates as “n/a” failed to reach 50% biofilm inhibition under the tested range of dosages.

Table 3. Patch test criteria.

Japanese standard	Score	Reaction
—	0.0	No reaction
±	0. 5	Slight erythema
+	1.0	Apparent erythema
+ +	2. 0	Erythema + edema, papules
+ + +	3.0	Erythema + edema + papules + vesicles
+ + + +	4. 0	Large blisters

Table 4. Classification of Cosmetics by Skin Irritation Index

Skin irritation index	1995 Classification
5. 0 or lower	Safe products
5. 0 ~ 15. 0	Acceptable products
15. 0 ~ 30. 0	Product requiring improvement
30.0 or higher	Hazardous products

Skin irritation index = (Overall score of the subject with the strongest reaction after 24 or 48 hours / Number of subjects) ×100

Table 5. Patch Test Data Profile

Sample name	Test sample			Negative control 1			Negative control 2			Negative control 3		
	s-SH 200 ppm			Saline			Water for injection			Vaseline		
Results	Classification		Index*	Classification		Index*	Classification		Index*	Classification		Index*
	Safe products		**0.0**	—		0.0	—		0.0	—		0.0
ID	2 hours	24 hours	Score	2 hours	24 hours	Score	2 hours	24 hours	Score	2 hours	24 hours	Score
1	—	—	0.0	—	—	0.0	—	—	0.0	—	—	0.0
2	—	—	0.0	—	—	0.0	—	—	0.0	—	—	0.0
3	—	—	0.0	—	—	0.0	—	—	0.0	—	—	0.0
4	—	—	0.0	—	—	0.0	—	—	0.0	—	—	0.0
5	—	—	0.0	—	—	0.0	—	—	0.0	—	—	0.0
7	—	—	0.0	—	—	0.0	—	—	0.0	—	—	0.0
8	—	—	0.0	—	—	0.0	—	—	0.0	—	—	0.0
9	—	—	0.0	—	—	0.0	—	—	0.0	—	—	0.0
10	—	—	0.0	—	—	0.0	—	—	0.0	—	—	0.0
11	—	—	0.0	—	—	0.0	—	—	0.0	—	—	0.0
13	—	—	0.0	—	—	0.0	—	—	0.0	—	—	0.0
14	—	—	0.0	—	—	0.0	—	—	0.0	—	—	0.0
15	—	—	0.0	—	—	0.0	—	—	0.0	—	—	0.0
16	—	—	0.0	—	—	0.0	—	—	0.0	—	—	0.0
17	—	—	0.0	—	—	0.0	—	—	0.0	—	—	0.0
18	—	—	0.0	—	—	0.0	—	—	0.0	—	—	0.0
19	—	—	0.0	—	—	0.0	—	—	0.0	—	—	0.0
20	—	—	0.0	—	—	0.0	—	—	0.0	—	—	0.0
21	—	—	0.0	—	—	0.0	—	—	0.0	—	—	0.0
45	—	—	0.0	—	—	0.0	—	—	0.0	—	—	0.0

Figure 1. Effect of Glycated Keratin on Viability of *S. epidermidis* at 24 Hours

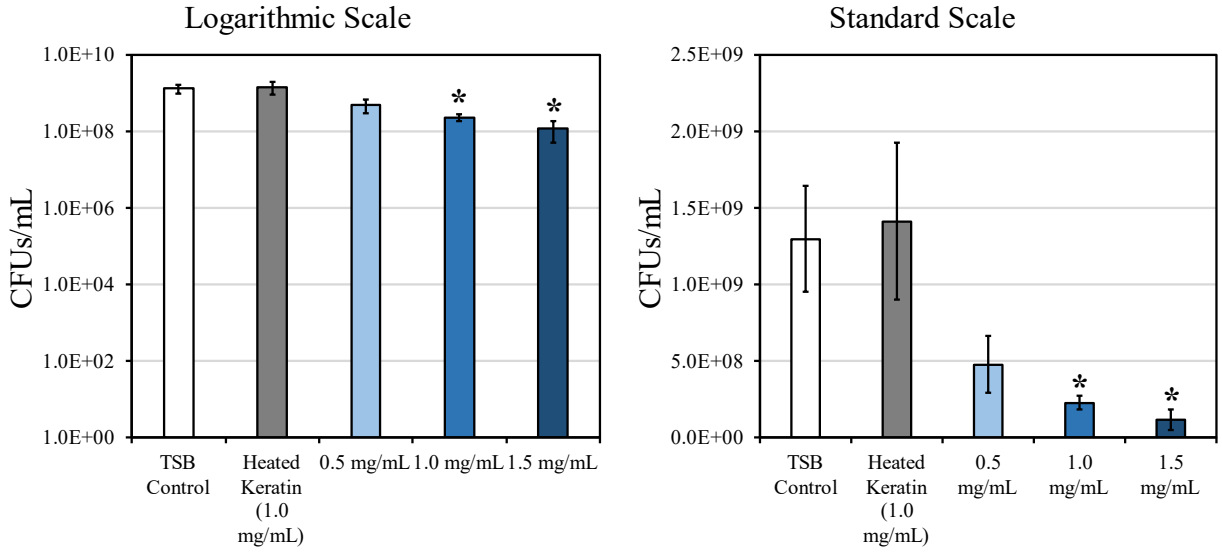

S. epidermidis viable cell count after 24 hours of incubation with increasing glycated keratin concentration. Results represented in logarithmic (left) and standard scale (right). n = 3. Mean ± standard deviation. Statistical difference calculated by Student's t-test versus Control. *$p < 0.05$.

Figure 2. Effect of Glycated Keratin on Viability of *S. epidermidis* at 72 Hours

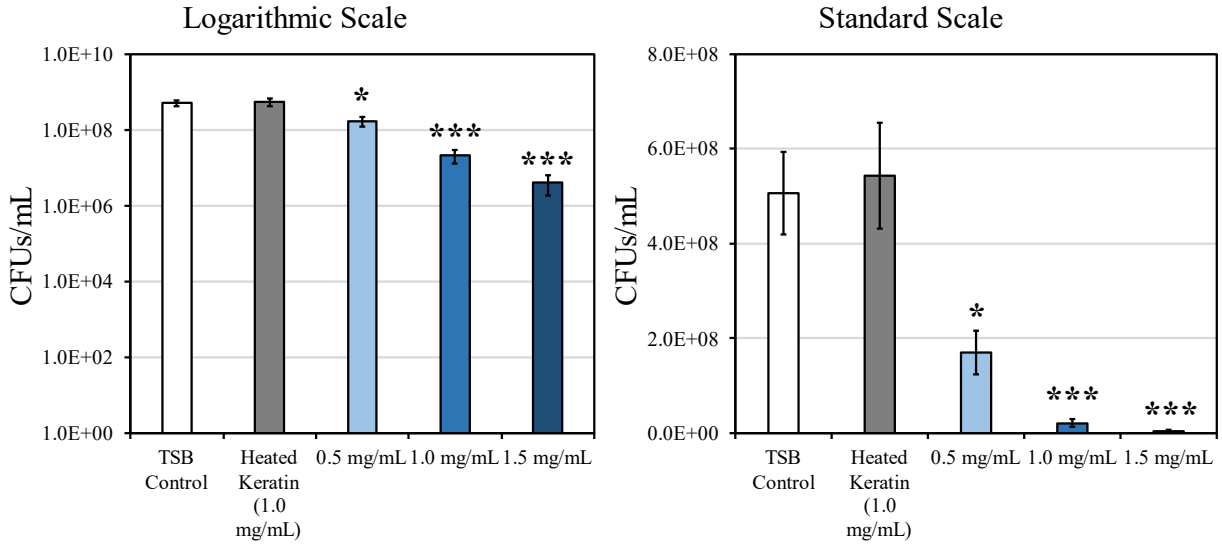

S. epidermidis viable cell count after72 hours of incubation with increasing glycated keratin concentration. Results represented in logarithmic (left) and standard scale (right). n = 3. Mean ± standard deviation. Statistical difference calculated by Student's t-test versus Control. *$p < 0.05$, *** $p < 0.001$.

Figure 3. Glycation Model HPLC Chromatograph

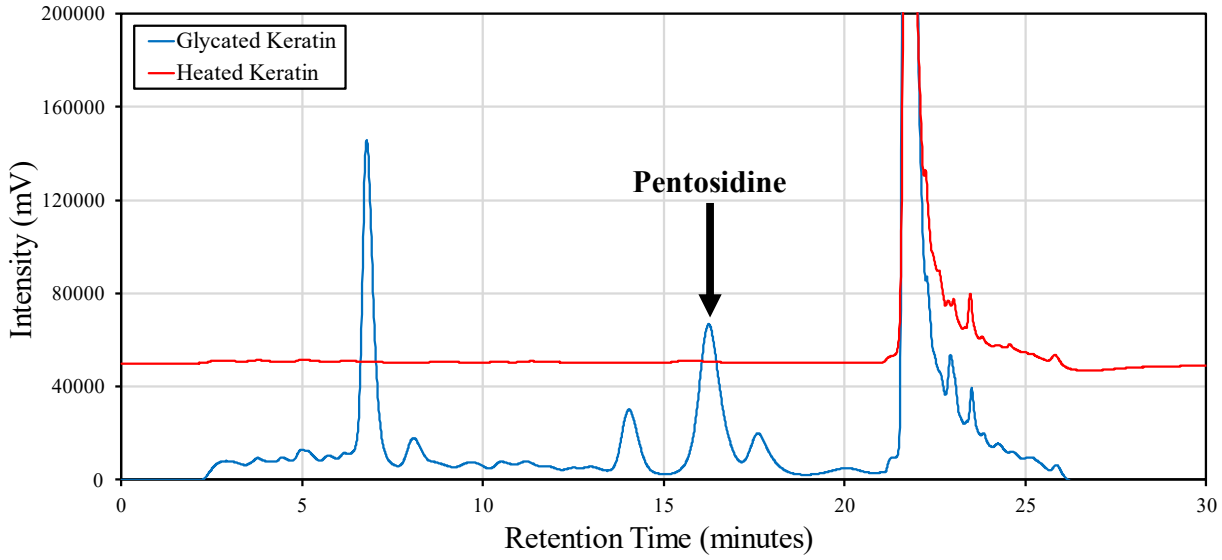

High-Performance Liquid Chromatography Spectrum of Glycated and Un-Glycated Keratin. Peak indicated by arrow represents pentosidine. Other peaks show the presence of unknown glucose-keratin adjuncts. Values of Heated Keratin Intensity are shifted upwards by 50 000 units for better visibility.

Figure 4. Effect of Free Pentosidine on Viability of *S. epidermidis*

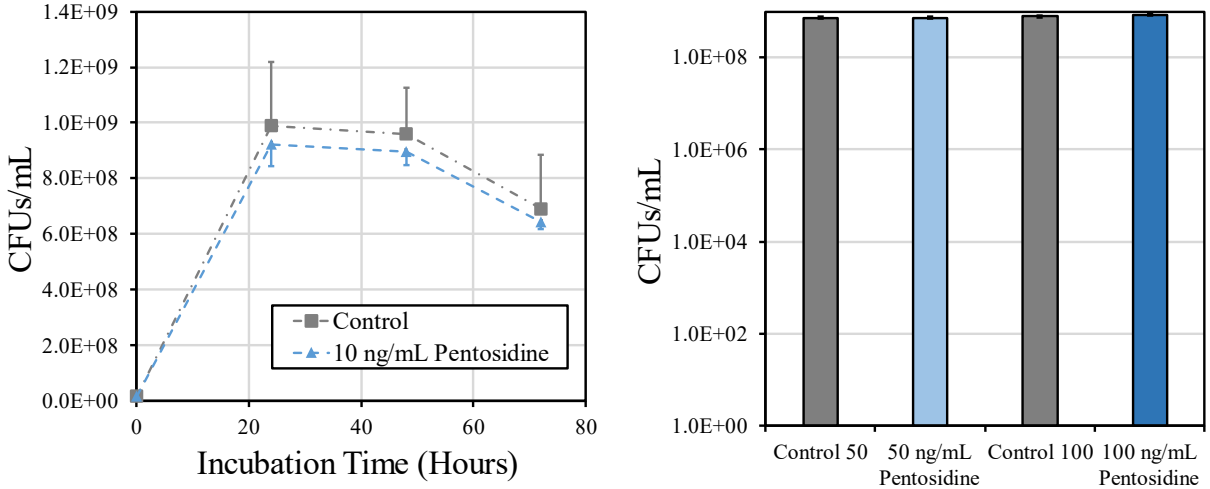

Effect of 10 ng/mL of free pentosidine on *S. epidermidis* viable cell count over time (left). 24-hour cell viability of *S. epidermidis* incubated with 50 and 100 ng/mL of pentosidine compared to control cultures. Logarithmic scale. n = 3. Mean ± standard deviation. Statistical difference calculated by Student's t-test versus Control. Not significant.

Figure 5. Effect of Free CML on Viability of *S. epidermidis*

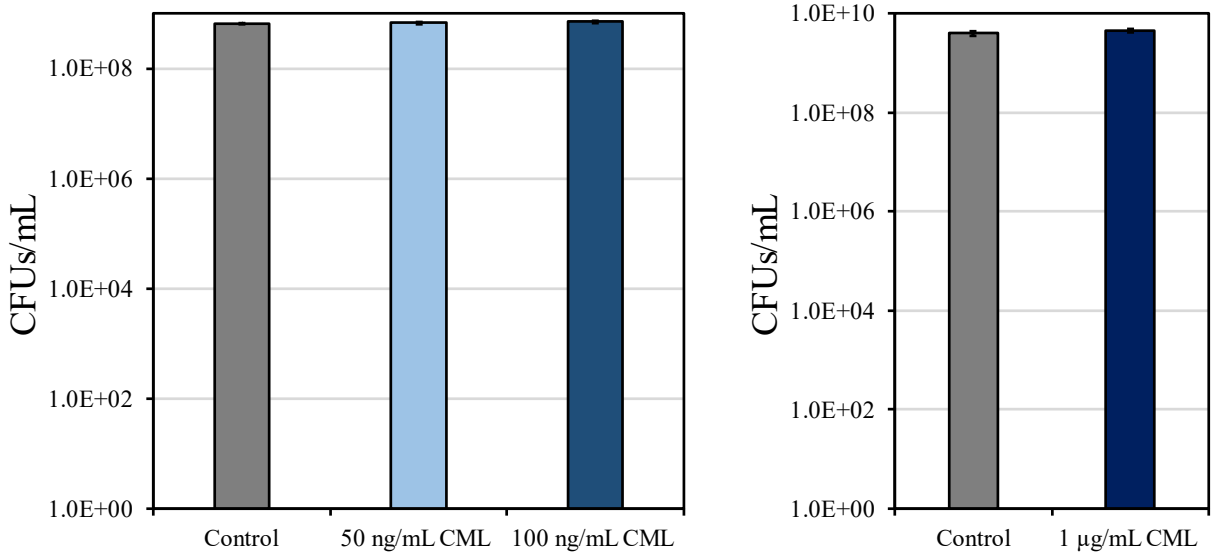

Effect of 50 and 100 ng/mL of free carboxymethyl lysine (CML) on *S. epidermidis* viable cell count at 24 hours post incubation (left). Effect of 1 µg/mL free CML on 24-hour cell viability of *S. epidermidis*(right). Logarithmic scale. n = 3. Mean ± standard deviation. Statistical difference calculated by Student's t-test versus Control. Not significant.

Figure 6. Growth Curve Comparison of *S. epidermidis* and *S. aureus* with Glycated Keratin

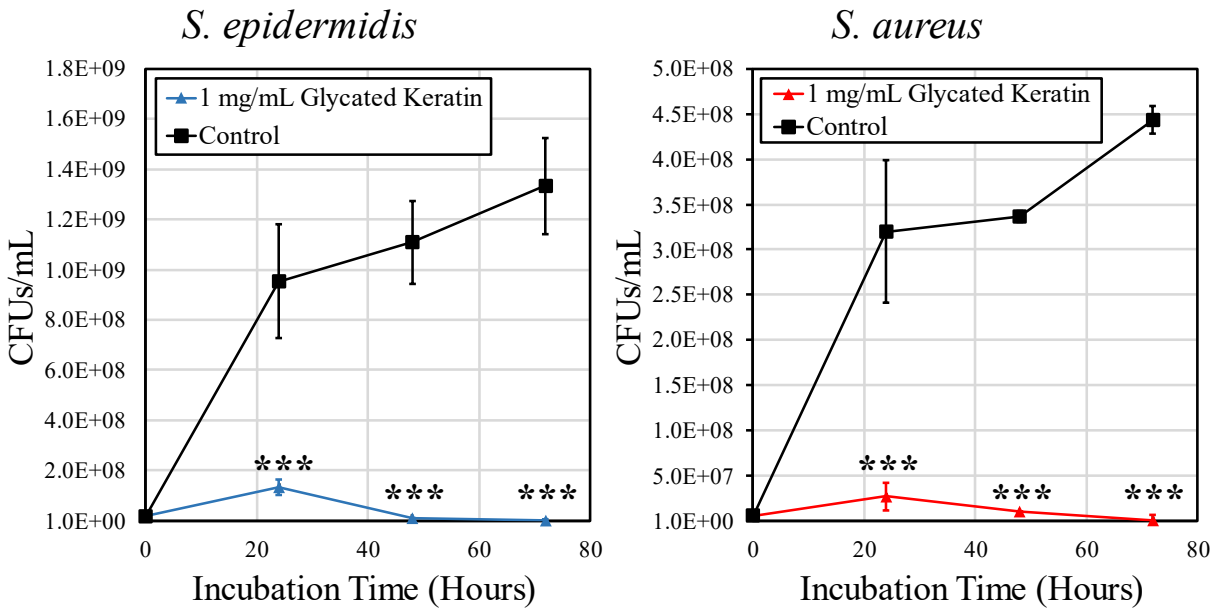

Viable cell counts of *S. epidermidis* (left) and *S. aureus* (right) over a period of 72 hours in growth media containing 1.0 mg/mL glycated keratin. Standard Scale. n = 3. Mean ± standard deviation. Statistical difference calculated by Student's t-test versus Control. *** $p < 0.001$.

Figure 7. Growth Inhibitory Effect of Glycated Keratin: Close-Up at 24 Hours

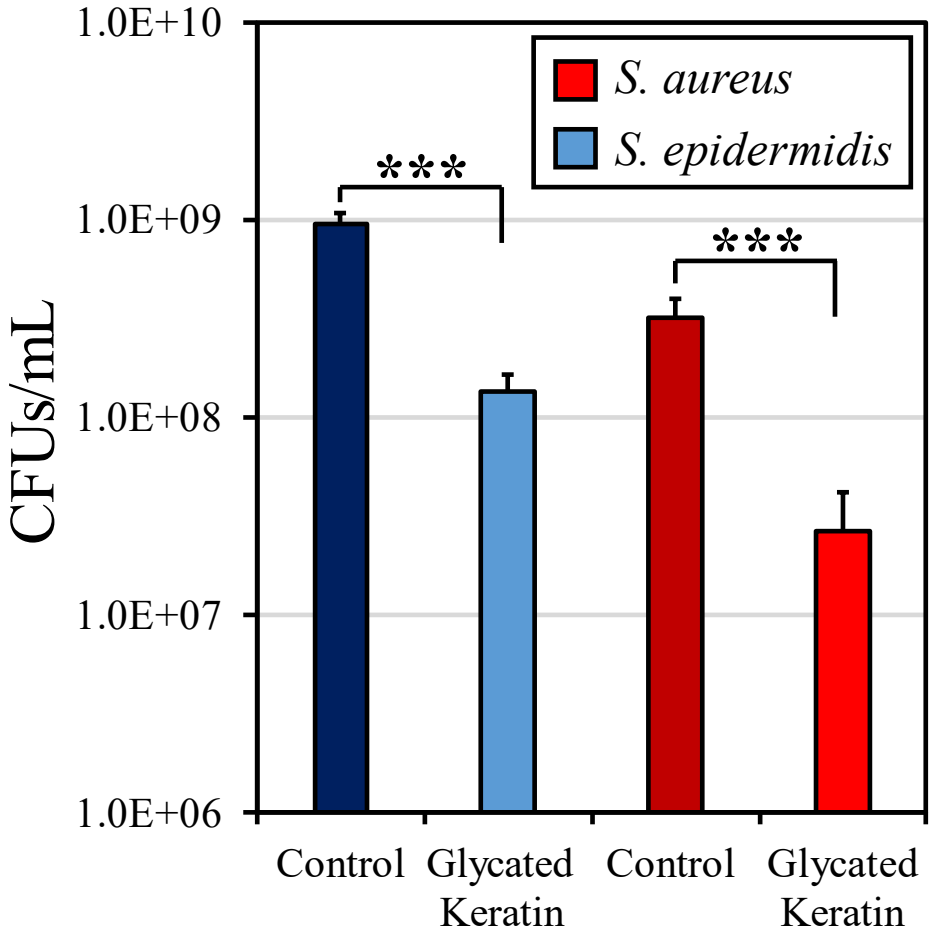

24-hour cell viability of planktonic cultures of *S. epidermidis* and *S. aureus* in media with 1.0 mg/mL glycated keratin. Logarithmic scale. n = 3. Mean ± standard deviation. Statistical difference calculated by Student's t-test. *** $p < 0.001$.

Figure 8. DNA Release from AGE Exposure in Non-Growth Media

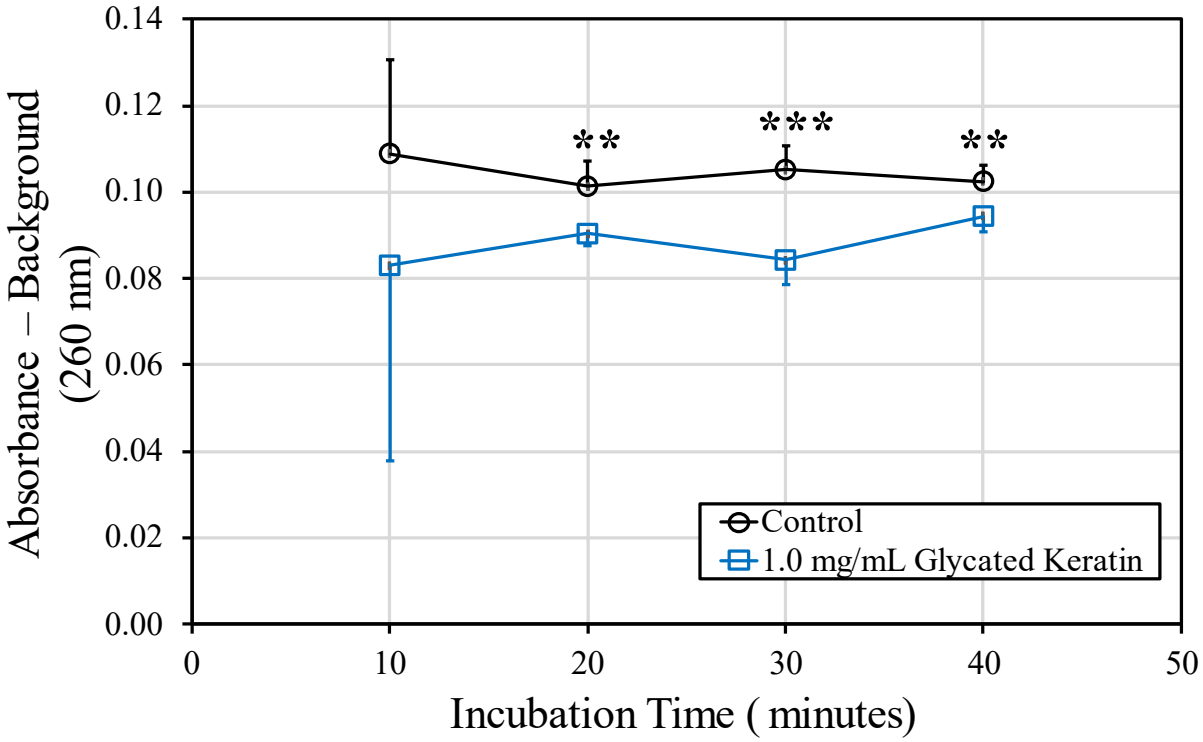

Release of intracellular material as indicated by absorbance at 260 nm of culture supernatant over a period of 40 minutes at 37°C in minimal media. n = 6.

Figure 9. Membrane Damage from AGE Exposure in Growing Culture

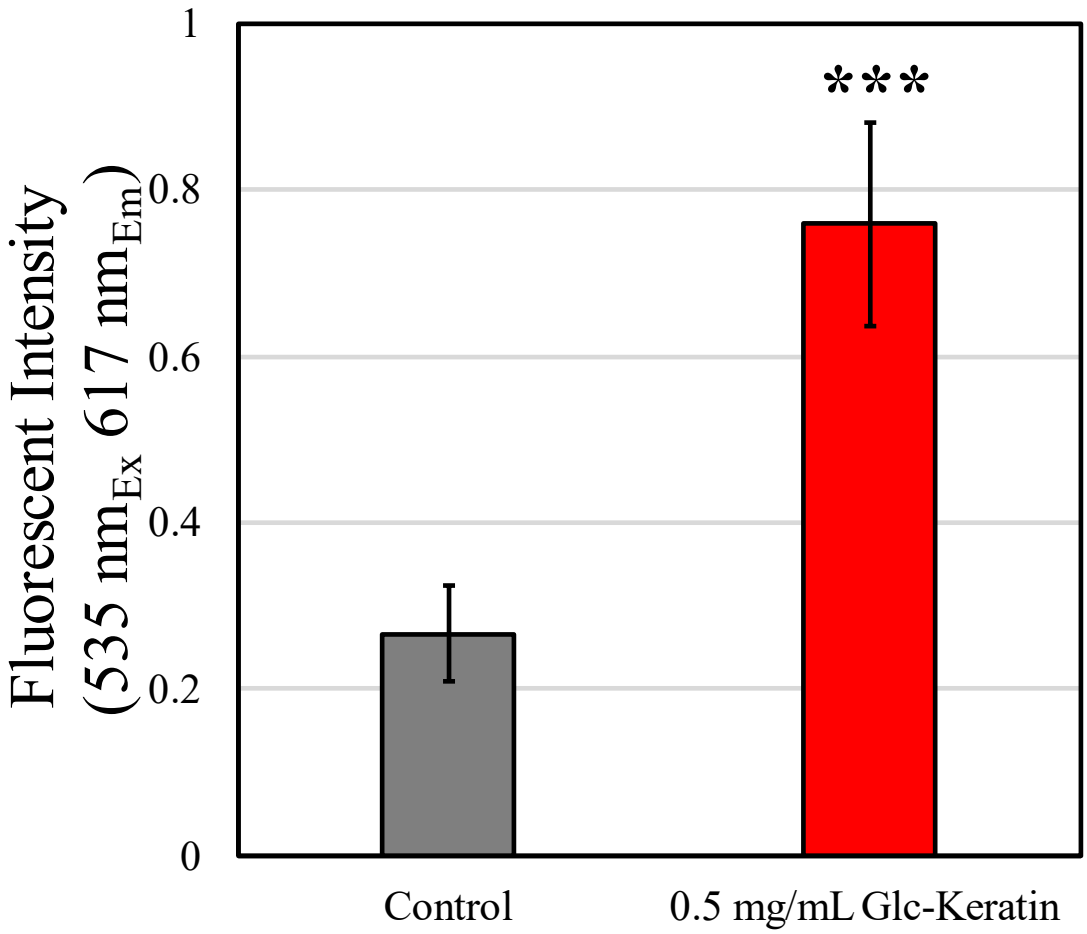

Membrane permeability determined by propidium iodide staining after 24 hours under planktonic conditions in TSB media. n = 14. Mean ± standard deviation. Statistical difference determined by Student's t-test. ***p< 0.001.

Figure 10. Membrane Damage in Growing and Non-Growth Cultures

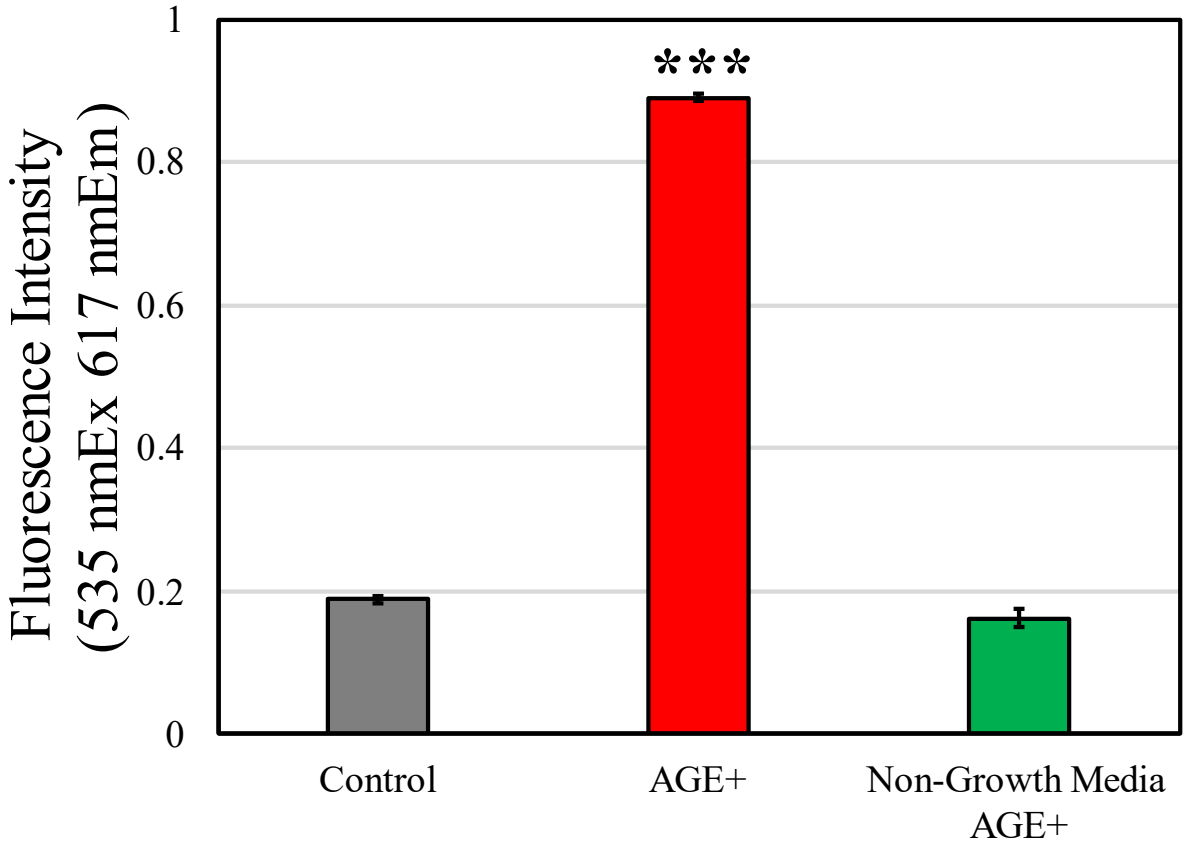

Membrane permeability determined by propidium iodide staining after 24 hours under planktonic conditions in TSB media (Control), TSB with 0.5 mg/mL glycated keratin, and non-growth media with 0.5 mg/mL glycated keratin. n = 6. Mean ± standard deviation. Statistical difference determined by Student's t-test compared to Control. ***$p < 0.001$.

Figure 11. *S. aureus* Sedimentation Assay

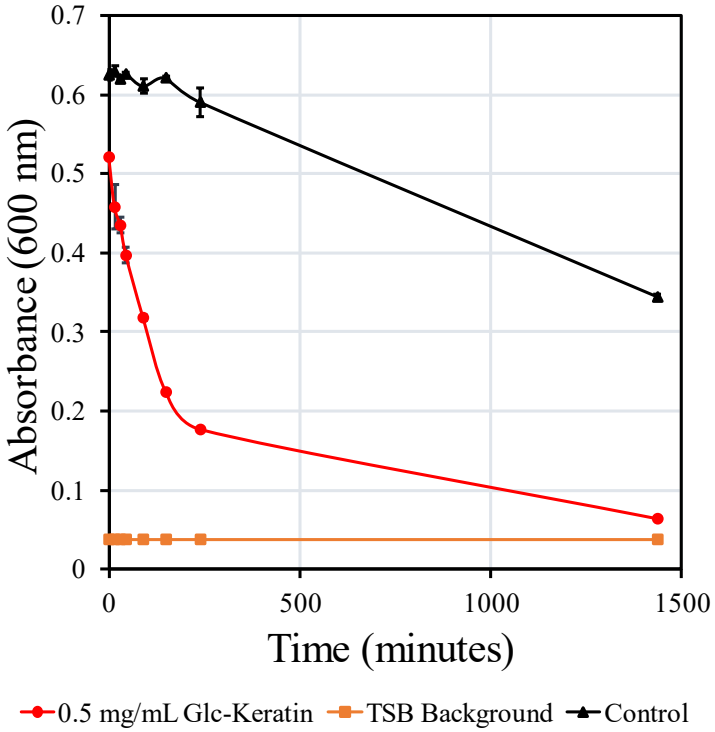

Measurement of cellular aggregation induce by 0.5 mg/mL glycated keratin via sedimentation. Sample tubes kept at 4°C and aliquots collected from upper portion of solution over time. Turbidity measured by absorbance at 600 nm. n = 3. Mean ± standard deviation.

Figure 12. Glycated Keratin Induced Cellular Aggregation

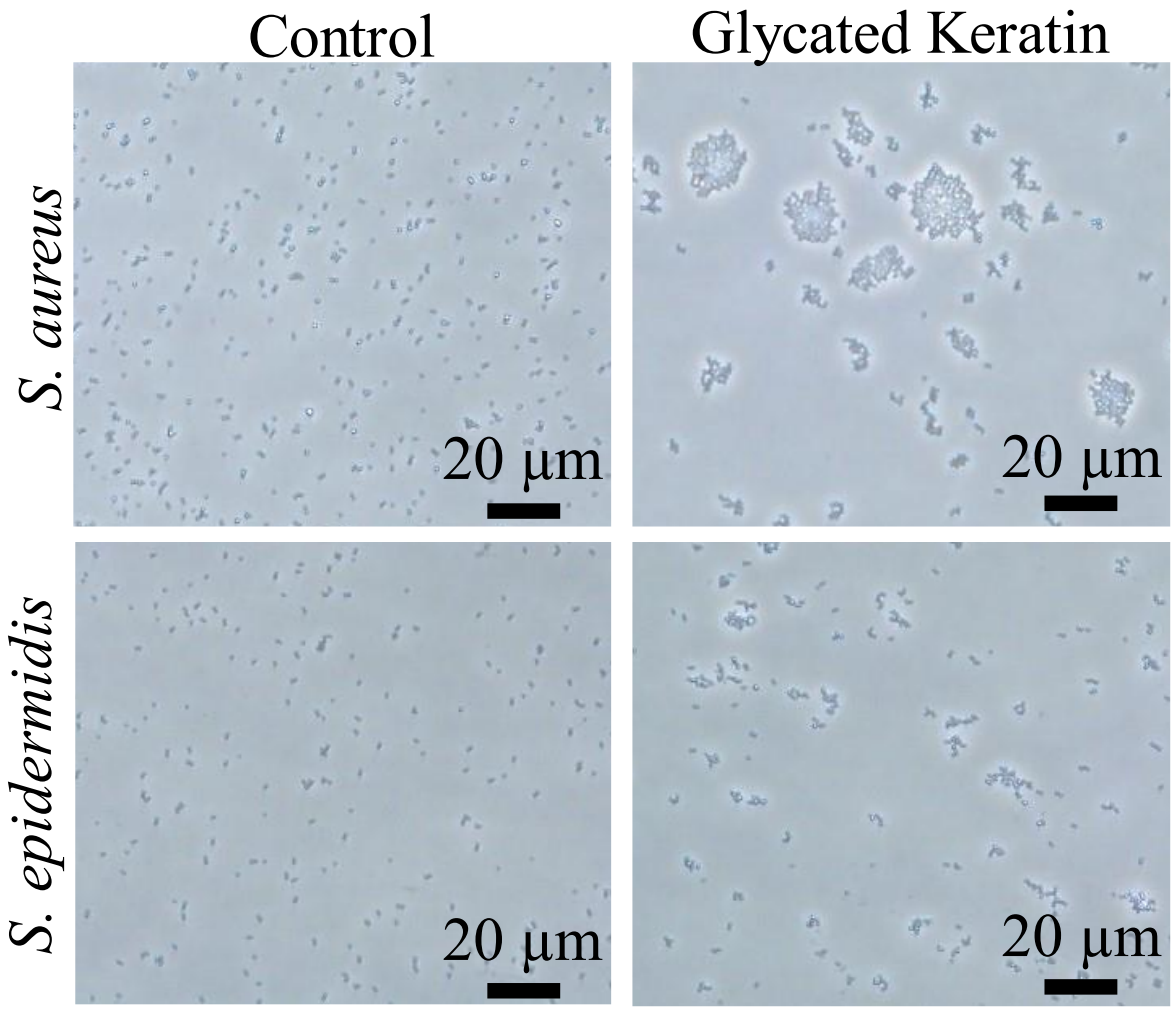

Representative bright-field microscopy images of *S. aureus* and *S. epidermidis* cellular aggregation after 24 hours under planktonic conditions. Images captured at 400X magnification.

Figure 13. Glycated Keratin Induced Cellular Aggregation

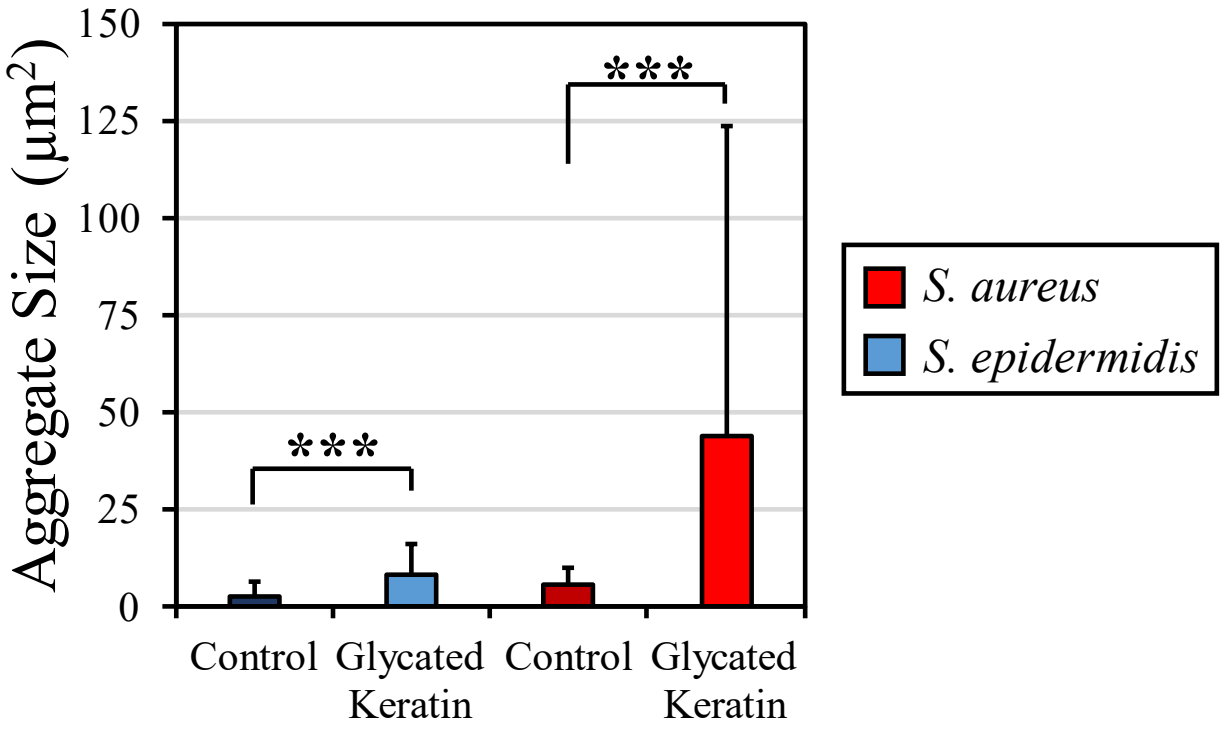

Mean bacterial aggregate size. Samples were vortexed and 2 μL inoculates were transferred to microscope slides. n = 10. Mean ± standard deviation. Statistical difference determined by Student's t-test. *** $p < 0.001$

Figure 14. Potential Pathway for Initiation of Cellular Aggregation.

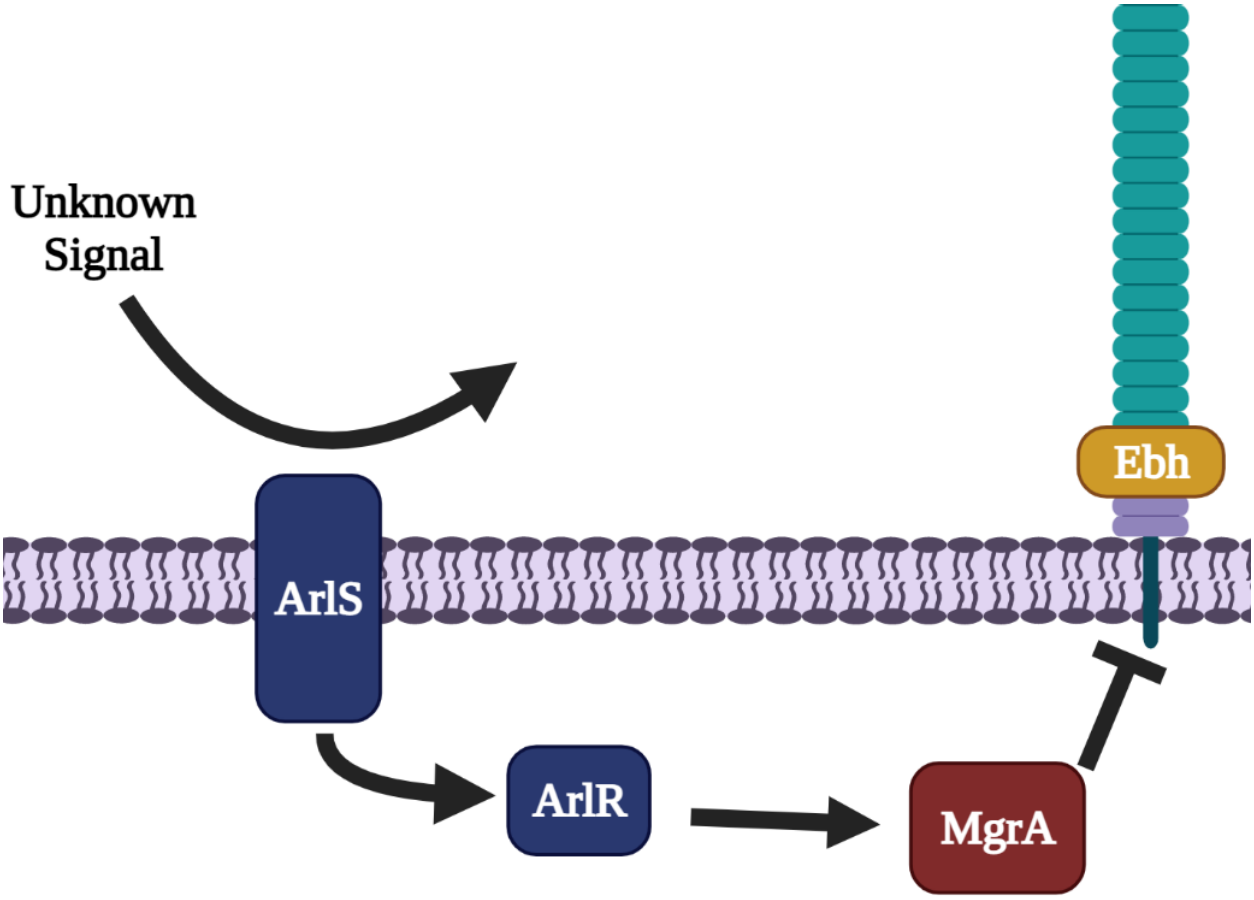

ArlS and ArlR, two-component response regulator; MgrA, HTH-type transcriptional regulator; Ebh, extracellular matrix binding protein.

Figure 15. Glycated Keratin Induced Biofilm Formation

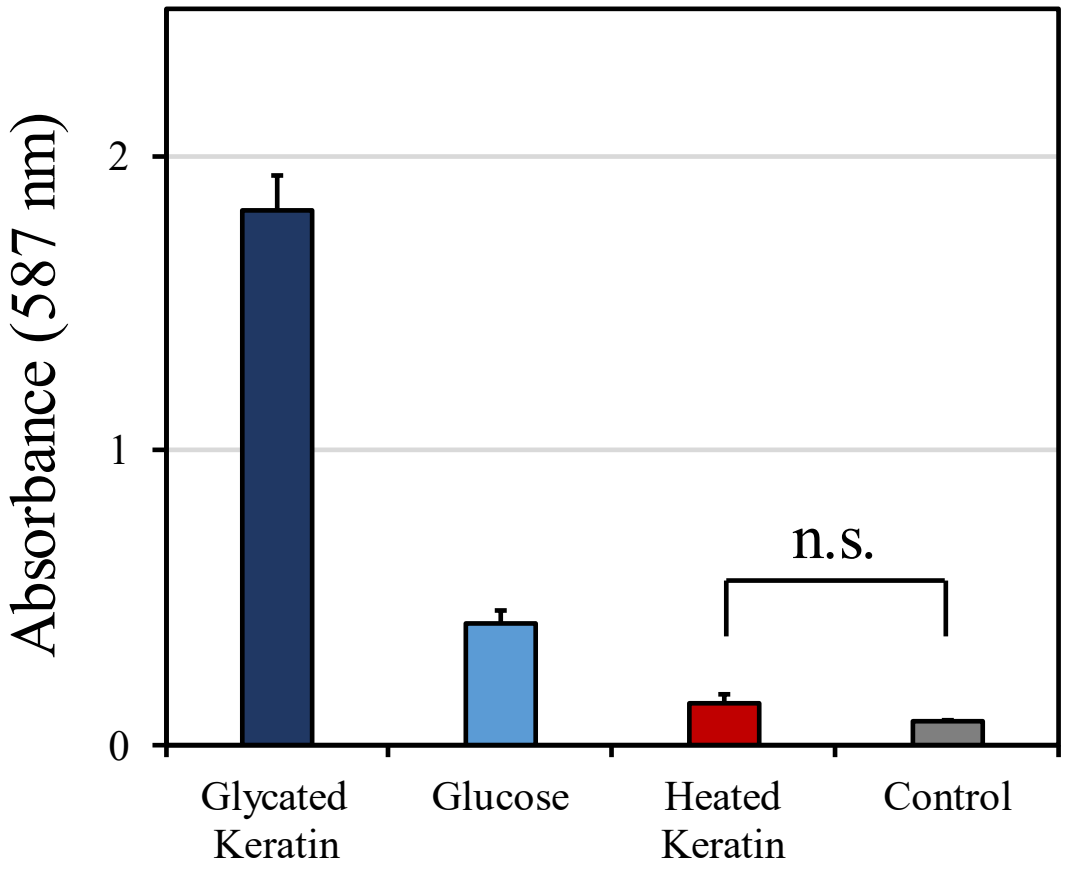

Increase in biofilm formation by addition of 0.5 mg/mL of keratin. Glucose conditions contain 5.0 mg/mL of glucose, double the concentration of standard TSB. Statistical difference was calculated via One-way ANOVA followed by Tukey's test. $p < 0.001$. n.s. = not significant.

Figure 16. Difference in Biofilm Response: *S. epidermidis* vs. *S. aureus*

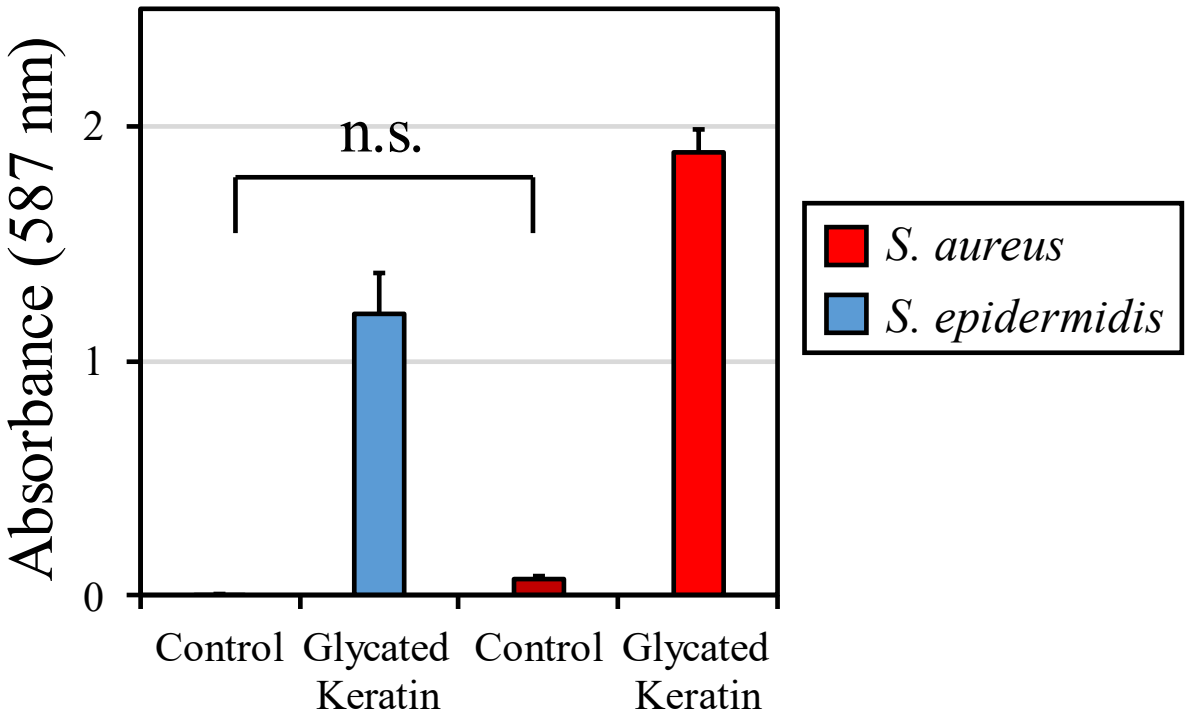

(B) Difference in biofilm formation between *S. epidermidis* and *S. aureus*. n = 8. Mean ± standard deviation. Statistical difference was calculated via One-way ANOVA followed by Tukey's test. $p < 0.001$. n.s. = not significant

Figure 17. Glycated Keratin Dose-Response Relationship

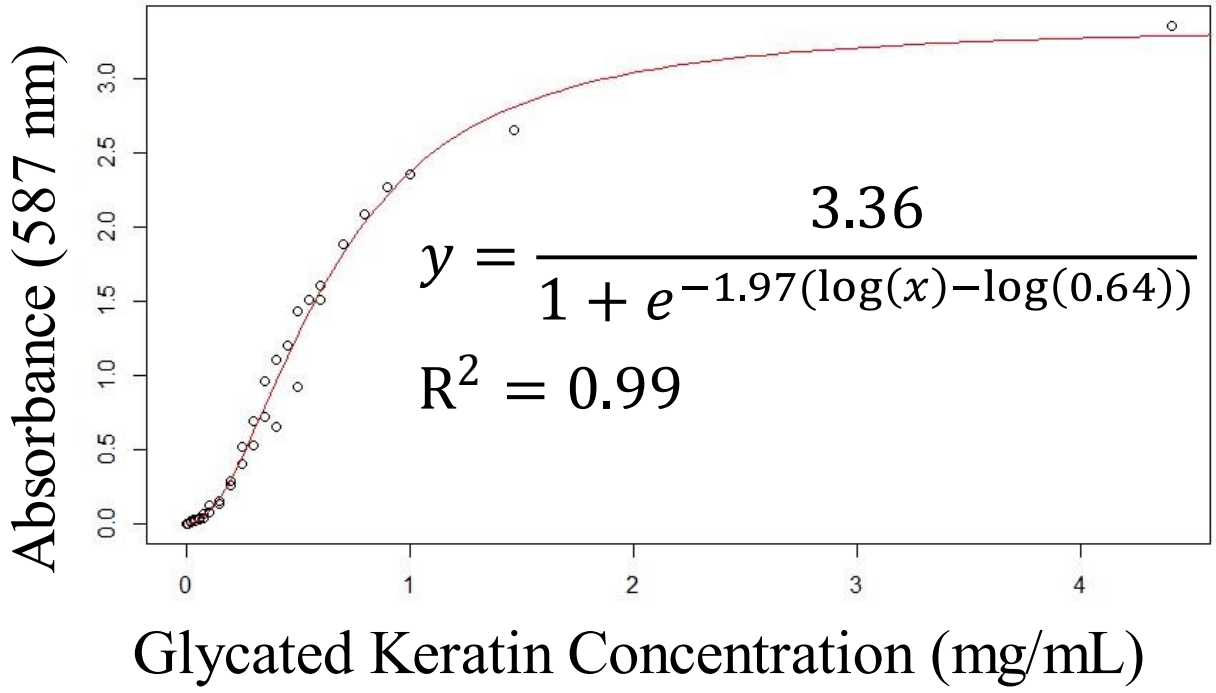

Dose-response relationship of *S. aureus* biofilm formation and >10 kDA glucose-keratin concentration. Biofilms were stained with crystal violet and absorbance was measured at 587 nm after 48 hours of growth under static conditions at 37°C. Each data point represents the mean of eight samples. Midpoint = 0.64. R^2 = 0.99.

Figure 18. Heated Keratin Dose-Response Relationship.

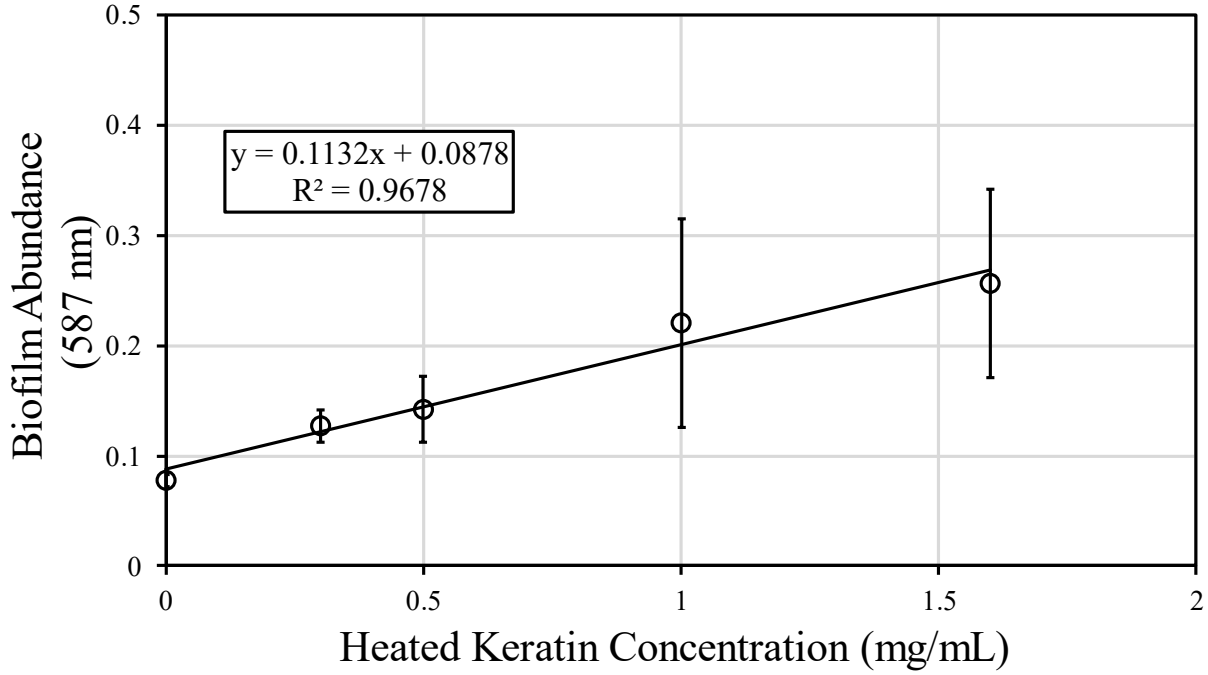

Dose-response relationship of *S. aureus* biofilm formation and > 10kDa heated-keratin concentration. Heated keratin was prepared following the same protocol as glycated keratin, without the addition of glucose to the sample solution. Biofilms were stained with crystal violet and absorbance was measured at 587 nm after 48 hours of growth under static conditions at 37°C. n = 8. Mean ± standard deviation.

Figure 19. Glucose Dose-Response Relationship.

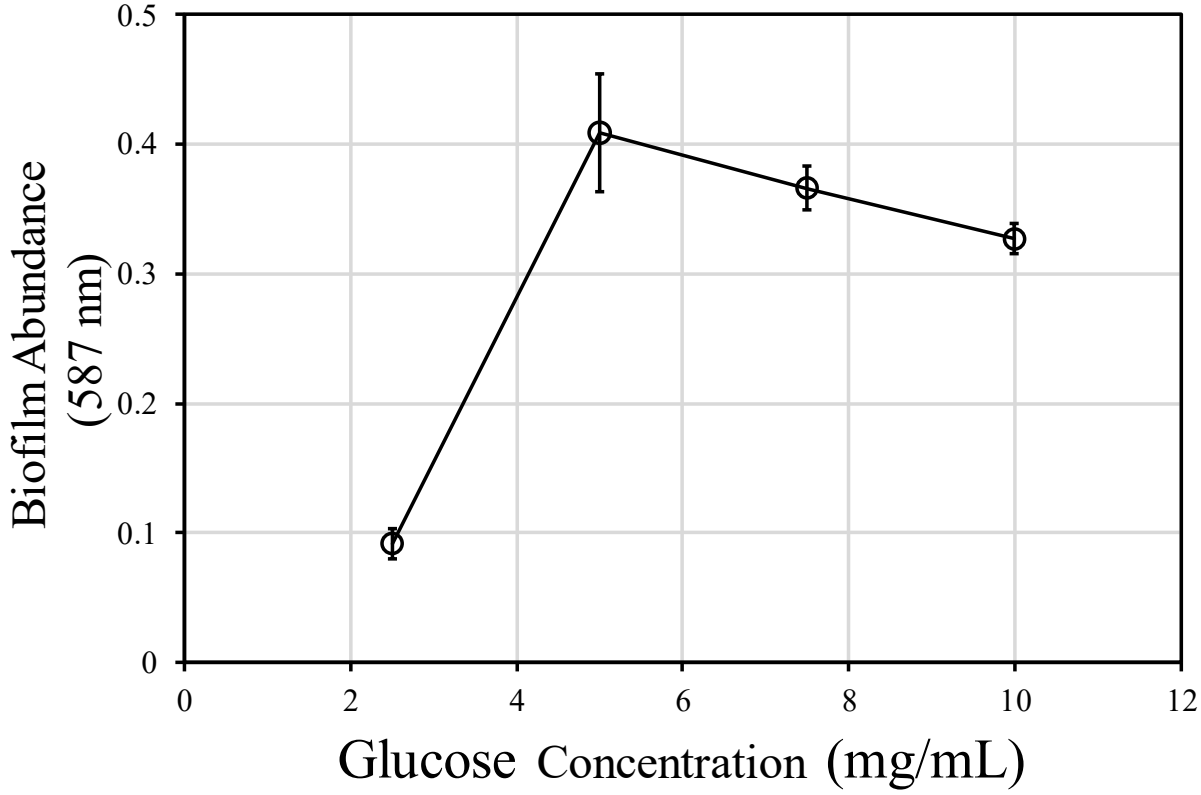

Dose-response relationship of *S. aureus* biofilm formation and media glucose concentration. Biofilms were stained with crystal violet and absorbance was measured at 587 nm after 48 hours of growth under static conditions at 37°C. n = 8. Mean ± standard deviation.

Figure 20. Biofilm Response by Molecular Weight Fractions

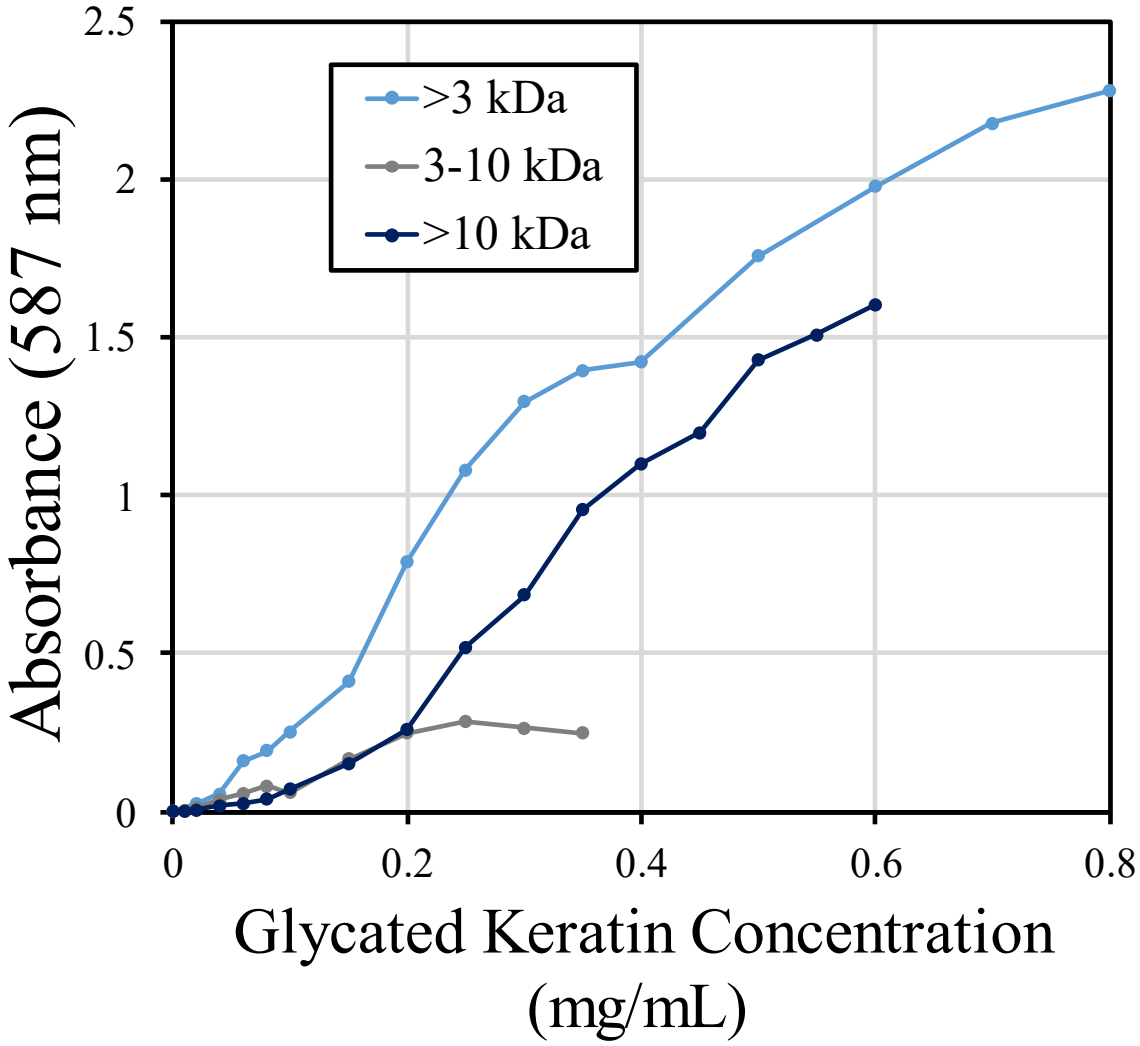

Biofilm promotion by different molecular weight fractions of glycated keratin over a range of dosages. Biofilms were stained with crystal violet and absorbance was measured at 587 nm after 48 hours of growth under static conditions at 37°C n = 8.

Figure 21. Biofilm Response by Molecular Weight Fraction at 0.25 mg/mL

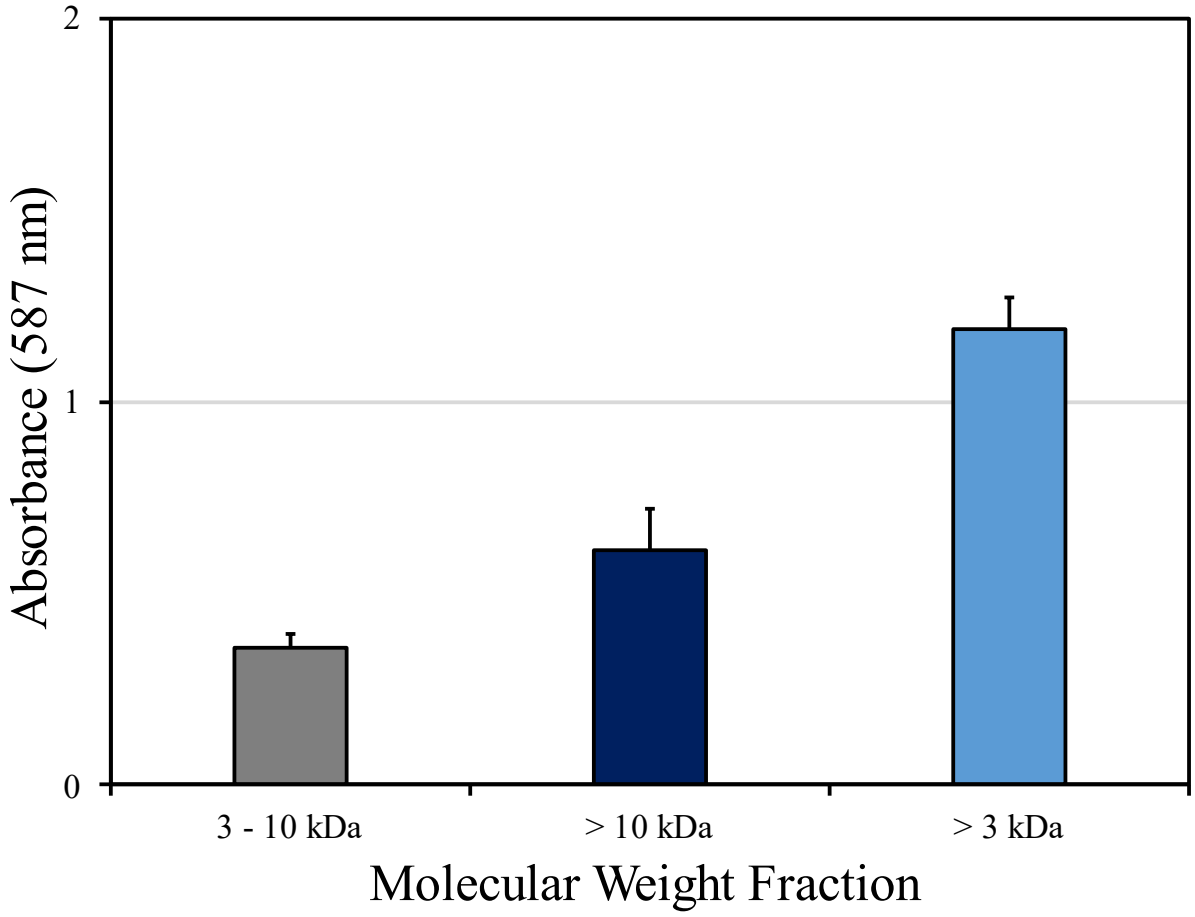

Biofilm promotion by different molecular weight fractions of glycated keratin at a dosage of 0.25 mg/mL. Biofilms were stained with crystal violet and absorbance was measured at 587 nm after 48 hours of growth under static conditions at 37°C n = 8. Mean ± standard deviation. Statistical difference was calculated by One-way ANOVA and Tukey's test. $p < 0.001$ between all sample groups.

Figure 22. Influence of Growth Phase on AGE-Induced Biofilm Formation

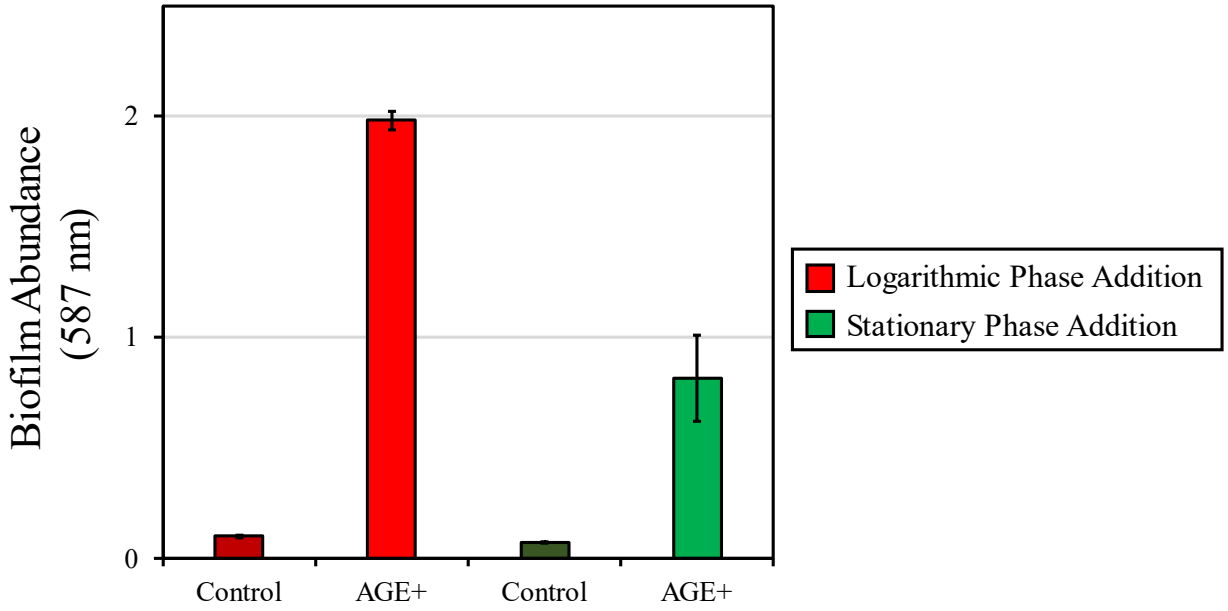

The effect of the timing of glycated keratin addition to *S. aureus* culture based on growth phase. For logarithmic phase samples, *S. aureus* overnight stock was inoculated into TSB media containing 0.5 mg/mL glycated keratin. For stationary phase addition, cells were collected from 24-hour *S. aureus* cultures in the post-logarithmic growth phase and resuspended in fresh media containing 0.5 mg/mL glycated keratin. Biofilms were stained with crystal violet and absorbance was measured at 587 nm after 48 hours of growth under static conditions at 37°C. n = 8. Mean ± standard deviation. Statistical difference was calculated via One-way ANOVA followed by Tukey's test. $p < 0.001$ between all sample groups.

Figure 23. Media Fluorescent AGE Decrease

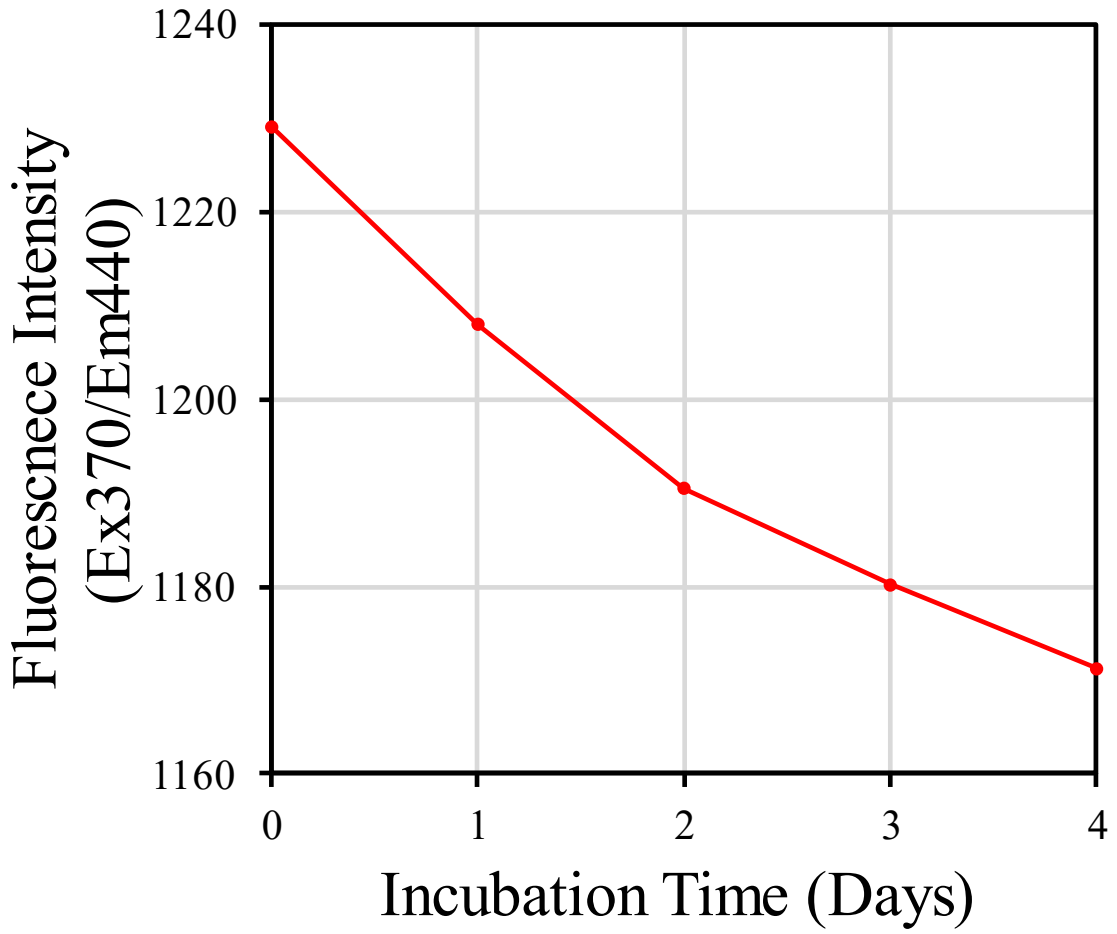

Apparent decrease of fluorescent AGE content in *S. aureus* planktonic culture over time. TSB growth media with 1 mg/mL glycated keratin. Fluorescence intensity values are standardized in reference to 5 µg/mL quinine sulphate solution as 1000 units. n = 3.

Figure 24. Fluorescent AGE Metabolism

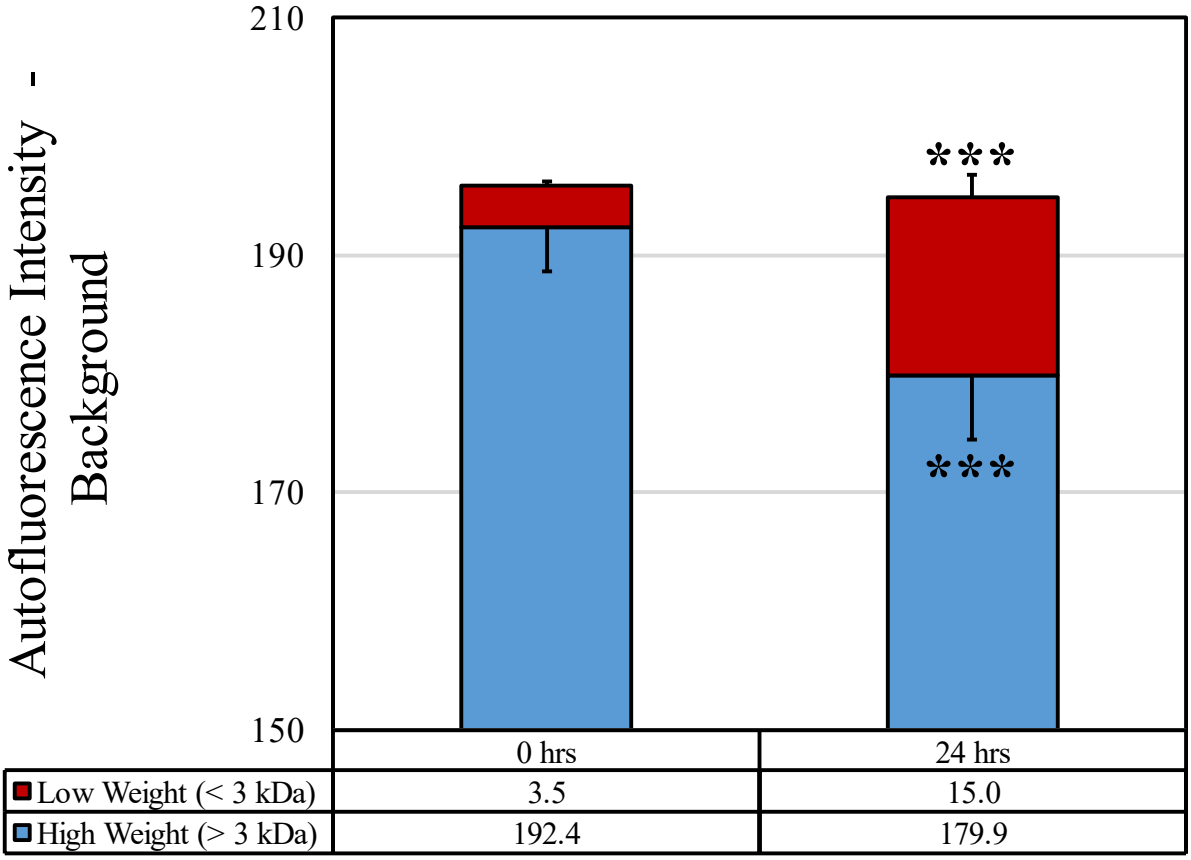

	0 hrs	24 hrs
Low Weight (< 3 kDa)	3.5	15.0
High Weight (> 3 kDa)	192.4	179.9

1 mL aliquots of overnight stock were resuspended in the equivalent volume of minimal media; 1 mg/mL of glucose-keratin was added to the test condition. After 24 hours of incubation under planktonic conditions, media supernatant was collected and filtered to separate high and low molecular weight glycated proteins (greater or less than 3 kDa). n = 5. Mean ± standard deviation. Absorbance values were standardized in reference to 5 µg/mL quinine sulphate solution as 1000 units, and background values of un-inoculated solution were subtracted. Statistical difference calculated by Student's t-test compared to time-zero. *** $p < 0.001$.

Figure 25. Aminoguanidine Biofilm Inhibition Effect

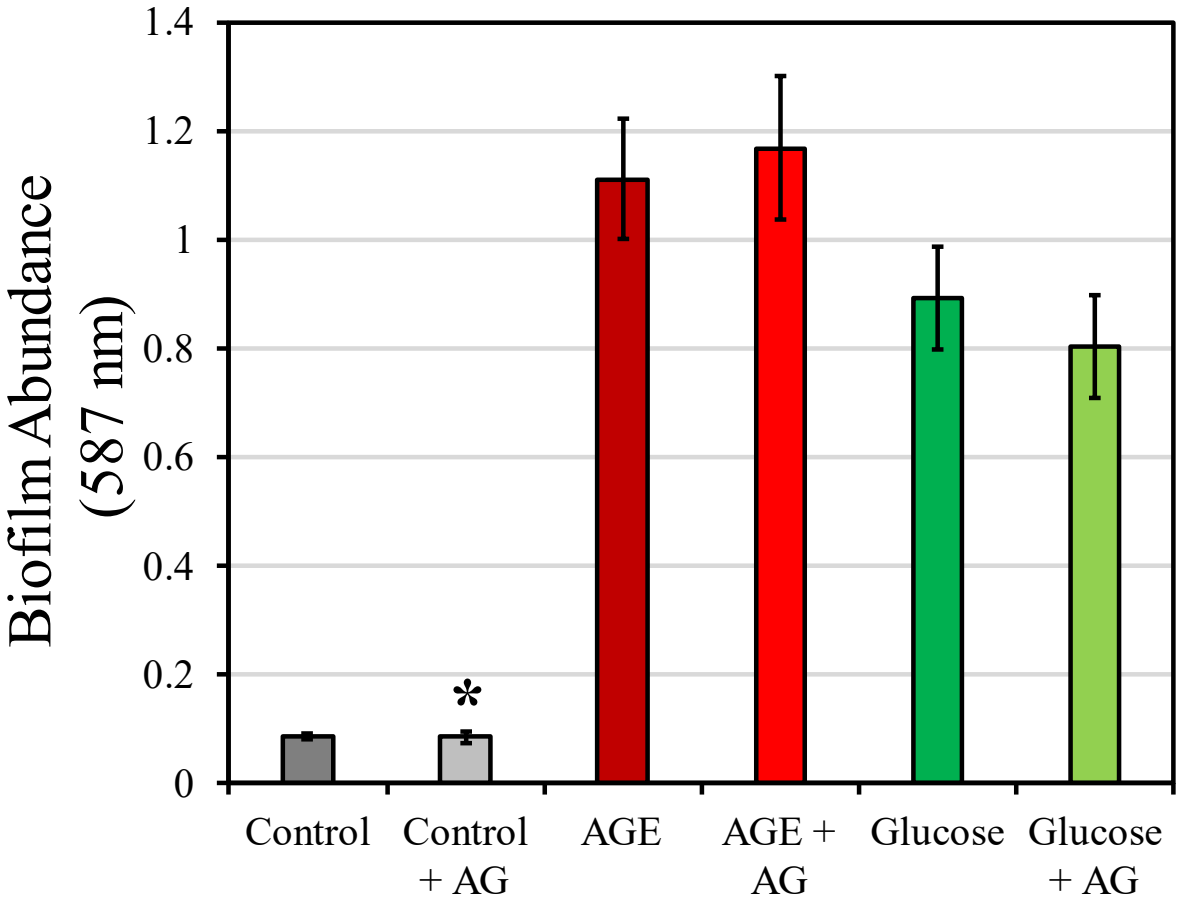

Effect of 0.1 mg/mL aminoguanidine on *S. aureus* biofilm formation in 0.1 mg/mL glycated keratin and 5.0 mg/mL glucose cultures. Biofilms were stained with crystal violet and absorbance was measured at 587 nm after 48 hours of growth under static conditions at 37°C. n = 8. Mean ± standard deviation. Statistical difference determined by Student's t-test compared to controls.

Figure 26. Aminoguanidine Cell Viability

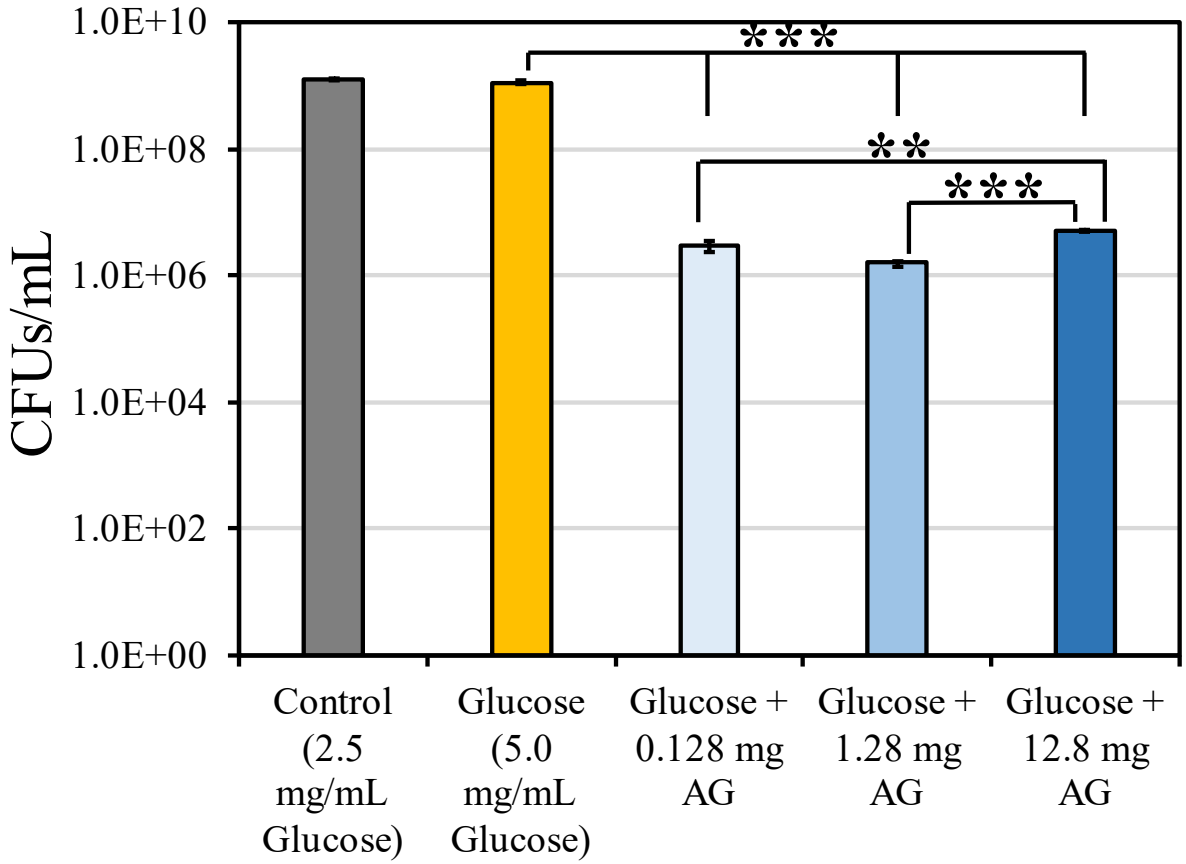

Effect of aminoguanidine on *S. aureus* cell viability after 72 hours under elevated glucose conditions (5.0 mg/mL). n = 3. Mean ± Standard Deviation. Statistical difference was calculated via One-way ANOVA followed by Tukey's test. ** $p < 0.01$, *** $p < 0.001$.

Figure 27. Ascorbic Acid: Cell Viability and Biofilm Inhibition

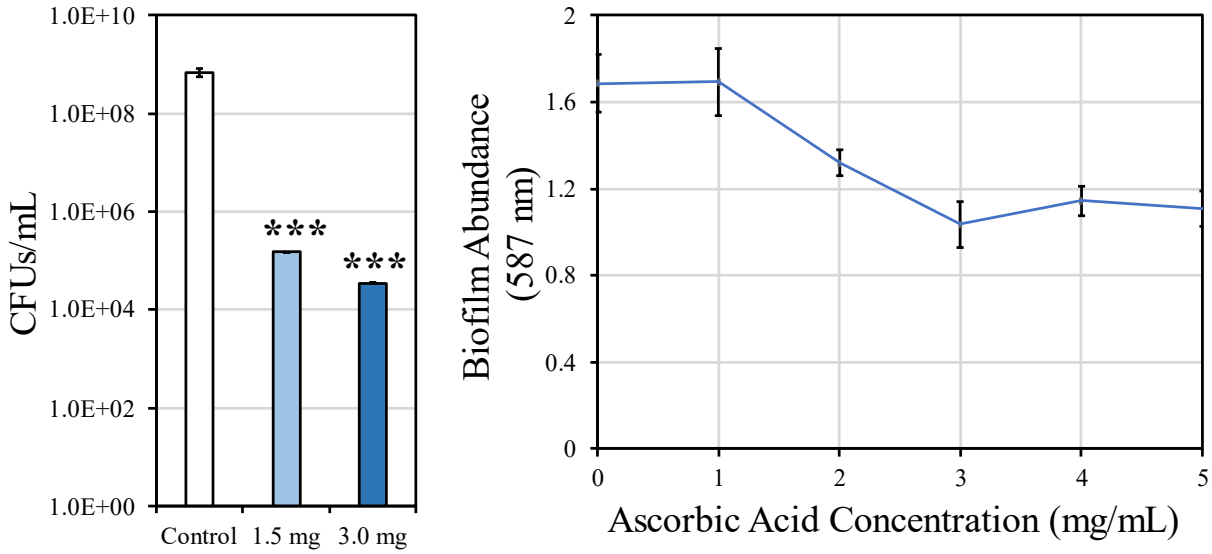

(Left) *S. aureus* cell viability after 24 hours of incubation under planktonic conditions with added ascorbic acid. n = 3. Mean ± Standard Deviation. Statistical difference determined by Student's t-test compared to control. *** $p < 0.001$.

(Right) Effect of ascorbic acid on *S. aureus* biofilm formation provoked by 0.5 mg/mL of glycated keratin. Biofilm assayed after 48 hours of growth under static conditions. n = 8. Mean ± standard deviation.

Figure 28. Effect of Ascorbic Acid on Baseline *S. aureus* Biofilm Formation

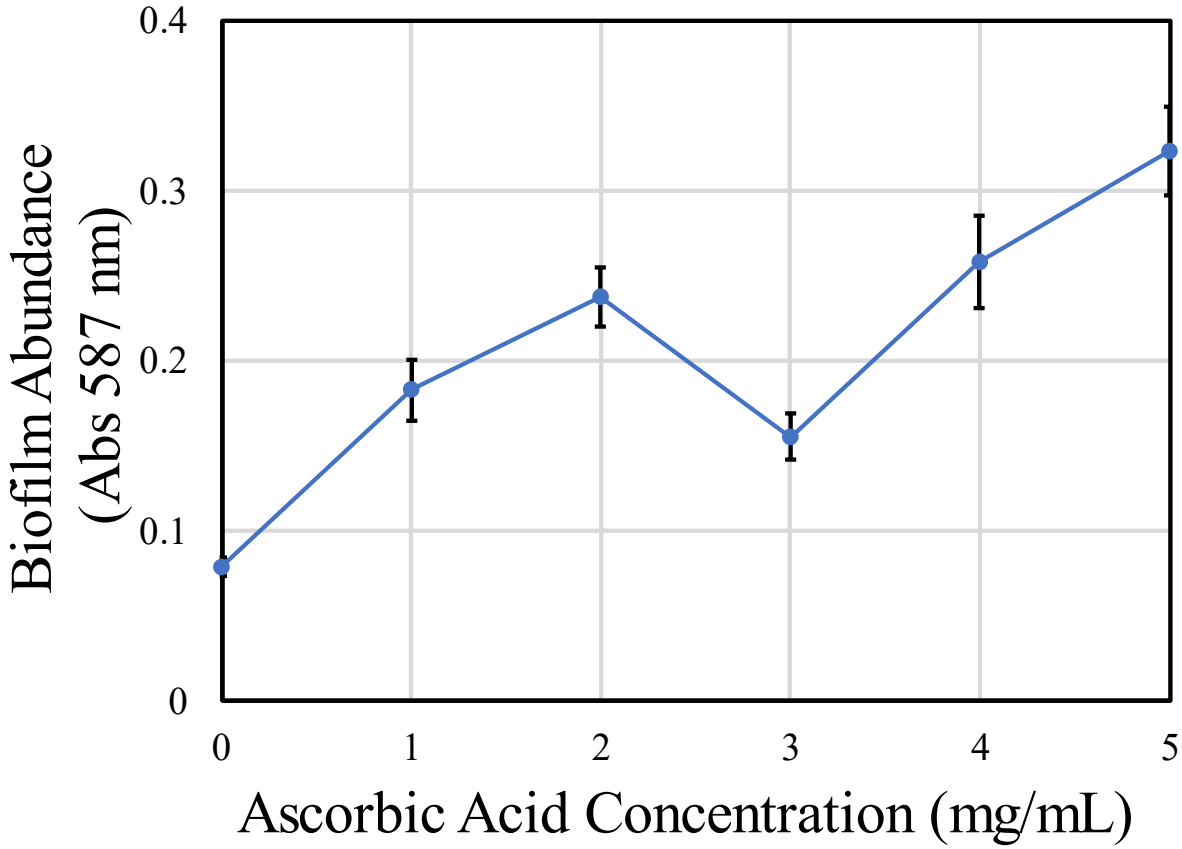

S. aureus biofilm response to various concentrations of ascorbic acid. Biofilm assayed after 48 hours of growth under static conditions. n = 8. Mean ± standard deviation.

Figure 29. Astaxanthin: Cell Viability and Biofilm Inhibition

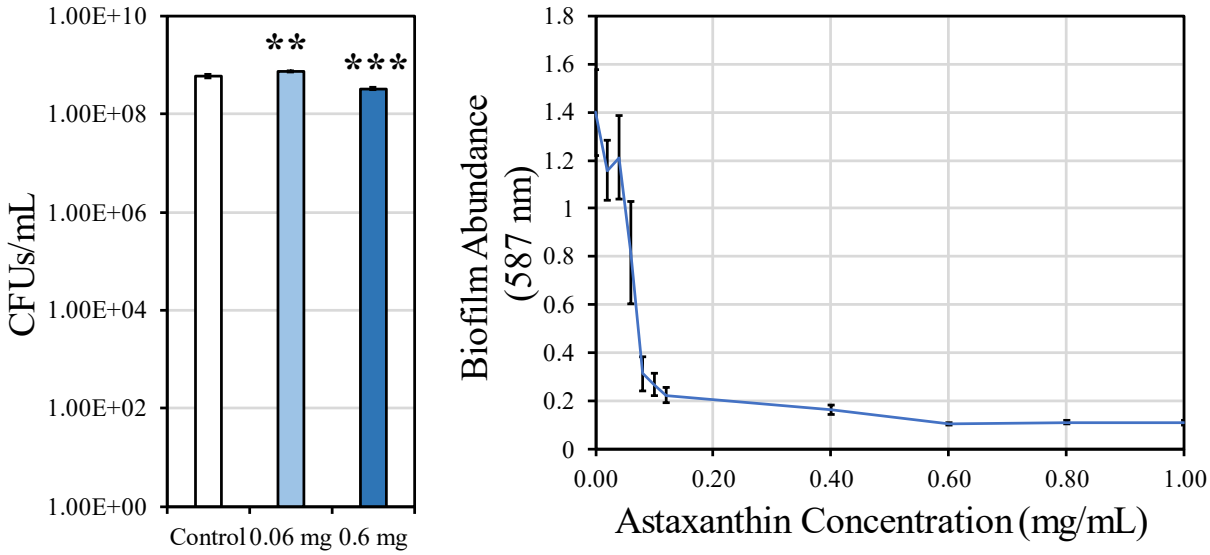

(Left) *S. aureus* cell viability after 24 hours of incubation under planktonic conditions with added astaxanthin. n = 3. Mean ± Standard Deviation. Statistical difference determined by Student's t-test compared to control. ** $p < 0.01$, *** $p < 0.001$.

(Right) Effect of astaxanthin on *S. aureus* biofilm formation provoked by 0.5 mg/mL of glycated keratin. Biofilm assayed after 48 hours of growth under static conditions. n = 8. Mean ± standard deviation.

Figure 30. Effect of Astaxanthin on Baseline *S. aureus* Biofilm Formation

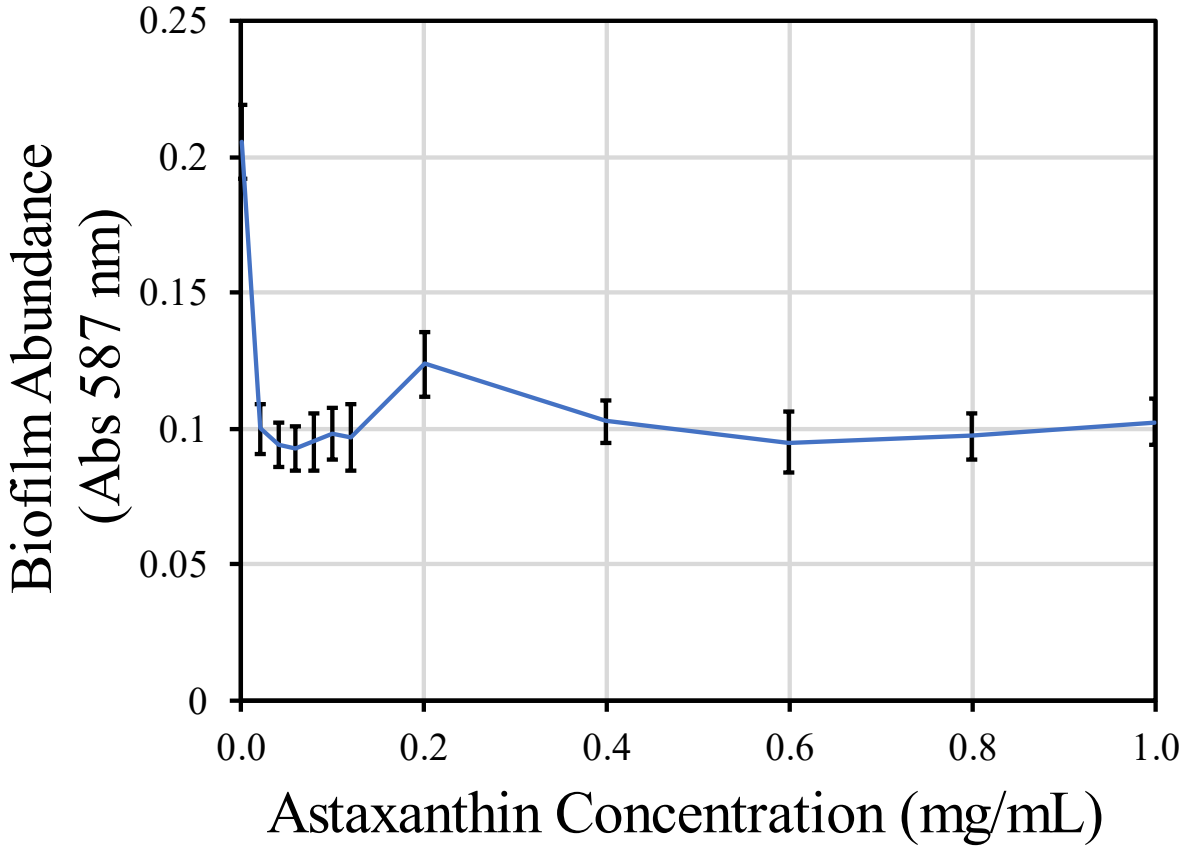

S. aureus biofilm response to various concentrations of astaxanthin. Biofilm assayed after 48 hours of growth under static conditions. n = 8. Mean ± standard deviation.

Figure 31. Dose-Response Curve of Astaxanthin Biofilm Inhibition

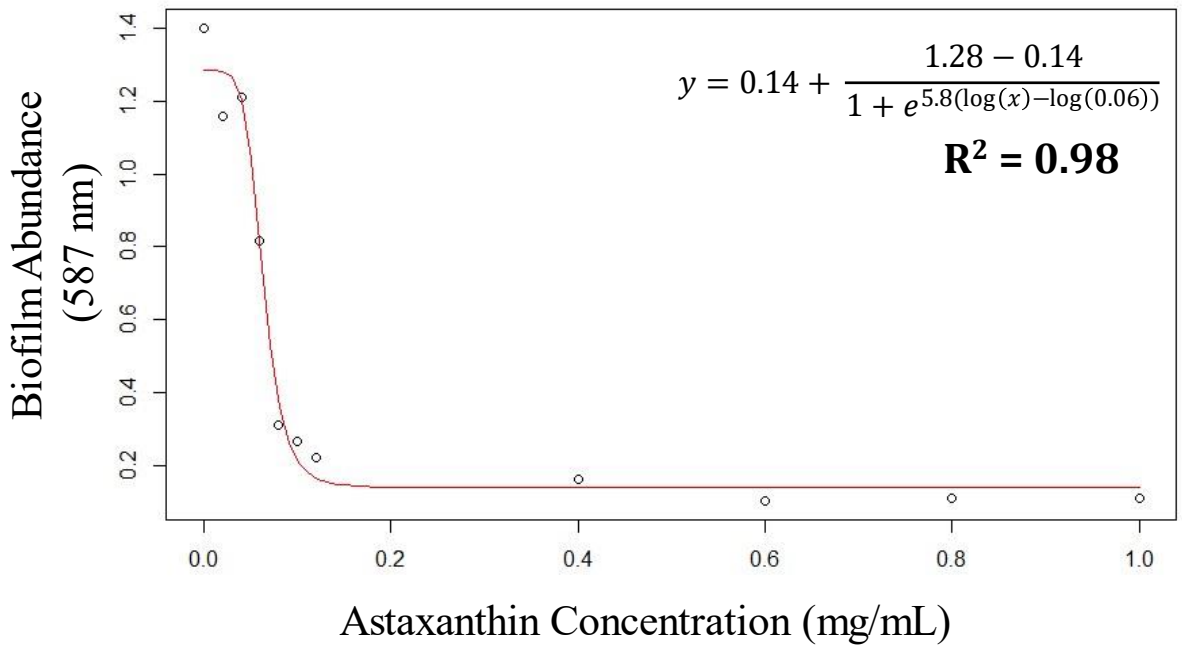

Dose-response relationship of *S. aureus* biofilm abundance induced by exposure to 0.5 mg/mL glycated keratin, and astaxanthin concentration. Biofilms were stained with crystal violet and absorbance was measured at 587 nm after 48 hours of growth under static conditions at 37°C. Each data point represents the mean of eight samples. Midpoint = 0.06. $R^2 = 0.98$.

Figure 32. Astaxanthin Culture Microscope Capture

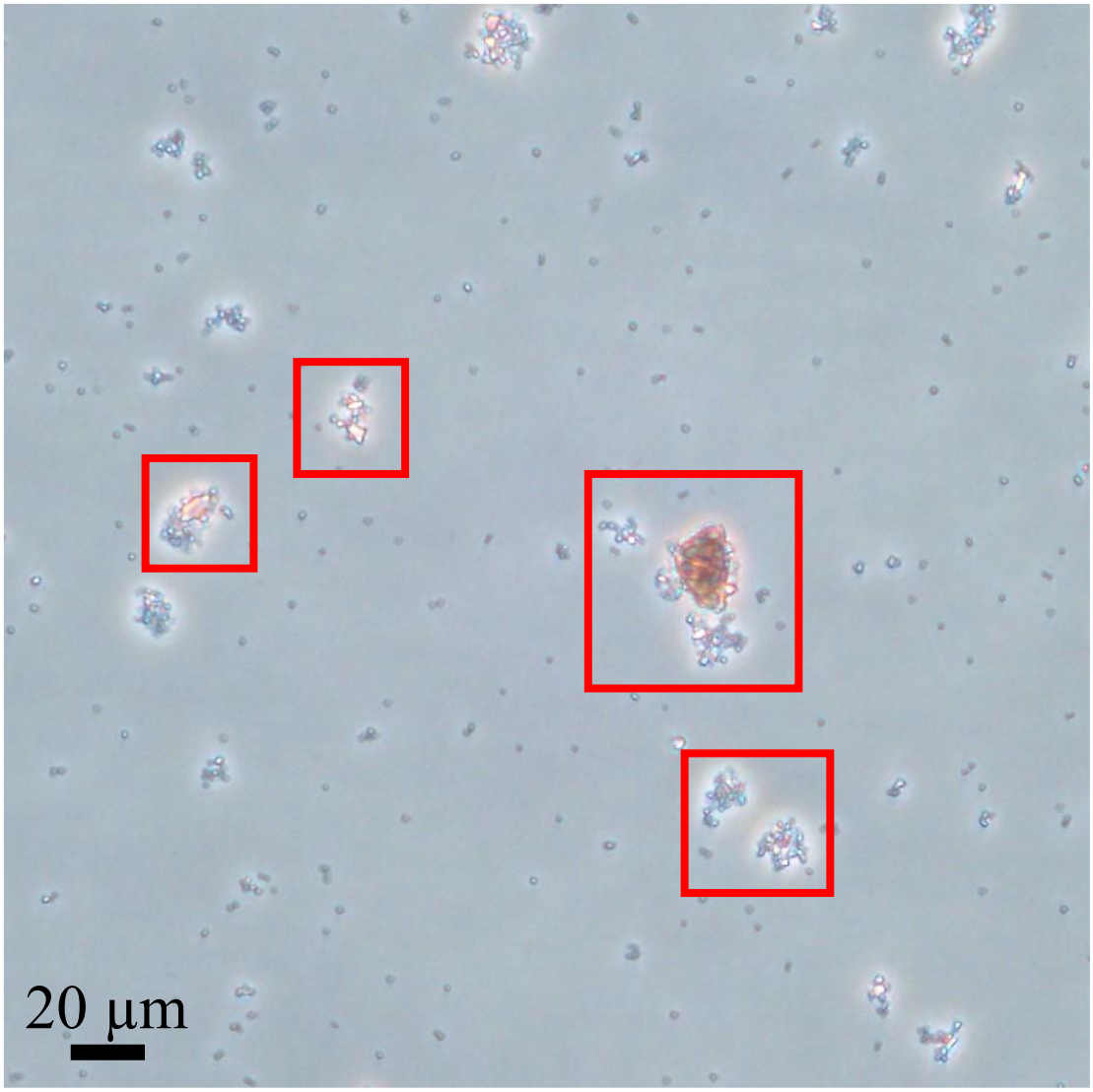

Representative microscope image capture at 400X magnification of *S. aureus* aggregates observed in 0.6 mg/mL astaxanthin control culture after 24 hours under planktonic conditions. Red boxes indicate small *S. aureus* aggregates around red structures which appear to be small particles/crystals of astaxanthin that failed to fully dissolve in the mixed water and DMSO solution at this concentration.

Figure 33. Clove: Cell Viability and Biofilm Inhibition

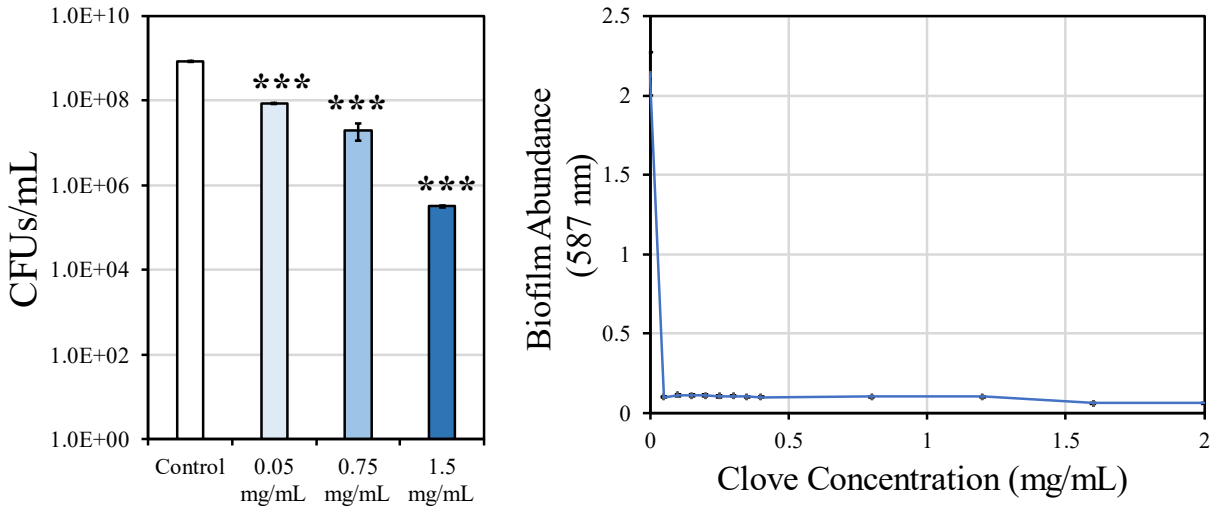

(Left) *S. aureus* cell viability after 24 hours of incubation under planktonic conditions with added clove extract. n = 3. Mean ± Standard Deviation. Statistical difference determined by Student's t-test compared to control. *** $p < 0.001$.

(Right) Effect of clove extract on *S. aureus* biofilm formation provoked by 0.5 mg/mL of glycated keratin. Biofilm assayed after 48 hours of growth under static conditions. n = 8. Mean ± standard deviation.

Figure 34. Effect of Clove Extract on Baseline *S. aureus* Biofilm Formation

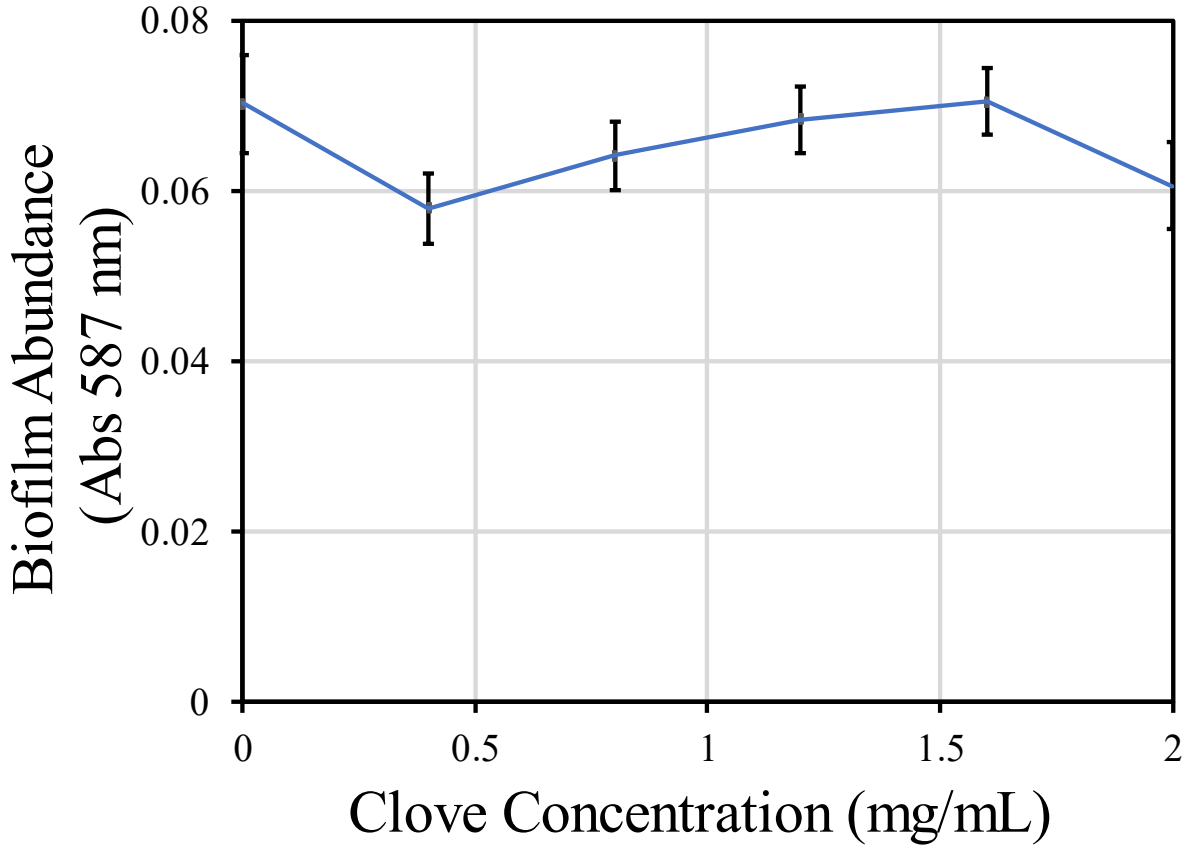

S. aureus biofilm response to various concentrations of clove extract. Biofilm assayed after 48 hours of growth under static conditions. n = 8. Mean ± standard deviation.

Figure 35. Melatonin: Cell Viability and Biofilm Inhibition

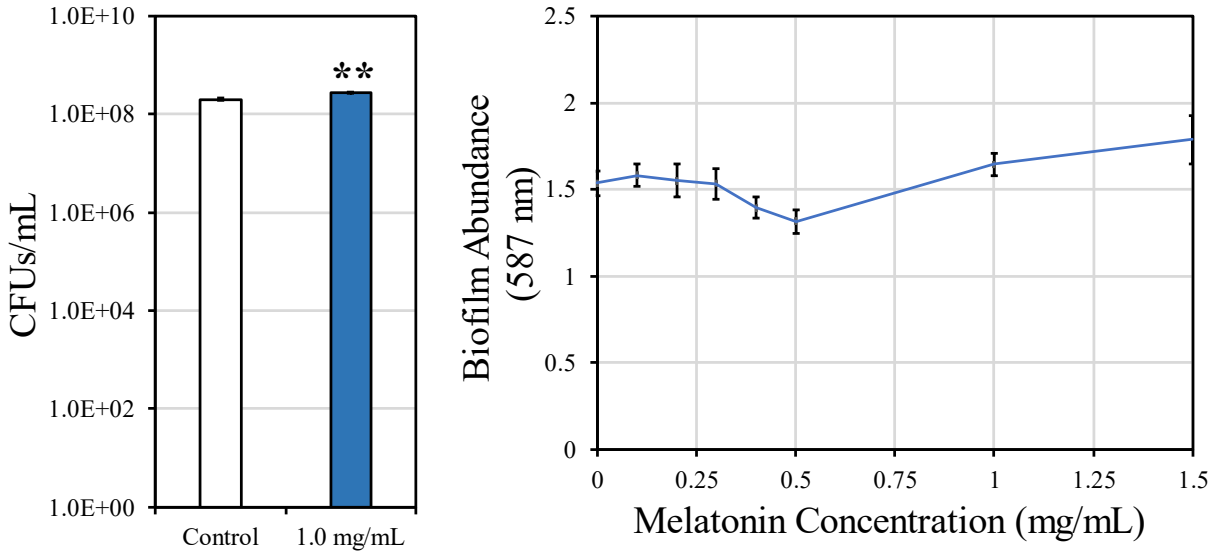

(Left) *S. aureus* cell viability after 24 hours of incubation under planktonic conditions with added melatonin. n = 3. Mean ± Standard Deviation. Statistical difference determined by Student's t-test compared to control. ** $p < 0.01$.

(Right) Effect of melatonin on *S. aureus* biofilm formation provoked by 0.5 mg/mL of glycated keratin. Biofilm assayed after 48 hours of growth under static conditions. n = 8. Mean ± standard deviation.

Figure 36. Effect of Melatonin on Baseline *S. aureus* Biofilm Formation

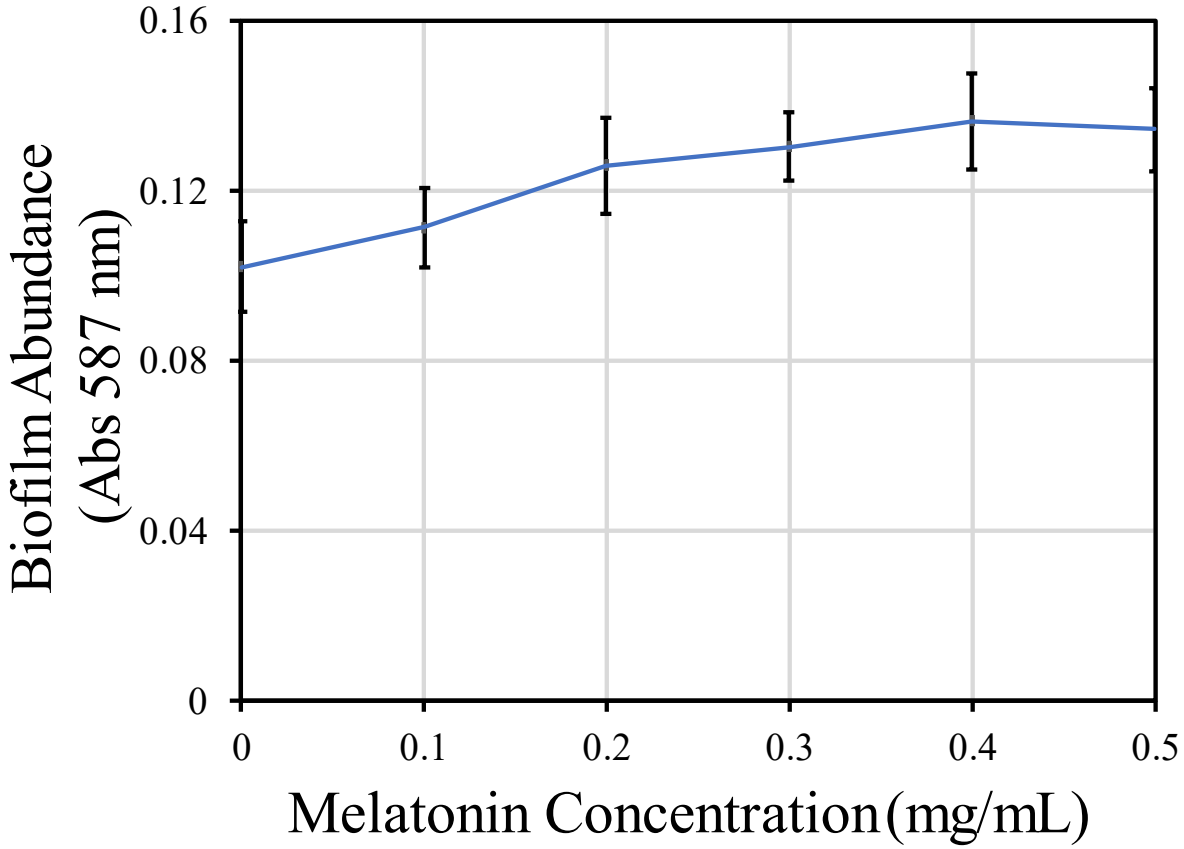

S. aureus biofilm response to various concentrations of melatonin. Biofilm assayed after 48 hours of growth under static conditions. n = 8. Mean ± standard deviation.

Figure 37. Effect of PTB on Baseline *S. aureus* Biofilm Formation

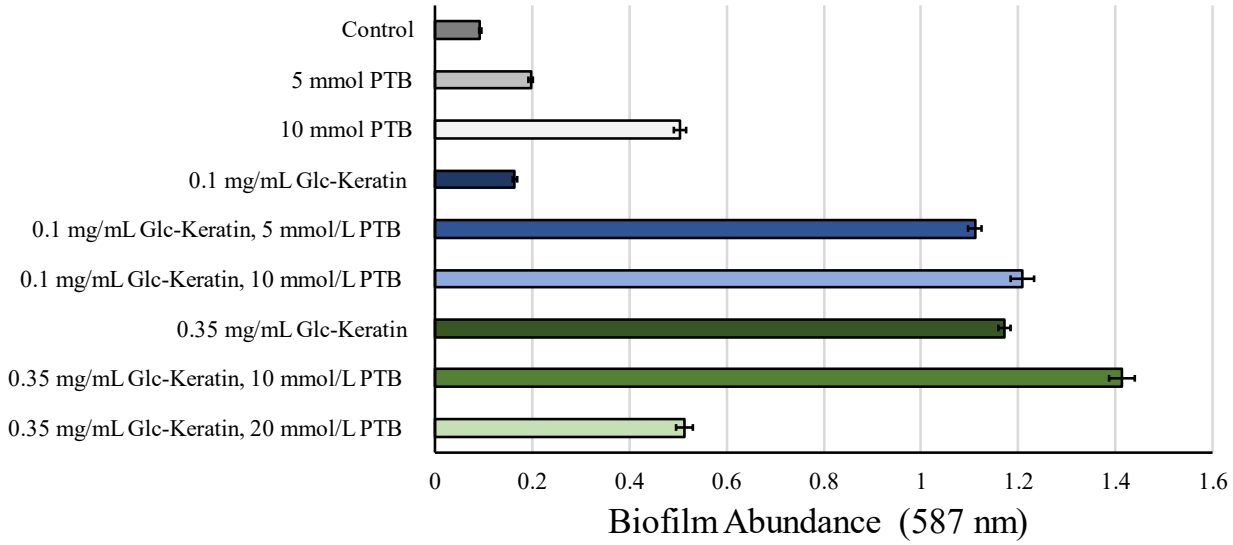

S. aureus biofilm response to various concentrations of PTB. Biofilm assayed after 48 hours of growth under static conditions. n = 8. Mean ± standard deviation.

Figure 38. PTB: Cell Viability and Biofilm Inhibition

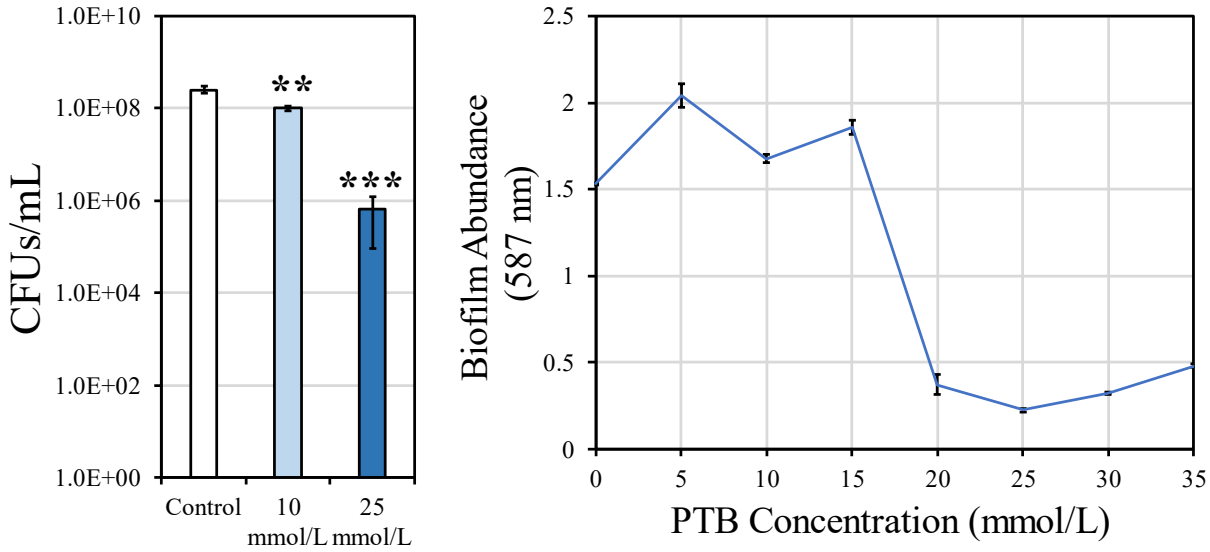

(Left) *S. aureus* cell viability after 24 hours of incubation under planktonic conditions with added PTB. n = 3. Mean ± Standard Deviation. Statistical difference determined by Student's t-test compared to control. ** $p < 0.01$, *** $p < 0.001$.

(Right) Effect of PTB on *S. aureus* biofilm formation provoked by 0.5 mg/mL of glycated keratin. Biofilm assayed after 48 hours of growth under static conditions. n = 8. Mean ± standard deviation.

Figure 39. Rosemary Extract: Cell Viability and Biofilm Inhibition

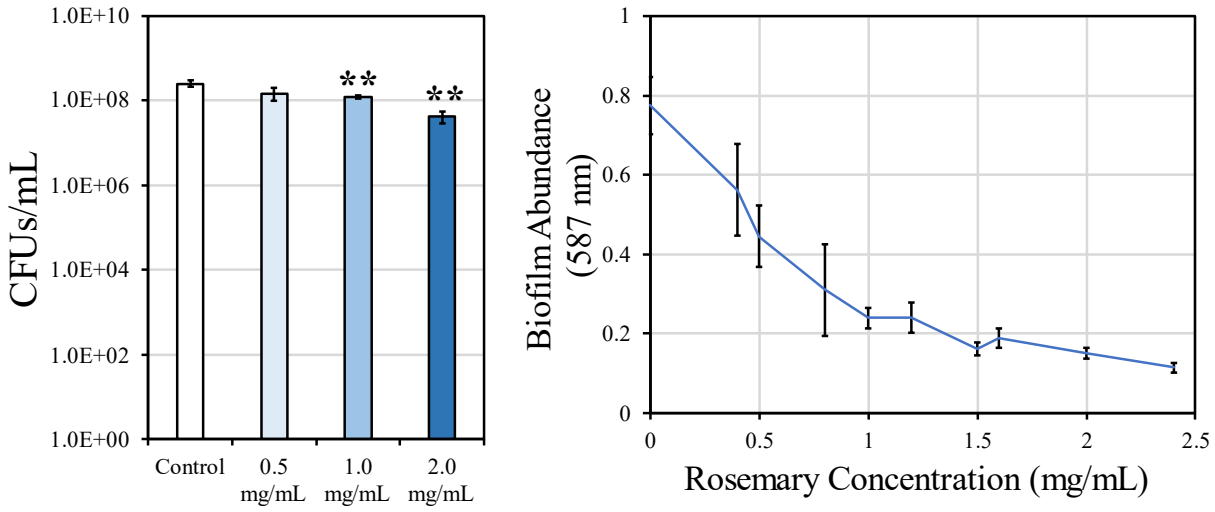

(Left) *S. aureus* cell viability after 24 hours of incubation under planktonic conditions with added rosemary extract. n = 3. Mean ± Standard Deviation. Statistical difference determined by Student's t-test compared to control. ** p <0.01.

(Right) Effect of rosemary extract on *S. aureus* biofilm formation provoked by 0.5 mg/mL of glycated keratin. Biofilm assayed after 48 hours of growth under static conditions. n = 8. Mean ± standard deviation.

Figure 40. Effect of Rosemary Extract on Baseline *S. aureus* Biofilm Formation

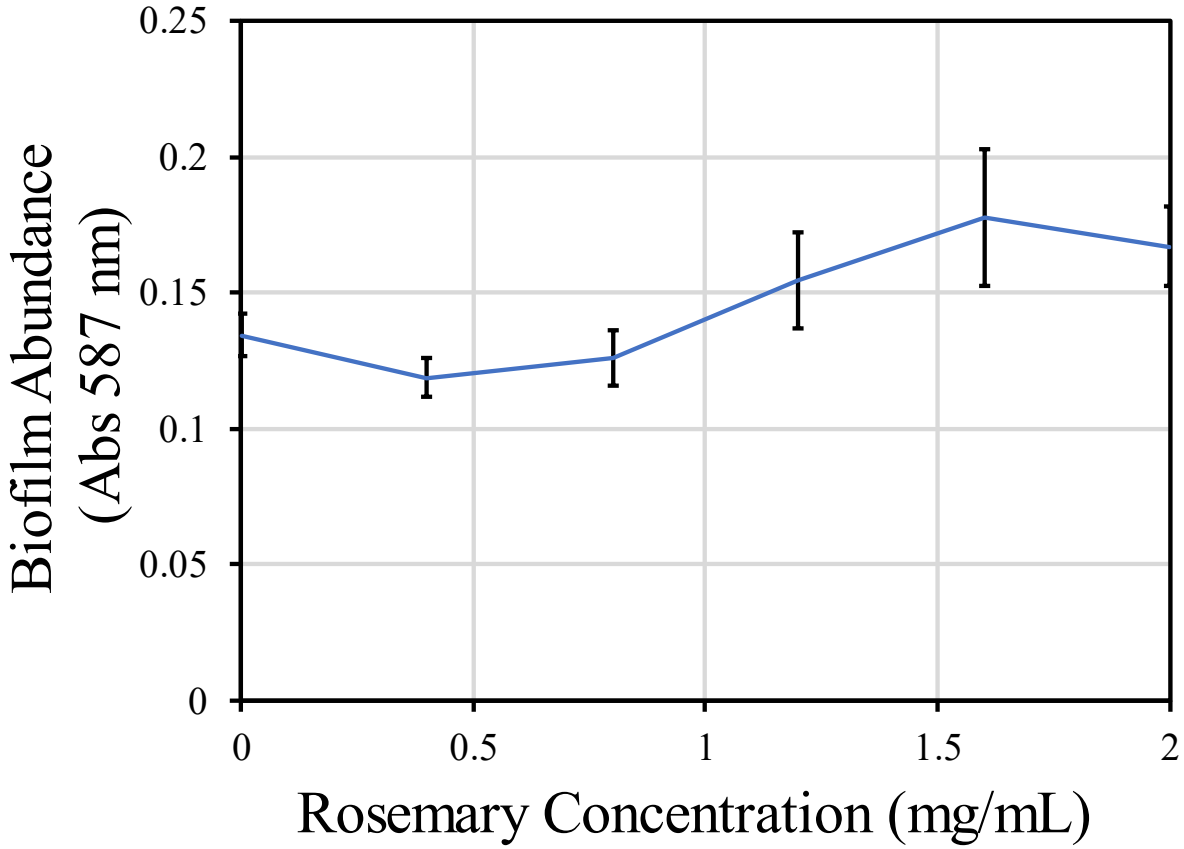

S. aureus biofilm response to various concentrations of rosemary extract. Biofilm assayed after 48 hours of growth under static conditions. n = 8. Mean ± standard deviation.

Figure 41. Dose-Response Curve of Rosemary Extract Biofilm Inhibition

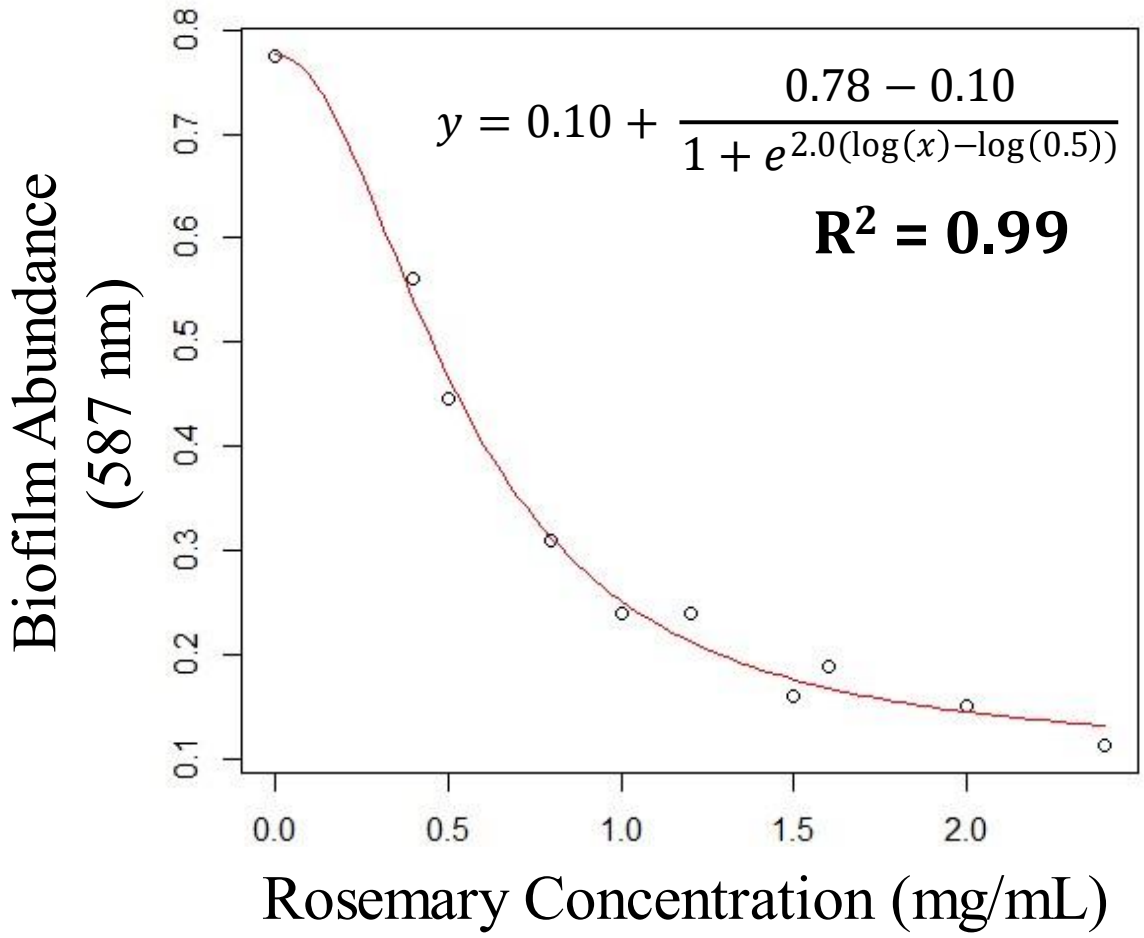

Dose-response relationship of *S. aureus* biofilm abundance induced by exposure to 0.5 mg/mL glycated keratin and rosemary extract concentration. Biofilms were stained with crystal violet and absorbance was measured at 587 nm after 48 hours of growth under static conditions at 37°C. Each data point represents the mean of eight samples. Midpoint = 0.5. $R^2 = 0.99$.

Figure 42. Glycative Stress and Immune Cell Functioning

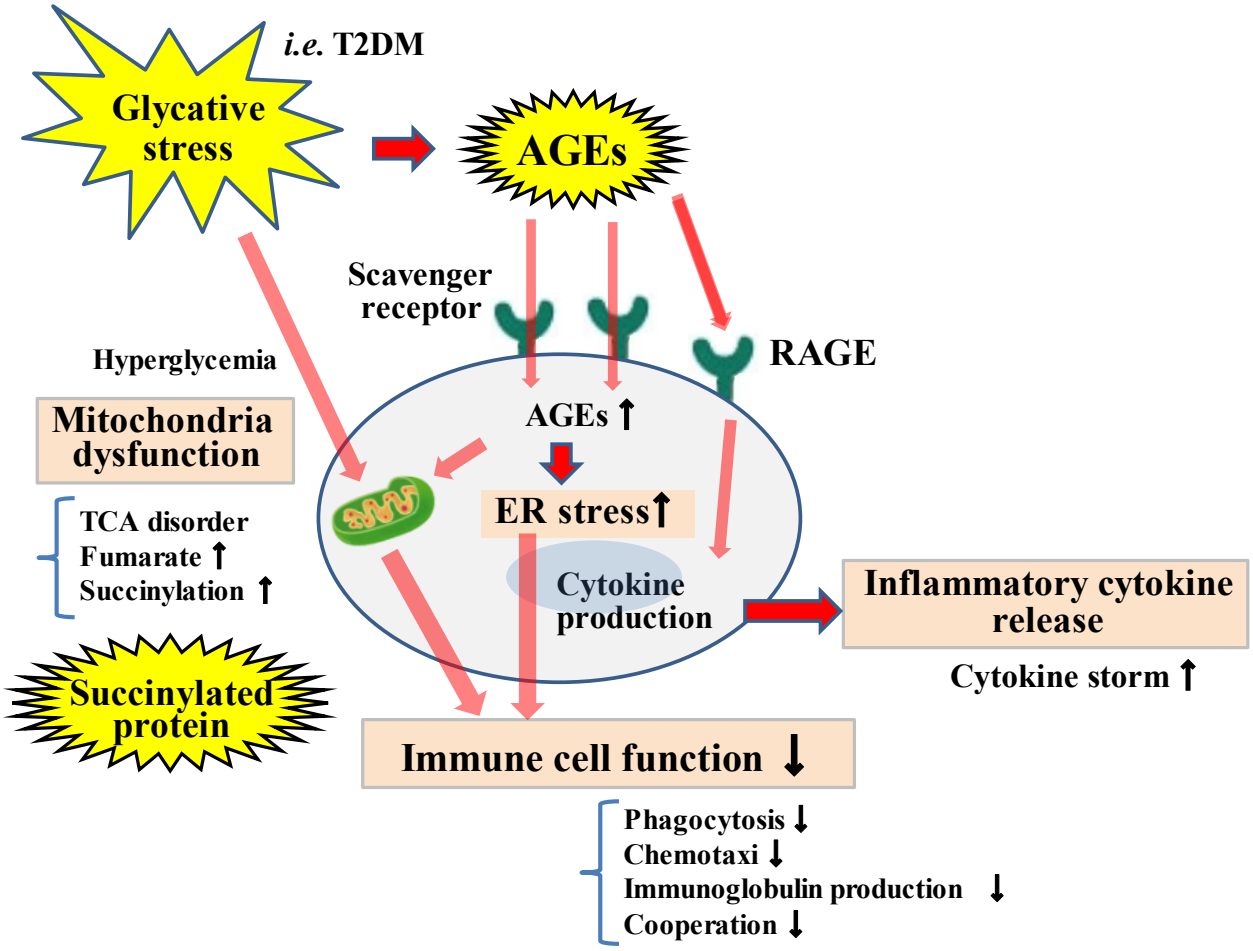

AGEs, advanced glycation endproducts; RAGE, receptor for AGEs; T2DM, type 2 diabetes mellitus; TCA, tricarboxylic acid; ER, endoplasmic reticulum.

Figure 43. Glycative Stress and Skin Microflora.

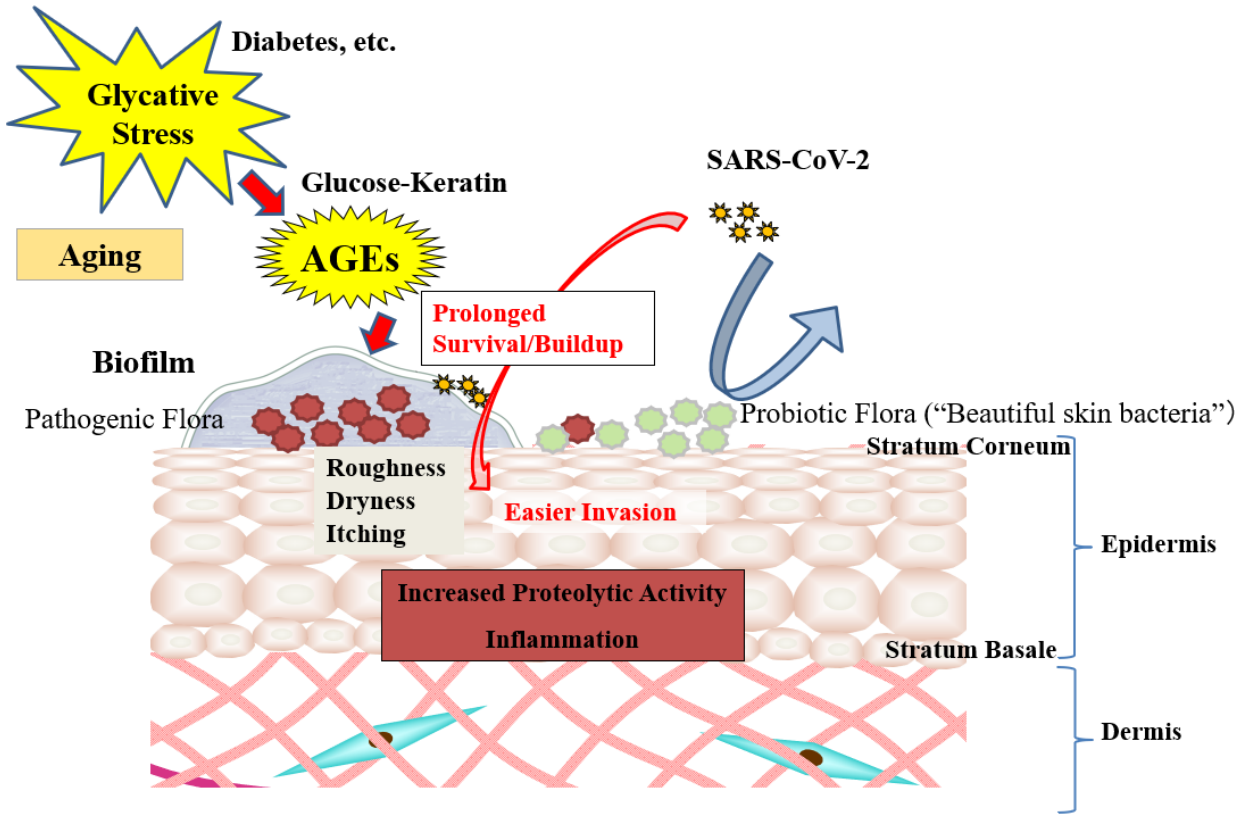

AGEs, advanced glycation endproducts.

Figure 44. Hand Sanitizer Bactericidal Efficacy Test

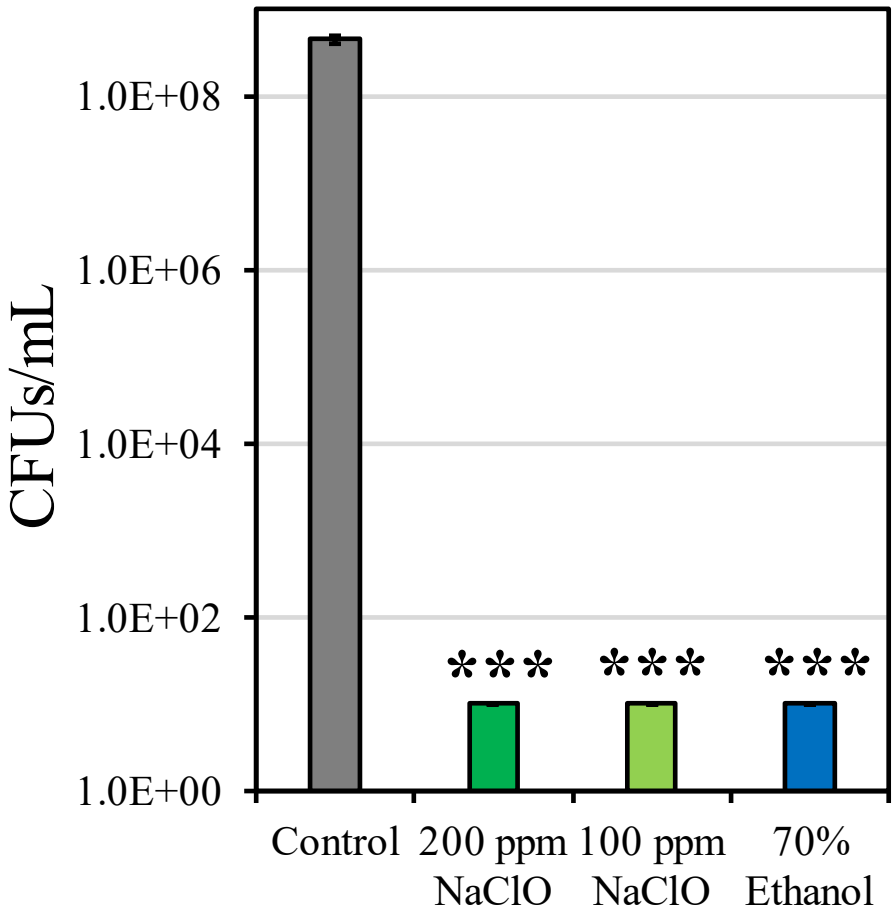

Cell viability of *S. aureus* after 5-minute exposure to hand sanitizing solutions. 1.0E+01 CFUs/mL (10 CFU/mL) is the theoretical minimum detection limit, although no viable colonies were observed. n = 3. Mean ± Standard Deviation. Statistical difference calculated by Student's t-test compared to control. *** $p < 0.001$.

REFERENCES

1. Genuth S, Sun W, Cleary P, et al. Glycation and Carboxymethyllysine Levels in Skin Collagen Predict the Risk of Future 10-Year Progression of Diabetic Retinopathy and Nephropathy in the Diabetes Control and Complications Trial and Epidemiology of Diabetes Interventions and Complications P. *Diabetes*. 2005;54(11):3103-3111.

2. Sambola A, Ruiz-Meana M, Barba I, et al. Glycative and oxidative stress are associated with altered thrombus composition in diabetic patients with ST-elevation myocardial infarction. *Int J Cardiol*. 2017;243:9-14.

3. Rungratanawanich W, Qu Y, Wang X, Essa MM, Song B-J. Advanced glycation end products (AGEs) and other adducts in aging-related diseases and alcohol-mediated tissue injury. *Exp Mol Med*. 2021;53(2):168-188.

4. Haque E, Kamil M, Hasan A, et al. Advanced glycation end products (AGEs), protein aggregation and their cross talk: new insight in tumorigenesis. *Glycobiology*. 2020;30(1):2-18.

5. Teissier T, Boulanger É. The receptor for advanced glycation end-products (RAGE) is an important pattern recognition receptor (PRR) for inflammaging. *Biogerontology*. 2019;20(3):279-301.

6. Yamamoto M, Sugimoto T. Advanced Glycation End Products, Diabetes, and Bone Strength. *Curr Osteoporos Rep*. 2016;14(6):320-326.

7. Son S, Hwang I, Han SH, Shin J-S, Shin OS, Yu J-W. Advanced glycation end products impair NLRP3 inflammasome–mediated innate immune responses in macrophages. *J Biol Chem*. 2017;292(50):20437-20448.

8. Gkogkolou P, Böhm M. Advanced glycation end products: Keyplayers in skin aging? *Dermatoendocrinol*. 2012;4(3):259-270.

9. Yagi M, Yonei Y. Glycative stress and skin aging. *Glycative Stress Res*. 2018;5(1):50-54.

10. Thomas DP, Delbridge L, Morris D, Howell MJ. Cyclohexanone extraction: An improvement in the thiobarbituric acid method for the determination of nonenzymatic

glycosylation of hair and epidermal keratin. *Scand J Clin Lab Invest*. 1984;44(5):457-461.

11. Paisey RB, Clamp JR, Kent MJ, Light ND, Hopton M, Hartog M. Glycosylation of hair: Possible measure of chronic hyperglycaemia. *Br Med J*. 1984;288(6418):669-671.

12. Bakan E, Bakan N. Glycosylation of nail in diabetics: possible marker of long-term hyperglycemia. *Clin Chim Acta*. 1985;147(1):1-5.

13. Corstjens H, Dicanio D, Muizzuddin N, et al. Glycation associated skin autofluorescence and skin elasticity are related to chronological age and body mass index of healthy subjects. *Exp Gerontol*. 2008;43(7):663-667.

14. Lee EJ, Kim JY, Oh SH. Advanced glycation end products (AGEs) promote melanogenesis through receptor for AGEs. *Sci Rep*. 2016;6(June):1-11.

15. Mironova R, Niwa T, Hayashi H, Dimitrova R, Ivanov I. Evidence for non-enzymatic glycosylation in Escherichia coli. *Mol Microbiol*. 2001;39(4):1061-1068.

16. Cohen-Or I, Katz C, Ron EZ. Metabolism of AGEs - Bacterial AGEs Are Degraded by Metallo-Proteases. *PLoS One*. 2013;8(10):1-8.

17. Cohen-Or I, Katz C, Ron EZ. AGEs secreted by bacteria are involved in the inflammatory response. *PLoS One*. 2011;6(3).

18. Katz C, Cohen-Or I, Gophna U, Ron EZ. The Ubiquitous Conserved Glycopeptidase Gcp Prevents Accumulation of Toxic Glycated Proteins. Rappuoli R, ed. *MBio*. 2010;1(3).

19. Odamaki T, Kato K, Sugahara H, et al. Age-related changes in gut microbiota composition from newborn to centenarian: A cross-sectional study. *BMC Microbiol*. 2016;16(1):1-12.

20. Nagpal R, Mainali R, Ahmadi S, et al. Gut microbiome and aging: Physiological and mechanistic insights. *Nutr Heal Aging*. 2018;4(4):267-285.

21. Bien J, Palagani V, Bozko P. The intestinal microbiota dysbiosis and Clostridium difficile infection: is there a relationship with inflammatory bowel disease? *Therap Adv Gastroenterol*. 2013;6(1):53-68.

22. Françoise A, Héry-Arnaud G. The microbiome in cystic fibrosis pulmonary disease.

Genes (Basel). 2020;11(5).

23. Khanolkar RA, Clark ST, Wang PW, et al. Ecological Succession of Polymicrobial Communities in the Cystic Fibrosis Airways. *mSystems*. 2020;5(6):1-16.

24. Valdes AM, Walter J, Segal E, Spector TD. Role of the gut microbiota in nutrition and health. *BMJ*. Published online June 13, 2018:k2179.

25. Morais LH, Schreiber HL, Mazmanian SK. The gut microbiota–brain axis in behaviour and brain disorders. *Nat Rev Microbiol*. 2021;19(4):241-255.

26. Capone KA, Dowd SE, Stamatas GN, Nikolovski J. Diversity of the human skin microbiome early in life. *J Invest Dermatol*. 2011;131(10):2026-2032.

27. Wang Y, Kuo S, Shu M, et al. Implications of probiotics in acne vulgaris. *NIH Public Access*. 2015;25(8):411-424.

28. Cogen AL, Yamasaki K, Muto J, et al. *Staphylococcus epidermidis* antimicrobial δ-toxin (phenol-soluble modulin-γ) cooperates with host antimicrobial peptides to kill group A Streptococcus. *PLoS One*. 2010;5(1):1-7.

29. Sugimoto S, Iwamoto T, Takada K, et al. *Staphylococcus epidermidis* Esp degrades specific proteins associatedwith *Staphylococcus aureus* biofilm formation and host-pathogen interaction. *J Bacteriol*. 2013;195(8):1645-1655.

30. Miller LG, Eells SJ, David MZ, et al. *Staphylococcus aureus* skin infection recurrences among household members: An examination of host, behavioral, and pathogen-level predictors. *Clin Infect Dis*. 2015;60(5):753-763.

31. Secor PR, James GA, Fleckman P, Olerud JE, McInnerney K, Stewart PS. *Staphylococcus aureus* Biofilm and Planktonic cultures differentially impact gene expression, mapk phosphorylation, and cytokine production in human keratinocytes. *BMC Microbiol*. 2011;11(1):143.

32. Park HY, Kim CR, Huh IS, et al. *Staphylococcus aureus* colonization in acute and chronic skin lesions of patients with atopic dermatitis. *Ann Dermatol*. 2013;25(4):410-416.

33. Gong JQ, Lin L, Lin T, et al. Skin colonization by *Staphylococcus aureus* in patients with

eczema and atopic dermatitis and relevant combined topical therapy: A double-blind multicentre randomized controlled trial. *Br J Dermatol*. 2006;155(4):680-687.

34. Ortines R V., Liu H, Cheng LI, et al. Neutralizing Alpha-Toxin Accelerates Healing of *Staphylococcus aureus*-Infected Wounds in Nondiabetic and Diabetic Mice. *Antimicrob Agents Chemother*. 2018;62(3).

35. Nakamura M, Shimakawa T, Nakano S, et al. Screening for nasal carriage of *Staphylococcus aureus* among patients scheduled to undergo orthopedic surgery: Incidence of surgical site infection by nasal carriage. *J Orthop Sci*. 2017;22(4):778-782.

36. Muñoz P, Hortal J, Giannella M, et al. Nasal carriage of S. aureus increases the risk of surgical site infection after major heart surgery. *J Hosp Infect*. 2008;68(1):25-31.

37. Mulcahy ME, McLoughlin RM. *Staphylococcus aureus* and influenza a virus: Partners in coinfection. *MBio*. 2016;7(6):4-7.

38. Goncheva MI, Conceicao C, Tuffs SW, et al. *Staphylococcus aureus* Lipase 1 Enhances Influenza A Virus Replication. Palese P, ed. *MBio*. 2020;11(4):1-16.

39. Duployez C, Le Guern R, Tinez C, et al. Panton-Valentine Leukocidin–Secreting *Staphylococcus aureus* Pneumonia Complicating COVID-19. *Emerg Infect Dis*. 2020;26(8):1939-1941.

40. Ramsey SD, Newton K, Blough D, McCulloch DK, Sandhu N, Wagner EH. Patient-Level Estimates of the Cost of Complications in Diabetes in a Managed-Care Population. *Pharmacoeconomics*. 1999;16(3):285-295.

41. Redel H, Gao Z, Li H, et al. Quantitation and composition of cutaneous microbiota in diabetic and nondiabetic men. *J Infect Dis*. 2013;207(7):1105-1114.

42. Anafo RB, Atiase Y, Kotey FCN, et al. Methicillin-resistant *Staphylococcus aureus* (MRSA) nasal carriage among patients with diabetes at the Korle Bu Teaching Hospital. Bae T, ed. *PLoS One*. 2021;16(9):e0257004.

43. Tamer A, Karabay O, Ekerbicer H. *Staphylococcus aureus* nasal carriage and associated factors in type 2 diabetic patients. *Jpn J Infect Dis*. 2006;59(1):10-14.

44. Lin SY, Lin NY, Huang YY, Hsieh CC, Huang YC. Methicillin-resistant *Staphylococcus aureus* nasal carriage and infection among patients with diabetic foot ulcer. *J Microbiol Immunol Infect*. 2020;53(2):292-299.

45. Hansen MLU, Gotland N, Mejer N, Petersen A, Larsen AR, Benfield T. Diabetes increases the risk of disease and death due to *Staphylococcus aureus* bacteremia. A matched case-control and cohort study. *Infect Dis (Auckl)*. 2017;49(9):689-697.

46. Brown SJ, Kroboth K, Sandilands A, et al. Intragenic Copy Number Variation within Filaggrin Contributes to the Risk of Atopic Dermatitis with a Dose-Dependent Effect. *J Invest Dermatol*. 2012;132(1):98-104.

47. Leung AD, Schiltz AM, Hall CF, Liu AH. Severe atopic dermatitis is associated with a high burden of environmental *Staphylococcus aureus*. *Clin Exp Allergy*. 2008;38(5):789-793.

48. Ogonowska P, Gilaberte Y, Barańska-Rybak W, Nakonieczna J. Colonization With *Staphylococcus aureus* in Atopic Dermatitis Patients: Attempts to Reveal the Unknown. *Front Microbiol*. 2021;11(January):1-19.

49. Di Domenico EG, Cavallo I, Bordignon V, et al. Inflammatory cytokines and biofilm production sustain *Staphylococcus aureus* outgrowth and persistence: a pivotal interplay in the pathogenesis of Atopic Dermatitis. *Sci Rep*. 2018;8(1):9573.

50. Sonesson A, Przybyszewska K, Eriksson S, et al. Identification of bacterial biofilm and the *Staphylococcus aureus* derived protease, staphopain, on the skin surface of patients with atopic dermatitis. *Sci Rep*. 2017;7(1):8689.

51. Hong JY, Kim MJ, Hong JK, et al. In vivo quantitative analysis of advanced glycation end products in atopic dermatitis—Possible culprit for the comorbidities? *Exp Dermatol*. 2020;29(10):1012-1016.

52. Rendon A, Schäkel K. Psoriasis Pathogenesis and Treatment. *Int J Mol Sci*. 2019;20(6):1475.

53. Totté JEE, van der Feltz WT, Hennekam M, van Belkum A, van Zuuren EJ, Pasmans SGMA. Prevalence and odds of S taphylococcus aureus carriage in atopic dermatitis: a

systematic review and meta-analysis. *Br J Dermatol*. 2016;175(4):687-695.

54. Chang H-W, Yan D, Singh R, et al. Alteration of the cutaneous microbiome in psoriasis and potential role in Th17 polarization. *Microbiome*. 2018;6(1):154.

55. Ergun T, Yazici V, Yavuz D, et al. Advanced glycation end products, a potential link between psoriasis and cardiovascular disease: A case–control study. *Indian J Dermatol*. 2019;64(3):201.

56. Papagrigoraki A, Del Giglio M, Cosma C, Maurelli M, Girolomoni G, Lapolla A. Advanced glycation end products are increased in the skin and blood of patients with severe psoriasis. *Acta Derm Venereol*. 2017;97(7):782-787.

57. DELBRIDGE L, ELLIS CS, ROBERTSON K, LEQUESNE LP. Non-enzymatic glycosylation of keratin from the stratum corneum of the diabetic foot. *Br J Dermatol*. 1985;112(5):547-554. doi:10.1111/j.1365-2133.1985.tb15262.x

58. Márová I, Záhejský J, Sehnalová H. Non-enzymatic glycation of epidermal proteins of the stratum corneum in diabetic patients. *Acta Diabetol*. 1995;32(1):38-43.

59. Kim KW, Lee SB. Inhibitory Effect of Maillard Reaction Products on Growth of the Aerobic Marine Hyperthermophilic Archaeon Aeropyrum pernix. *Appl Environ Microbiol*. 2003;69(7):4325-4328.

60. Ozer A, Altuntas CZ, Izgi K, et al. Advanced glycation end products facilitate bacterial adherence in urinary tract infection in diabetic mice. *Pathog Dis*. 2015;73(5):1-10.

61. Snelson M, Coughlan M. Dietary Advanced Glycation End Products: Digestion, Metabolism and Modulation of Gut Microbial Ecology. *Nutrients*. 2019;11(2):215.

62. Hiramoto S, Itoh K, Shizuuchi S, et al. Melanoidin, a Food Protein-Derived Advanced Maillard Reaction Product, Suppresses Helicobacter pylori in vitro and in vivo. *Helicobacter*. 2004;9(5):429-435.

63. Haasbroek K, Takabe W, Yagi M, Yonei Y. The effect of glycative stress on human symbiotic bacterium *Staphylococcus epidermidis*. *Glycative Stress Res*. 2019;6(3):142-150.

64. Hori M, Yagi M, Nomoto K, Ichijo R, Shimode A, Kitano T YY. Experimental models for advanced glycation end product formation using albumin, collagen, elastin, keratin and proteoglycan. *Anti-Aging Med*. 2012;9(6):125-134.

65. Merritt JH, Kadouri DE, O'Toole GA. Growing and Analyzing Static Biofilms. In: *Current Protocols in Microbiology*. John Wiley & Sons, Inc.; 2005.

66. McKenzie K, Maclean M, Grant MH, Ramakrishnan P, MacGregor SJ, Anderson JG. The effects of 405 nm light on bacterial membrane integrity determined by salt and bile tolerance assays, leakage of UV-absorbing material and SYTOX green labelling. *Microbiology*. 2016;162(9):1680-1688.

67. Yanagisawa K, Makita Z, Shiroshita K, et al. Specific fluorescence assay for advanced glycation end products in blood and urine of diabetic patients. *Metabolism*. 1998;47(11):1348-1353.

68. R Core Team. R: A language and environment for statistical computing. Published online 2020. http://www.r-project.org/

69. Ritz C, Baty F, Streibig JC, Gerhard D. Dose-response analysis using R. Xia Y, ed. *PLoS One*. 2015;10(12):e0146021.

70. Lewis IM. THE INHIBITION OF PHYTOMONAS MALVACEARA IN CULTURE MEDIA CONTAINING SUGARS. *J Bacteriol*. 1930;19(6):423-433.

71. Fulmer, EI; Huesselmann B. The Production of a Yeast Growth Stimulant by Heating Media Under Pressure. *Iowa State Coll J Sci*. 1927;1(1):411-418.

72. Smiley KL, Niven CF, Sherman JM. The Nutrition of Streptococcus salivarius . *J Bacteriol*. 1943;45(5):445-454.

73. Spingarn NE, Weisburger JH. Formation of mutagens in cooked foods. I. Beef. *Cancer Lett*. 1979;7(5):259-264.

74. Kim S-B, Kim I-S, Yeum D-M, Park Y-H. Mutagenicity of Maillard reaction products from d-glucose-amino acid mixtures and possible roles of active oxygens in the mutagenicity. *Mutat Res Repair*. 1991;254(1):65-69.

75. Jemmali M. Influence of the Maillard Reaction Products on Some Bacteria of the Intestinal Flora. *J Appl Bacteriol*. 1969;32(2):151-155.

76. Rufián-Henares JA, de la Cueva SP. Antimicrobial Activity of Coffee Melanoidins□A Study of Their Metal-Chelating Properties. *J Agric Food Chem*. 2009;57(2):432-438.

77. Kennedy L, Mehl TD, Elder E. Nonenzymatic glycosylation of serum and plasma proteins. *Diabetes*. 1982;31(Suppl. 3II):52-56.

78. Kawabata K, Yoshikawa H, Saruwatari K, et al. The presence of Nε-(Carboxymethyl) lysine in the human epidermis. *Biochim Biophys Acta - Proteins Proteomics*. 2011;1814(10):1246-1252.

79. Rurián-Henares JA, Morales FJ. Antimicrobial activity of melanoidins against Escherichia coli is mediated by a membrane-damage mechanism. *J Agric Food Chem*. 2008;56(7):2357-2362.

80. Crosby HA, Tiwari N, Kwiecinski JM, et al. The *Staphylococcus aureus* ArlRS two-component system regulates virulence factor expression through MgrA. *Mol Microbiol*. 2020;113(1):103-122.

81. Liang X, Zheng L, Landwehr C, Lunsford D, Holmes D, Ji Y. Global Regulation of Gene Expression by ArlRS, a Two-Component Signal Transduction Regulatory System of *Staphylococcus aureus*. *J Bacteriol*. 2005;187(15):5486-5492.

82. Crosby HA, Schlievert PM, Merriman JA, King JM, Salgado-Pabón W, Horswill AR. The *Staphylococcus aureus* Global Regulator MgrA Modulates Clumping and Virulence by Controlling Surface Protein Expression. Otto M, ed. *PLOS Pathog*. 2016;12(5):e1005604.

83. Walker JN, Crosby HA, Spaulding AR, et al. The *Staphylococcus aureus* ArlRS Two-Component System Is a Novel Regulator of Agglutination and Pathogenesis. Peschel A, ed. *PLoS Pathog*. 2013;9(12):e1003819.

84. Dastgheyb SS, Hammoud S, Ketonis C, et al. Staphylococcal Persistence Due to Biofilm Formation in Synovial Fluid Containing Prophylactic Cefazolin. *Antimicrob Agents Chemother*. 2015;59(4):2122-2128.

85. Haaber J, Cohn MT, Frees D, Andersen TJ, Ingmer H. Planktonic Aggregates of *Staphylococcus aureus* Protect against Common Antibiotics. Otto M, ed. *PLoS One*. 2012;7(7):e41075.

86. Alhede M, Lorenz M, Fritz BG, et al. Bacterial aggregate size determines phagocytosis efficiency of polymorphonuclear leukocytes. *Med Microbiol Immunol*. 2020;209(6):669-680.

87. Josefsson E, Hartford O, O'Brien L, Patti JM, Foster T. Protection against Experimental *Staphylococcus aureus* Arthritis by Vaccination with Clumping Factor A, a Novel Virulence Determinant. *J Infect Dis*. 2001;184(12):1572-1580.

88. McAdow M, Kim HK, DeDent AC, Hendrickx APA, Schneewind O, Missiakas DM. Preventing *Staphylococcus aureus* Sepsis through the Inhibition of Its Agglutination in Blood. Sullam PM, ed. *PLoS Pathog*. 2011;7(10):e1002307.

89. Moreillon P, Entenza JM, Francioli P, et al. Role of *Staphylococcus aureus* coagulase and clumping factor in pathogenesis of experimental endocarditis. *Infect Immun*. 1995;63(12):4738-4743.

90. Vernachio J, Bayer AS, Le T, et al. Anti-Clumping Factor A Immunoglobulin Reduces the Duration of Methicillin-Resistant *Staphylococcus aureus* Bacteremia in an Experimental Model of Infective Endocarditis. *Antimicrob Agents Chemother*. 2003;47(11):3400-3406.

91. Staats A, Burback PW, Eltobgy M, et al. Synovial Fluid-Induced Aggregation Occurs across *Staphylococcus aureus* Clinical Isolates and is Mechanistically Independent of Attached Biofilm Formation. Zhang K, ed. *Microbiol Spectr*. 2021;9(2).

92. Kaplan JB, Izano EA, Gopal P, et al. Low Levels of β-Lactam Antibiotics Induce Extracellular DNA Release and Biofilm Formation in *Staphylococcus aureus*. Dunman P, Pier G, eds. *MBio*. 2012;3(4).

93. Corno G, Coci M, Giardina M, Plechuk S, Campanile F, Stefani S. Antibiotics promote aggregation within aquatic bacterial communities. *Front Microbiol*. 2014;5.

94. Ricciardi BF, Muthukrishnan G, Masters E, Ninomiya M, Lee CC, Schwarz EM. *Staphylococcus aureus* Evasion of Host Immunity in the Setting of Prosthetic Joint

Infection: Biofilm and Beyond. *Curr Rev Musculoskelet Med*. 2018;11(3):389-400.

95. Silva-Santana G, Lenzi-Almeida KC, Lopes VGS, Aguiar-Alves F. Biofilm formation in catheter-related infections by Panton-Valentine leukocidin-producing *Staphylococcus aureus*. *Int Microbiol*. 2016;19(4):199-207.

96. Tsukahara H, Shibata R, Ohta N, et al. High levels of urinary pentosidine, an advanced glycation end product, in children with acute exacerbation of atopic dermatitis: Relationship with oxidative stress. *Metabolism*. 2003;52(12):1601-1605.

97. Kopeć-Pyciarz K, Makulska I, Zwolińska D, Łaczmański Ł, Baran W. Skin autofluorescence, as a measure of age accumulation in individuals suffering from chronic plaque psoriasis. *Mediators Inflamm*. 2018;2018:6-9.

98. Ng CY, Huang YH, Chu CF, Wu TC, Liu SH. Risks for *Staphylococcus aureus* colonization in patients with psoriasis: a systematic review and meta-analysis. *Br J Dermatol*. 2017;177(4):967-977.

99. Gupta S, Laskar N, Kadouri DE. Evaluating the Effect of Oxygen Concentrations on Antibiotic Sensitivity, Growth, and Biofilm Formation of Human Pathogens. *Microbiol Insights*. 2016;9:MBI.S40767.

100. Cramton SE, Ulrich M, Götz F, Döring G. Anaerobic Conditions Induce Expression of Polysaccharide Intercellular Adhesin in *Staphylococcus aureus* and *Staphylococcus epidermidis*. O'Brien AD, ed. *Infect Immun*. 2001;69(6):4079-4085.

101. Mashruwala AA, Guchte A van de, Boyd JM. Impaired respiration elicits SrrAB-dependent programmed cell lysis and biofilm formation in *Staphylococcus aureus*. *Elife*. 2017;6.

102. Efthimiou G, Tsiamis G, Typas MA, Pappas KM. Transcriptomic Adjustments of *Staphylococcus aureus* COL (MRSA) Forming Biofilms Under Acidic and Alkaline Conditions. *Front Microbiol*. 2019;10.

103. Rode TM, Langsrud S, Holck A, Møretrø T. Different patterns of biofilm formation in *Staphylococcus aureus* under food-related stress conditions. *Int J Food Microbiol*. 2007;116(3):372-383.

104. Slany M, Oppelt J, Cincarova L. Formation of *Staphylococcus aureus* Biofilm in the Presence of Sublethal Concentrations of Disinfectants Studied via a Transcriptomic Analysis Using Transcriptome Sequencing (RNA-seq). Schaffner DW, ed. *Appl Environ Microbiol*. 2017;83(24).

105. O'Neill E, Pozzi C, Houston P, et al. A Novel *Staphylococcus aureus* Biofilm Phenotype Mediated by the Fibronectin-Binding Proteins, FnBPA and FnBPB. *J Bacteriol*. 2008;190(11):3835-3850.

106. Herman-Bausier P, Valotteau C, Pietrocola G, et al. Mechanical Strength and Inhibition of the *Staphylococcus aureus* Collagen-Binding Protein Cna. *MBio*. 2016;7(5).

107. Trivedi S, Uhlemann A-C, Herman-Bausier P, et al. The Surface Protein SdrF Mediates *Staphylococcus epidermidis* Adherence to Keratin. *J Infect Dis*. 2017;215(12):1846-1854.

108. Pepper ED, Farrell MJ, Nord G, Finkel SE. Antiglycation Effects of Carnosine and Other Compounds on the Long-Term Survival of Escherichia coli. *Appl Environ Microbiol*. 2010;76(24):7925-7930.

109. Thornalley PJ. Use of aminoguanidine (Pimagedine) to prevent the formation of advanced glycation endproducts. *Arch Biochem Biophys*. 2003;419(1):31-40.

110. Hellwig M, Auerbach C, Müller N, et al. Metabolization of the Advanced Glycation End Product N -ε-Carboxymethyllysine (CML) by Different Probiotic E. coli Strains. *J Agric Food Chem*. 2019;67(7):1963-1972.

111. Hellwig M, Bunzel D, Huch M, Franz CMAP, Kulling SE, Henle T. Stability of Individual Maillard Reaction Products in the Presence of the Human Colonic Microbiota. *J Agric Food Chem*. 2015;63(30):6723-6730.

112. Narda M, Peno-Mazzarino L, Krutmann J, Trullas C, Granger C. Novel Facial Cream Containing Carnosine Inhibits Formation of Advanced Glycation End-Products in Human Skin. *Skin Pharmacol Physiol*. 2018;31(6):324-331.

113. Hiron A, Borezée-Durant E, Piard J-C, Juillard V. Only One of Four Oligopeptide Transport Systems Mediates Nitrogen Nutrition in *Staphylococcus aureus*. *J Bacteriol*. 2007;189(14):5119-5129.

114. Mack D, Fischer W, Krokotsch A, et al. The intercellular adhesin involved in biofilm accumulation of *Staphylococcus epidermidis* is a linear beta-1,6-linked glucosaminoglycan: purification and structural analysis. *J Bacteriol*. 1996;178(1):175-183.

115. Heilmann C, Schweitzer O, Gerke C, Vanittanakom N, Mack D, Götz F. Molecular basis of intercellular adhesion in the biofilm-forming *Staphylococcus epidermidis*. *Mol Microbiol*. 1996;20(5):1083-1091.

116. Vuong C, Voyich JM, Fischer ER, et al. Polysaccharide intercellular adhesin (PIA) protects *Staphylococcus epidermidis* against major components of the human innate immune system. *Cell Microbiol*. 2004;6(3):269-275.

117. Wu Y, Wang J, Xu T, et al. The Two-Component Signal Transduction System ArlRS Regulates *Staphylococcus epidermidis* Biofilm Formation in an ica-Dependent Manner. Otto M, ed. *PLoS One*. 2012;7(7):e40041.

118. Arciola CR, Campoccia D, Ravaioli S, Montanaro L. Polysaccharide intercellular adhesin in biofilm: structural and regulatory aspects. *Front Cell Infect Microbiol*. 2015;5.

119. van Schaik W, Abee T. The role of σB in the stress response of Gram-positive bacteria – targets for food preservation and safety. *Curr Opin Biotechnol*. 2005;16(2):218-224.

120. Valle J, Vergara-Irigaray M, Merino N, Penadés JR, Lasa I. σ B Regulates IS 256 - Mediated *Staphylococcus aureus* Biofilm Phenotypic Variation. *J Bacteriol*. 2007;189(7):2886-2896.

121. Chan PF, Foster SJ, Ingham E, Clements MO. The *Staphylococcus aureus* Alternative Sigma Factor ς B Controls the Environmental Stress Response but Not Starvation Survival or Pathogenicity in a Mouse Abscess Model. *J Bacteriol*. 1998;180(23):6082-6089.

122. Latasa C, Solano C, Penadés JR, Lasa I. Biofilm-associated proteins. *C R Biol*. 2006;329(11):849-857.

123. Tormo MÁ, Knecht E, Götz F, Lasa I, Penadés JR. Bap-dependent biofilm formation by pathogenic species of Staphylococcus: evidence of horizontal gene transfer? *Microbiology*. 2005;151(7):2465-2475.

124. Cucarella C, Tormo MA, Úbeda C, et al. Role of Biofilm-Associated Protein Bap in the Pathogenesis of Bovine *Staphylococcus aureus*. *Infect Immun*. 2004;72(4):2177-2185.

125. Cucarella C, Solano C, Valle J, Amorena B, Lasa I, Penadés JR. Bap, a *Staphylococcus aureus* Surface Protein Involved in Biofilm Formation. *J Bacteriol*. 2001;183(9):2888-2896.

126. Kavanaugh JS, Flack CE, Lister J, et al. Identification of Extracellular DNA-Binding Proteins in the Biofilm Matrix. Losick R, ed. *MBio*. 2019;10(3).

127. Sugimoto S, Sato F, Miyakawa R, et al. Broad impact of extracellular DNA on biofilm formation by clinically isolated Methicillin-resistant and -sensitive strains of *Staphylococcus aureus*. *Sci Rep*. 2018;8(1):2254.

128. Memmi G, Nair DR, Cheung A. Role of ArlRS in Autolysis in Methicillin-Sensitive and Methicillin-Resistant *Staphylococcus aureus* Strains. *J Bacteriol*. 2012;194(4):759-767.

129. Ranjit DK, Endres JL, Bayles KW. *Staphylococcus aureus* CidA and LrgA Proteins Exhibit Holin-Like Properties. *J Bacteriol*. 2011;193(10):2468-2476.

130. Savva CG, Dewey JS, Deaton J, et al. The holin of bacteriophage lambda forms rings with large diameter. *Mol Microbiol*. 2008;69(4):784-793.

131. Rice KC, Mann EE, Endres JL, et al. The cidA murein hydrolase regulator contributes to DNA release and biofilm development in *Staphylococcus aureus*. *Proc Natl Acad Sci*. 2007;104(19):8113-8118.

132. Groicher KH, Firek BA, Fujimoto DF, Bayles KW. The *Staphylococcus aureus* lrgAB Operon Modulates Murein Hydrolase Activity and Penicillin Tolerance. *J Bacteriol*. 2000;182(7):1794-1801.

133. Sharma-Kuinkel BK, Mann EE, Ahn J-S, Kuechenmeister LJ, Dunman PM, Bayles KW. The *Staphylococcus aureus* LytSR Two-Component Regulatory System Affects Biofilm Formation. *J Bacteriol*. 2009;191(15):4767-4775.

134. Kazi RS, Banarjee RM, Deshmukh AB, Patil G V., Jagadeeshaprasad MG, Kulkarni MJ. Glycation inhibitors extend yeast chronological lifespan by reducing advanced glycation

end products and by back regulation of proteins involved in mitochondrial respiration. *J Proteomics*. 2017;156:104-112.

135. Moores J. Vitamin C: a wound healing perspective. *Br J Community Nurs*. 2013;18(Sup12):S6-S11.

136. Padayatty SJ, Katz A, Wang Y, et al. Vitamin C as an Antioxidant: Evaluation of Its Role in Disease Prevention. *J Am Coll Nutr*. 2003;22(1):18-35.

137. Mousavi S, Bereswill S, Heimesaat MM. Immunomodulatory and antimicrobial effects of vitamin C. *Eur J Microbiol Immunol*. 2019;9(3):73-79.

138. Shivaprasad D, Taneja NK, Lakra A, Sachdev D. In vitro and in situ abrogation of biofilm formation in E. coli by vitamin C through ROS generation, disruption of quorum sensing and exopolysaccharide production. *Food Chem*. 2021;341:128171.

139. Eydou Z, Jad BN, Elsayed Z, Ismail A, Magaogao M, Hossain A. Investigation on the effect of vitamin C on growth & biofilm-forming potential of Streptococcus mutans isolated from patients with dental caries. *BMC Microbiol*. 2020;20(1):231.

140. Pandit S, Ravikumar V, Abdel-Haleem AM, et al. Low Concentrations of Vitamin C Reduce the Synthesis of Extracellular Polymers and Destabilize Bacterial Biofilms. *Front Microbiol*. 2017;8.

141. Mirani ZA, Khan MN, Siddiqui A, et al. Ascorbic acid augments colony spreading by reducing biofilm formation of methicillin resistant *Staphylococcus aureus*. *Iran J Basic Med Sci*. 2018;21(2):175-180.

142. Vinson JA, Howard TB. Inhibition of protein glycation and advanced glycation end products by ascorbic acid and other vitamins and nutrients. *J Nutr Biochem*. 1996;7(12):659-663.

143. Song Q, Liu J, Dong L, Wang X, Zhang X. Novel advances in inhibiting advanced glycation end product formation using natural compounds. *Biomed Pharmacother*. 2021;140:111750.

144. Kırmusaoğlu S, Kaşıkçı H. Identification of ica -dependent biofilm production by

Staphylococcus aureus clinical isolates and antibiofilm effects of ascorbic acid against biofilm production. *J Clin Pathol*. 2020;73(5):261-266.

145. Sztretye M, Dienes B, Gönczi M, et al. Astaxanthin: A Potential Mitochondrial-Targeted Antioxidant Treatment in Diseases and with Aging. *Oxid Med Cell Longev*. 2019;2019:1-14.

146. Park CH, Xu FH, Roh S-S, et al. Astaxanthin and Corni Fructus Protect Against Diabetes-Induced Oxidative Stress, Inflammation, and Advanced Glycation End Product in Livers of Streptozotocin-Induced Diabetic Rats. *J Med Food*. 2015;18(3):337-344.

147. Sun Z, Liu J, Zeng X, et al. Astaxanthin is responsible for antiglycoxidative properties of microalga Chlorella zofingiensis. *Food Chem*. 2011;126(4):1629-1635.

148. Haasbroek K, Takabe W, Yagi M, Yonei Y. High-fat Diet Induced Dysbiosis & Amelioration by Astaxanthin. *Rad Hrvat Akad Znan i Umjet Med Znan*. 2019;49(December):58-66.

149. Zhang L, Gu B, Wang Y. Clove essential oil confers antioxidant activity and lifespan extension in C. elegans via the DAF-16/FOXO transcription factor. *Comp Biochem Physiol Part C Toxicol Pharmacol*. 2021;242:108938.

150. Han X, Parker TL. Anti-inflammatory activity of clove (Eugenia caryophyllata) essential oil in human dermal fibroblasts. *Pharm Biol*. 2017;55(1):1619-1622.

151. Barboza JN, da Silva Maia Bezerra Filho C, Silva RO, Medeiros JVR, de Sousa DP. An Overview on the Anti-inflammatory Potential and Antioxidant Profile of Eugenol. *Oxid Med Cell Longev*. 2018;2018:1-9.

152. Nirmala MJ, Durai L, Gopakumar V, Nagarajan R. Anticancer and antibacterial effects of a clove bud essential oil-based nanoscale emulsion system. *Int J Nanomedicine*. 2019;Volume 14:6439-6450.

153. Kubatka P, Uramova S, Kello M, et al. Antineoplastic effects of clove buds (Syzygium aromaticum L.) in the model of breast carcinoma. *J Cell Mol Med*. 2017;21(11):2837-2851.

154. Nuñez L, D'Aquino M. Microbicide activity of clove essential oil (Eugenia caryophyllata). *Brazilian J Microbiol*. 2012;43(4):1255-1260.

155. Prashar A, Locke IC, Evans CS. Cytotoxicity of clove (Syzygium aromaticum) oil and its major components to human skin cells. *Cell Prolif*. 2006;39(4):241-248.

156. Tarocco A, Caroccia N, Morciano G, et al. Melatonin as a master regulator of cell death and inflammation: molecular mechanisms and clinical implications for newborn care. *Cell Death Dis*. 2019;10(4):317.

157. Jin H, Zhang Z, Wang C, et al. Melatonin protects endothelial progenitor cells against AGE-induced apoptosis via autophagy flux stimulation and promotes wound healing in diabetic mice. *Exp Mol Med*. 2018;50(11):1-15.

158. Dontsov AE, Vospelnikova ND, Zack PP, Ostrovsky MA. Antiglycation activity of melatonin. *Dokl Biochem Biophys*. 2017;475(1):283-286.

159. Takabe W, Mitsuhashi R, Parengkuan L, Yagi M, Yonei Y. Cleaving effect of melatonin on crosslinks in advanced glycation end products. *Glycative Stress Res*. 2016;3(1):038-043.

160. Paulose JK, Wright JM, Patel AG, Cassone VM. Human Gut Bacteria Are Sensitive to Melatonin and Express Endogenous Circadian Rhythmicity. Yamazaki S, ed. *PLoS One*. 2016;11(1):e0146643.

161. Park YS, Kim SH, Park JW, et al. Melatonin in the colon modulates intestinal microbiota in response to stress and sleep deprivation. *Intest Res*. 2020;18(3):325-336.

162. Kim SW, Kim S, Son M, Cheon JH, Park YS. Melatonin controls microbiota in colitis by goblet cell differentiation and antimicrobial peptide production through Toll-like receptor 4 signalling. *Sci Rep*. 2020;10(1):2232.

163. Jiao J, Ma Y, Chen S, et al. Melatonin-Producing Endophytic Bacteria from Grapevine Roots Promote the Abiotic Stress-Induced Production of Endogenous Melatonin in Their Hosts. *Front Plant Sci*. 2016;7.

164. Bishayi B, Adhikary R, Nandi A, Sultana S. Beneficial Effects of Exogenous Melatonin in

Acute *Staphylococcus aureus* and Escherichia coli Infection-Induced Inflammation and Associated Behavioral Response in Mice After Exposure to Short Photoperiod. *Inflammation*. 2016;39(6):2072-2093.

165. Tekbas OF, Ogur R, Korkmaz A, Kilic A, Reiter RJ. Melatonin as an antibiotic: new insights into the actions of this ubiquitous molecule. *J Pineal Res*. 2008;44(2):222-226.

166. Masadeh M, Alzoubi K, Al-azzam S, Khabour O, Al-buhairan A. Ciprofloxacin-Induced Antibacterial Activity Is Atteneuated by Pretreatment with Antioxidant Agents. *Pathogens*. 2016;5(1):28.

167. ATROSHI F, RIZZO A, WESTERMARCK T, ALI-VEHMAS T. EFFECTS OF TAMOXIFEN, MELATONIN, COENZYME Q10, ANDl-CARNITINE SUPPLEMENTATION ON BACTERIAL GROWTH IN THE PRESENCE OF MYCOTOXINS. *Pharmacol Res*. 1998;38(4):289-295.

168. Nogueira LM, Sampson JN, Chu LW, et al. Individual Variations in Serum Melatonin Levels through Time: Implications for Epidemiologic Studies. Behrens T, ed. *PLoS One*. 2013;8(12):e83208.

169. Hsing AW, Meyer TE, Niwa S, Quraishi SM, Chu LW. Measuring Serum Melatonin in Epidemiologic Studies. *Cancer Epidemiol Biomarkers Prev*. 2010;19(4):932-937.

170. Zhdanova I V., Wurtman RJ, Balcioglu A, Kartashov AI, Lynch HJ. Endogenous Melatonin Levels and the Fate of Exogenous Melatonin: Age Effects. *Journals Gerontol Ser A Biol Sci Med Sci*. 1998;53A(4):B293-B298.

171. Slominski A, Tobin DJ, Zmijewski MA, Wortsman J, Paus R. Melatonin in the skin: synthesis, metabolism and functions. *Trends Endocrinol Metab*. 2008;19(1):17-24.

172. Kim T-K, Lin Z, Tidwell WJ, Li W, Slominski AT. Melatonin and its metabolites accumulate in the human epidermis in vivo and inhibit proliferation and tyrosinase activity in epidermal melanocytes in vitro. *Mol Cell Endocrinol*. 2015;404:1-8.

173. Song R, Ren L, Ma H, et al. Melatonin promotes diabetic wound healing in vitro by regulating keratinocyte activity. *Am J Transl Res*. 2016;8(11):4682-4693.

174. Aldini G, Vistoli G, Stefek M, et al. Molecular strategies to prevent, inhibit, and degrade advanced glycoxidation and advanced lipoxidation end products. *Free Radic Res*. 2013;47(sup1):93-137.

175. Cooper ME, Thallas V, Forbes J, Scalbert E, Sastra S, Darby I, Soulis T. The cross-link breaker, N-phenacylthiazolium bromide prevents vascular advanced glycation end-product accumulation. *Diabetologia*. 2000 May;43(5):660-4.

176. Hollenbach S, Thampi P, Viswanathan T, Abraham EC. Cleavage of in vitro and in vivo formed lens protein cross-links by a novel cross-link breaker. *Mol Cell Biochem*. 2003;243(1-2):73-80.

177. Chang P-C, Tsai S-C, Chong LY, Kao M-J. N-Phenacylthiazolium Bromide Inhibits the Advanced Glycation End Product (AGE)–AGE Receptor Axis to Modulate Experimental Periodontitis in Rats. *J Periodontol*. 2014;85(7):e268-e276.

178. Bradke BS, Vashishth D. N-Phenacylthiazolium Bromide Reduces Bone Fragility Induced by Nonenzymatic Glycation. Roeder RK, ed. *PLoS One*. 2014;9(7):e103199.

179. Nieto G, Ros G, Castillo J. Antioxidant and Antimicrobial Properties of Rosemary (Rosmarinus officinalis, L.): A Review. *Medicines*. 2018;5(3):98.

180. Shen Y, Han J, Zheng X, et al. Rosemary leaf extract inhibits glycation, breast cancer proliferation, and diabetes risks. *Appl Sci*. 2020;10(7).

181. Jean D, Pouligon M, Dalle C. Evaluation in vitro of AGE-crosslinks breaking ability of rosmarinic acid. *Glycative Stress Res*. 2015;2(1):204-207.

182. Azar WS, Njeim R, Fares AH, et al. COVID-19 and diabetes mellitus: how one pandemic worsens the other. *Rev Endocr Metab Disord*. 2020;21(4):451-463.

183. Mozafari N, Azadi S, Mehdi-Alamdarlou S, Ashrafi H, Azadi A. Inflammation: A bridge between diabetes and COVID-19, and possible management with sitagliptin. *Med Hypotheses*. 2020;143:110111.

184. Rajpal A, Rahimi L, Ismail-Beigi F. Factors leading to high morbidity and mortality of COVID-19 in patients with type 2 diabetes. *J Diabetes*. 2020;12(12):895-908.

185. Krause M, Gerchman F, Friedman R. Coronavirus infection (SARS-CoV-2) in obesity and diabetes comorbidities: is heat shock response determinant for the disease complications? *Diabetol Metab Syndr*. 2020;12(1):63.

186. Nakamura J, Kamiya H, Haneda M, et al. Causes of death in Japanese patients with diabetes based on the results of a survey of 45,708 cases during 2001-2010: Report of the Committee on Causes of Death in Diabetes Mellitus. *J Diabetes Investig*. 2017;8(3):397-410.

187. Barron E, Bakhai C, Kar P, et al. Associations of type 1 and type 2 diabetes with COVID-19-related mortality in England: a whole-population study. *Lancet Diabetes Endocrinol*. 2020;8(10):813-822.

188. Holman N, Knighton P, Kar P, et al. Risk factors for COVID-19-related mortality in people with type 1 and type 2 diabetes in England: a population-based cohort study. *Lancet Diabetes Endocrinol*. 2020;8(10):823-833.

189. Lansbury L, Lim B, Baskaran V, Lim WS. Co-infections in people with COVID-19: a systematic review and meta-analysis. *J Infect*. 2020;81(2):266-275.

190. Lai C-C, Wang C-Y, Hsueh P-R. Co-infections among patients with COVID-19: The need for combination therapy with non-anti-SARS-CoV-2 agents? *J Microbiol Immunol Infect*. 2020;53(4):505-512.

191. Sivitz WI, Yorek MA. Mitochondrial Dysfunction in Diabetes: From Molecular Mechanisms to Functional Significance and Therapeutic Opportunities. *Antioxid Redox Signal*. 2010;12(4):537-577.

192. Nagai R, Brock JW, Blatnik M, et al. Succination of Protein Thiols during Adipocyte Maturation. *J Biol Chem*. 2007;282(47):34219-34228.

193. Iwashima Y, Eto M, Hata A, et al. Advanced Glycation End Products-Induced Gene Expression of Scavenger Receptors in Cultured Human Monocyte-Derived Macrophages. *Biochem Biophys Res Commun*. 2000;277(2):368-380.

194. Hamasaki S, Kobori T, Yamazaki Y, et al. Effects of scavenger receptors-1 class A stimulation on macrophage morphology and highly modified advanced glycation end

product-protein phagocytosis. *Sci Rep*. 2018;8(1):5901.

195. Yamabe S, Hirose J, Uehara Y, et al. Intracellular accumulation of advanced glycation end products induces apoptosis via endoplasmic reticulum stress in chondrocytes. *FEBS J*. 2013;280(7):1617-1629.

196. Liu BF, Miyata S, Kojima H, et al. Low phagocytic activity of resident peritoneal macrophages in diabetic mice: relevance to the formation of advanced glycation end products. *Diabetes*. 1999;48(10):2074-2082.

197. Sannomiya P, Pereira MAA, Garcia-Leme J. Inhibition of leukocyte chemotaxis by serum factor in diabetes mellitus: Selective depression of cell responses mediated by complement-derived chemoattractants. *Agents Actions*. 1990;30(3-4):369-376.

198. Touré F, Zahm J-M, Garnotel R, et al. Receptor for advanced glycation end-products (RAGE) modulates neutrophil adhesion and migration on glycoxidated extracellular matrix. *Biochem J*. 2008;416(2):255-261.

199. Kaneshige H, Sakai H. The inhibitory effects of diabetic sera on in vitro production of cytoplasmic immunoglobulins in normal lymphocytes. *J Japan Diab Soc*. 1983;26:105-110.

200. Lin L, Park S, Lakatta EG. RAGE signaling in inflammation and arterial aging. *Front Biosci*. 2009;14(4):1403-1413.

201. Raony Í, Saggioro de Figueiredo C. Retinal outcomes of COVID-19: Possible role of CD147 and cytokine storm in infected patients with diabetes mellitus. *Diabetes Res Clin Pract*. 2020;165:108280.

202. Xu H, Zhong L, Deng J, et al. High expression of ACE2 receptor of 2019-nCoV on the epithelial cells of oral mucosa. *Int J Oral Sci*. 2020;12(1):8.

203. Hoffmann M, Kleine-Weber H, Schroeder S, et al. SARS-CoV-2 Cell Entry Depends on ACE2 and TMPRSS2 and Is Blocked by a Clinically Proven Protease Inhibitor. *Cell*. 2020;181(2):271-280.e8.

204. Hoffmann M, Kleine-Weber H, Pöhlmann S. A Multibasic Cleavage Site in the Spike

Protein of SARS-CoV-2 Is Essential for Infection of Human Lung Cells. *Mol Cell*. 2020;78(4):779-784.e5.

205. Jaimes JA, Millet JK, Whittaker GR. Proteolytic Cleavage of the SARS-CoV-2 Spike Protein and the Role of the Novel S1/S2 Site. *iScience*. 2020;23(6):101212.

206. Williams MR, Nakatsuji T, Sanford JA, Vrbanac AF, Gallo RL. *Staphylococcus aureus* Induces Increased Serine Protease Activity in Keratinocytes. *J Invest Dermatol*. 2017;137(2):377-384.

207. Burian M, Plange J, Schmitt L, et al. Adaptation of *Staphylococcus aureus* to the Human Skin Environment Identified Using an ex vivo Tissue Model. *Front Microbiol*. 2021;12.

208. Miedzobrodzki J, Kaszycki P, Bialecka A, Kasprowicz A. Proteolytic Activity of *Staphylococcus aureus* Strains Isolated from the Colonized Skin of Patients with Acute-Phase Atopic Dermatitis. *Eur J Clin Microbiol Infect Dis*. 2002;21(4):269-276.

209. Pietrocola G, Nobile G, Rindi S, Speziale P. *Staphylococcus aureus* Manipulates Innate Immunity through Own and Host-Expressed Proteases. *Front Cell Infect Microbiol*. 2017;7.

210. Stapels DAC, Ramyar KX, Bischoff M, et al. *Staphylococcus aureus* secretes a unique class of neutrophil serine protease inhibitors. *Proc Natl Acad Sci*. 2014;111(36):13187-13192.

211. Sungnak W, Huang N, Bécavin C, et al. SARS-CoV-2 entry factors are highly expressed in nasal epithelial cells together with innate immune genes. *Nat Med*. 2020;26(5):681-687.

212. Xue X, Mi Z, Wang Z, Pang Z, Liu H, Zhang F. High Expression of ACE2 on Keratinocytes Reveals Skin as a Potential Target for SARS-CoV-2. *J Invest Dermatol*. 2021;141(1):206-209.e1.

213. Visconti A, Bataille V, Rossi N, et al. Diagnostic value of cutaneous manifestation of SARS-CoV-2 infection*. *Br J Dermatol*. 2021;184(5):880-887.

214. Su C -J., Lee C -H. Viral exanthem in COVID-19, a clinical enigma with biological significance. *J Eur Acad Dermatology Venereol*. 2020;34(6).

215. Marzano AV, Cassano N, Genovese G, Moltrasio C, Vena GA. Cutaneous manifestations in patients with COVID-19: a preliminary review of an emerging issue. *Br J Dermatol*. 2020;183(3):431-442.

216. Fernandez-Nieto D, Ortega-Quijano D, Jimenez-Cauhe J, et al. Clinical and histological characterization of vesicular COVID-19 rashes: a prospective study in a tertiary care hospital. *Clin Exp Dermatol*. 2020;45(7):872-875.

217. Fischer H, Scherz J, Szabo S, et al. DNase 2 Is the Main DNA-Degrading Enzyme of the Stratum Corneum. Gartel A, ed. *PLoS One*. 2011;6(3):e17581.

218. Darlenski R, Tsankov N. COVID-19 pandemic and the skin: what should dermatologists know? *Clin Dermatol*. 2020;38(6):785-787.

219. Tao J, Song Z, Yang L, Huang C, Feng A, Man X. Emergency management for preventing and controlling nosocomial infection of the 2019 novel coronavirus: implications for the dermatology department. *Br J Dermatol*. 2020;182(6):1477-1478.

220. Hirose R, Ikegaya H, Naito Y, et al. Survival of Severe Acute Respiratory Syndrome Coronavirus 2 (SARS-CoV-2) and Influenza Virus on Human Skin: Importance of Hand Hygiene in Coronavirus Disease 2019 (COVID-19). *Clin Infect Dis*. Published online October 3, 2020.

221. Rundle CW, Presley CL, Militello M, et al. Hand hygiene during COVID-19: Recommendations from the American Contact Dermatitis Society. *J Am Acad Dermatol*. 2020;83(6):1730-1737.

222. Löffler H, Kampf G, Schmermund D, Maibach HI. How irritant is alcohol? *Br J Dermatol*. 2007;157(1):74-81.

223. Boyce JM, Kelliher S, Vallande N. Skin Irritation and Dryness Associated With Two Hand-Hygiene Regimens: Soap-and-Water Hand Washing Versus Hand Antisepsis With an Alcoholic Hand Gel. *Infect Control Hosp Epidemiol*. 2000;21(7):442-448.

224. Cartner T, Brand N, Tian K, et al. Effect of different alcohols on stratum corneum kallikrein 5 and phospholipase A 2 together with epidermal keratinocytes and skin irritation. *Int J Cosmet Sci*. 2017;39(2):188-196.

225. Kawamura T, Sasagawa S, Masuda T, Al. E. Basic research on patch test standardization. *Japanese J Dermatology*. 1970;80:301-314.

226. Sugai T. Cosmetics and Safety. *J Japanese Cosmet Sci Soc*. 1995;19:49-56.

227. Haasbroek K, Hashimoto M, Yokota S, Ishikawa N. Safety verification of stable sodium hypochlorite by 24-hour closed patch test method. *Glycative Stress Res*. 2021;8(2):110-114.